Energy, Mines and Resources Canada
Earth Physics Branch
1 Observatory Crescent
Ottawa Canada
K1A 0Y3

Énergie, Mines et Ressources Canada
Direction de la physique du globe
1 Place de l'Observatoire
Ottawa Canada
K1A 0Y3

Geothermal Service of Canada

Service géothermique du Canada

NATURE AND HISTORY OF GROUND ICE IN THE YUKON - ISOTOPE INVESTIGATIONS

F.A. Michel
Carleton University

Earth Physics Branch Open File Number 85-11
Dossier public de la Direction de la Physique du Globe No. 85-11

ABSTRACT

Massive ice and ice-rich sediments from a number of sites in central and northern Yukon have been examined stratigraphically and isotopically. Within the central Yukon, ice-wedge ice, segregated ice and frost-blister ice have been identified. Along the northern Yukon coastal plain, massive ice and ice-rich sediments, exposed in the headwalls of progressive thaw slides, have been interpreted as ice-wedge ice, segregated ice and buried glacier ice. The buried glacier ice, probably of early Wisconsinan age, exists near King Point, Kay Point, and on Herschel Island in what have been described as ice-thrust moraines. Each ice type displays a characteristic isotopic signature which is useful in identifying the origin of the ice.

RÉSUMÉ

La stratigraphie de la glace massive et des sédiments riches en glace est étudiée à plusieurs sites au centre et au nord du Yukon. Des échantillons recueillis à ces endroits sont analysés par des méthodes isotopiques. A l'intérieur du Yukon, la glace de fente, la glace de ségrégation et la glace d'aufeis sont identifiées. Le long de la plaine côtière du Yukon du nord la glace massive et les sédiments riches en glace, qui affleurent dans les parois frontales de coulées rétrogrades de sol provoquées par le dégel, ont plusieurs origines: glace de fente, glace de ségrégation et glace enfouie de glacier. La glace enfouie, datant probablement du début du Wisconsinien, existe près de King Point, Kay Point et sur l'île Herschel à l'intérieur de ce qui avait été décrit comme des moraines de chevauchement. Chaque type de glace a un caractère isotopique unique qui aide l'identification de son origine.

NATURE AND HISTORY OF GROUND ICE IN THE YUKON

- Isotope Investigations -

CONTRACT SERIAL NO. OST84-00292

FINAL REPORT

Prepared for

Department of Energy, Mines and Resources

Earth Physics Branch

by

F.A. Michel

Carleton University

April, 1985

ABSTRACT

Massive ice and ice-rich sediments from a number of sites in central and northern Yukon have been examined stratigraphically and isotopically. Within the central Yukon, ice-wedge ice, segregated ice and frost-blister ice have been identified. Along the northern Yukon coastal plain, massive ice and ice-rich sediments, exposed in the headwalls of retrogressive thaw slides, have been interpreted as ice-wedge ice, segregated ice and buried glacier ice. The buried glacier ice, probably of early Wisconsinan age, exists near King Point, Kay Point, and on Herschel Island in what have been described as ice-thrust moraines. Each ice type displays a characteristic isotopic signature which is useful in identifying the origin of the ice. Further research is required on the hydrogen isotope distribution and the ^{18}O-^{2}H relationships for each ice type.

TABLE OF CONTENTS

LIST OF FIGURES

Page

LIST OF TABLES

ACKNOWLEDGEMENTS

The author would like to thank A. Dufour, D. Good and M. Hare for their field assistance during 1983 and D. Good, M. Grant and D. van Everdingen for their field assistance during 1984. The laboratory assistance of D. Good, M. Grant and F. Dumovich and the typing by S. Thayer is also greatly appreciated. I would like to sincerely thank all of the staff of the Inuvik Weather Office, Environment Canada, for collecting precipitation samples during the past year.

The support provided by the Inuvik Research Laboratories, D.I.A.N.A, and the logistical support of the Polar Continental Shelf Project, E.M.R., are deeply appreciated. Financial support for this research has been provided by the Earth Physics Branch (contract OST84-00292), Energy, Mines and Resources Research Agreement Nos. 136, 287 and a NSERC operating grant (A2646) held by the author.

1. INTRODUCTION

1.1 Previous Studies

Initial investigations into the natural variations of stable isotopes in permafrost waters in northern Canada were undertaken by the author in 1976 (Fritz and Michel 1977). That study, which involved an examination of cores from the Mackenzie Valley and central Keewatin, revealed the existence of oxygen-18 variations of up to 15°/oo in permafrost-related ground ice. Additional detailed field studies at Illisarvik in the Mackenzie Delta during 1979 and 1980 demonstrated that many small-scale variations of less than 3°/oo are also preserved and that the isotopic profile can change dramatically over short distances (Michel and Fritz 1982a). A summary of typical isotopic compositions for various types of permafrost-related water in the Mackenzie Delta region has been presented by Mackay (1983). The preservation of small variations throughout the soil profile has been interpreted as an indication of negligible groundwater migration through the frozen soils (Michel 1982).

In an attempt to simulate natural variations under controlled conditions, a series of laboratory experiments were conducted during the 1977 to 1982 period (Michel 1982). These experiments have demonstrated that it is possible to generate small variations (less than 3°/oo) as a result of freezing. Furthermore, the experiments have shown that

variations in excess of 3°/oo (for oxygen-18) can be generated through fractionation under specialized conditions such as stationary freezing fronts and minor freeze-thaw cycles. Through the simultaneous study of deuterium isotopes it has also been possible to understand the significance of deuterium-oxygen-18 relationships which differ from the standard meteoric water line.

Within the Yukon, work has been undertaken on core material from the Dempster Highway pipeline route (Michel and Fritz 1982b, 1983) and the Alaska Highway pipeline route (Michel and Fritz 1982c). Significant isotope variations, which reflect recharge under different climatic conditions, exist along portions of the Dempster Highway route, while no such variations were detected along the Alaska Highway route, suggesting relatively recent recharge. More recently, isotopic investigations, in conjunction with separate stratigraphic and ice fabric studies, have been initiated at sites near Mayo and Dawson. A study of isotope fractionation during formation of frost-blister ice at North Fork Pass has recently been completed (Michel in preparation). In addition, several ice samples from the northern Yukon coastal plain, collected by J. S. Vincent of the Geological Survey of Canada in 1983, have been analysed for their isotopic composition.

1.2 Terms of Reference

As part of the ongoing investigations of groundwater in permafrost regions of Canada, this study was undertaken as a continuation of the previous research program. Specifically, the objectives of this study were:

1) to better understand the formation, nature and history of ground ice at selected locations in the Yukon, and
2) to better understand permafrost conditions in the region of study.

The major initiative of this study was to undertake an investigation of isotopic variations in ground ice. The key to these isotopic investigations is the fractionation which occurs between the isotopes of oxygen and hydrogen in the ice-water system during freezing. Various hypotheses for the origin of massive ground ice describe processes which should result in characteristic isotope signatures due to fractionation mechanisms. Thus, it should be possible to identify the origin of a particular ice mass. It is also necessary to understand stratigraphic relationships between the enclosing sediments and the internal structure of the ice if these ice masses are to be fully characterized in terms of formation and possible age.

1.3 Scope of the Report

This report describes the work completed and presents the data acquired during the contract period. Preliminary interpretations of the data are discussed in relation to

their significance in understanding the formation of ground ice at selected study sites in the Yukon. Investigations along the northern Yukon coastal plain are described in Chapter 2, while similar work within the central Yukon is presented in Chapter 3. This project was designed as the first phase of a two to three year program of study. Therefore, the results presented are still incomplete and interpretations are considered to be preliminary.

2. NORTHERN YUKON COAST

2.1 Introduction

During the months of June and July 1984, field work was concentrated along the northern coast of the Yukon. Camps were established at four sites where active retrogressive thaw slides were present. These were at or near Sabine Point, King Point, Kay Point and Herschel Island (Figure 2.1). Work at the first two sites was part of a broader study which included ice fabric investigations by French and Pollard of the University of Ottawa.

Sampling was undertaken using two methods. The first employed a portable hand-held STIHL drill and CRREL core barrel to obtain continuous core samples. On several occasions, especially at the Kay Point site, very stoney sediments prevented any substantial penetration. The second method, which became the dominant one during the summer, involved sampling the headwall of the thaw slide using ropes and an ice axe. This method proved to be quite suitable provided overhangs were minimal and the headwall sloped toward the thaw slide.

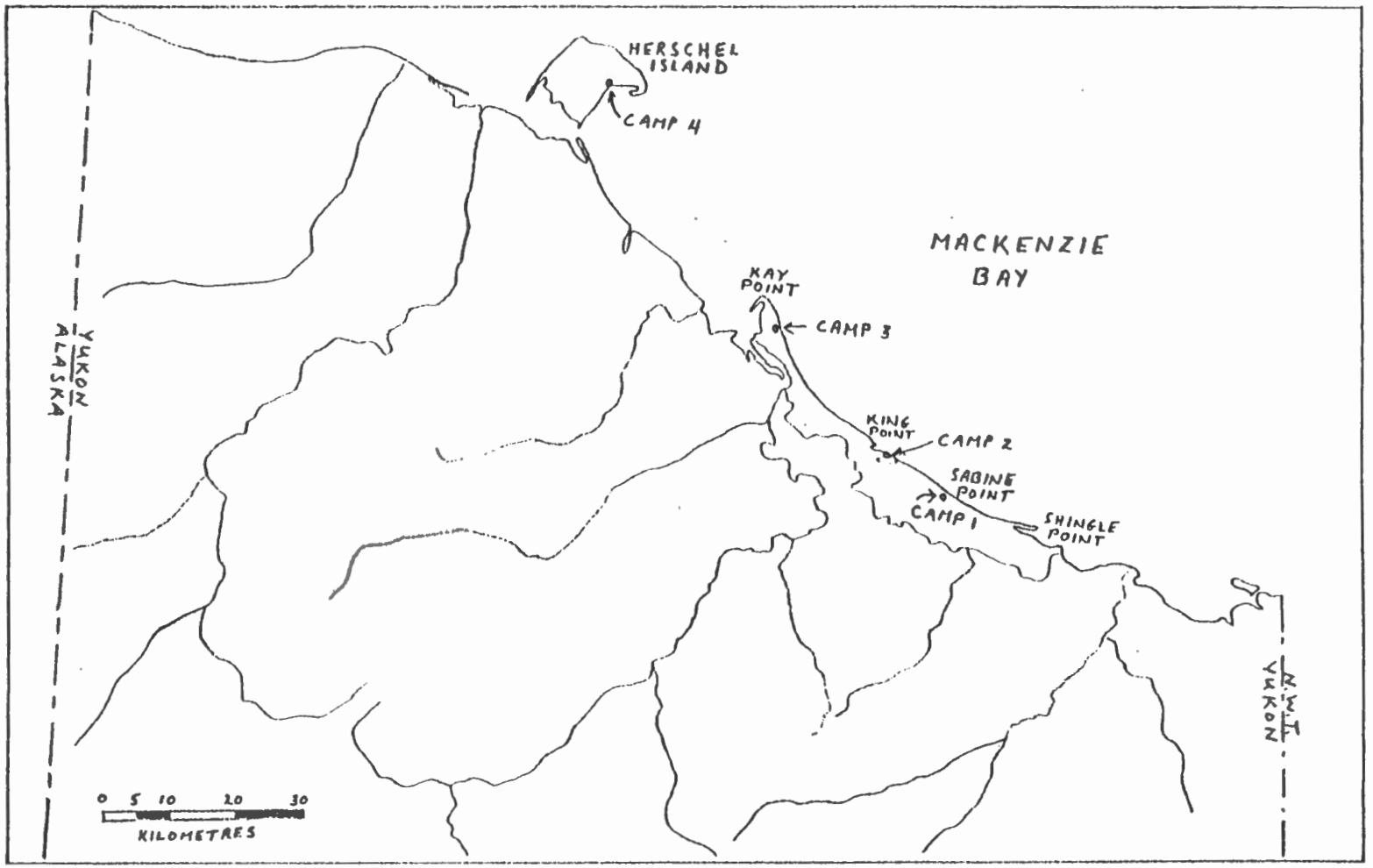

Figure 2.1 Location map of study sites along the northern Yukon coast.

In addition to these four sites, six grab samples of ice were provided by Dr. Vincent of the G.S.C. The staff of the Environment Canada weather office at Inuvik airport has been collecting precipitation samples during the past year.

2.2 Inuvik Precipitation

Since June 1984, precipitation samples have been collected at Inuvik for isotope analysis (Table 2.1). These data should be representative for at least the Mackenzie Delta region and probably the Yukon coastal plain. As can be seen from Table 2.1, the range in $\delta^{18}O$ values is quite large; -15.8 to -30.9 °/oo. Despite this large range, work by Michel (1982) has shown that water and ice in the active layer and upper permafrost zone consistently have $\delta^{18}O$ values in the -18 to 20°/oo range at Illisarvik. This range corresponds with the fall precipitation samples and suggests that most of the water saturating the active layer immediately prior to freezeback is derived from fall precipitation.

Since a full year has not yet elapsed since data collection began, any interpretation at present must be considered to be preliminary. The data which are available have been plotted in Figure 2.2. With the exception of one sample (June 11-30), all of the data plot very close to the

Table 2.1 Isotope data for Inuvik Airport precipitation

SAMPLE	$\delta^{18}O$ (°/oo SMOW)	$\delta^{2}H$ (°/oo SMOW)
June 3/84 snow	-20.9	-160
June 4/84 snow	-19.4	-152
June 11-30/84	-16.2	-136
July 1-21/84	-19.4	-148
July 22 - Aug. 8/84	-15.8	-119
Aug. 8-24/84	-18.7	-142
Aug 25 - Oct. 2/84	-19.0	-147
Oct. 3 - Dec 7 /84	-26.0	-192
Dec 8/84 - Feb 4/85	-30.9	-240
Feb 5 - April 8/85	-30.2	

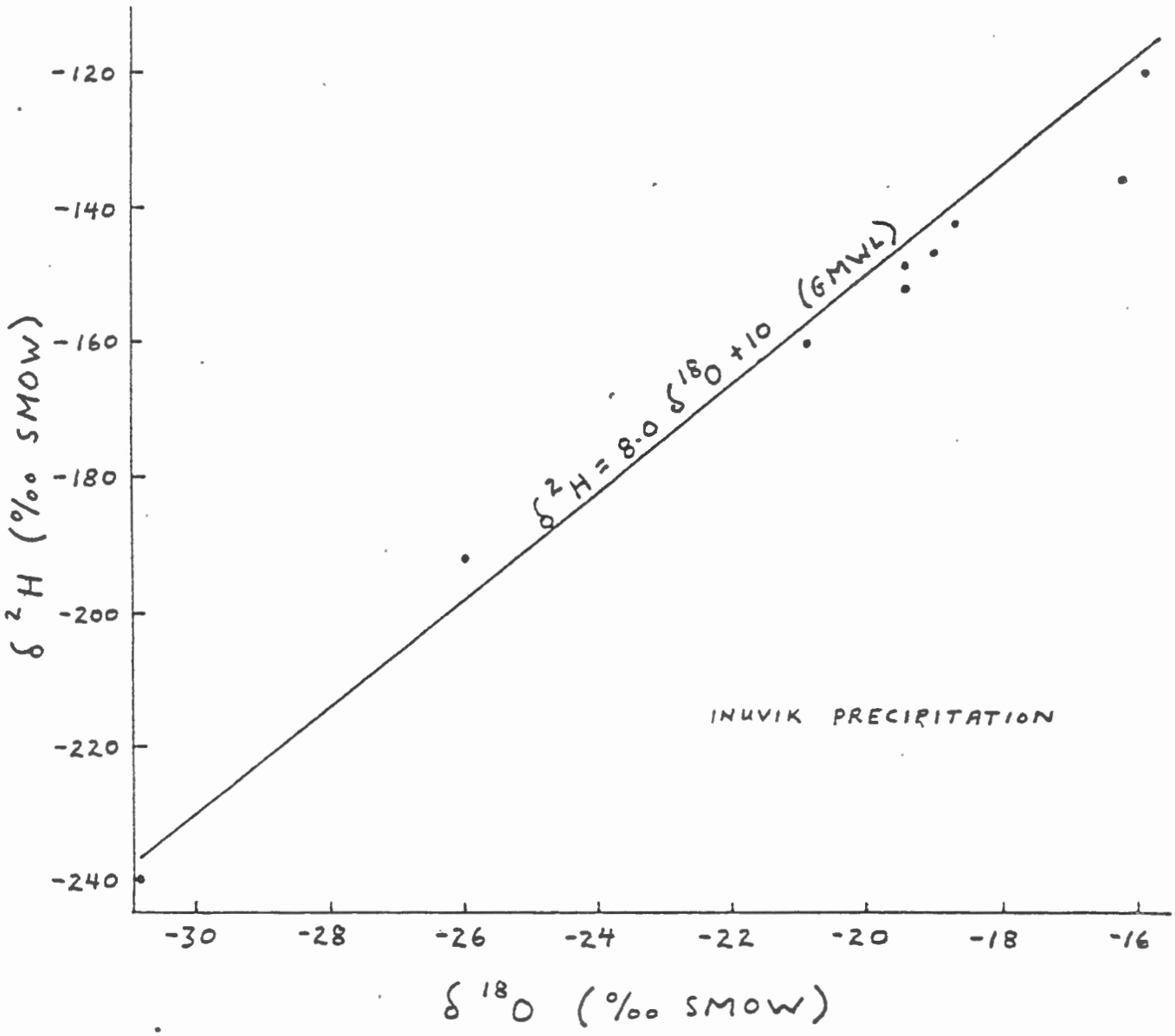

Figure 2.2 Relationship between ^{2}H and ^{18}O contents for Inuvik Airport precipitation. GMWL = global meteoric water line.

global meteoric water line. As additional data are collected, the definition of the local meteoric water line will improve. This line will be useful for comparison of isotopic data for various water and ice bodies in the region. It can also be used as a reference for discussion of various oxygen and hydrogen isotope relationships. Finally, it will permit the comparison of oxygen and hydrogen data for systems which are known to plot on the meteoric water line.

2.3 Grab Samples (Dr. J.S. Vincent)

A total of six grab samples of ice were collected by Dr. Vincent during field work in 1983. These samples have been analysed for their deuterium concentrations which are listed in Table 2.2. For the three ice wedge samples, the δ^2H values (-170 to -179°/oo) are similar to δ^2H values obtained for modern ice wedges in the Illisarvik area by Michel and Fritz (1982b). Based on the Inuvik precipitation data, the $\delta^{18}O$ values for these ice wedges would be in the -22 to -24°/oo range.

The three samples of massive ice have δ^2H values which are more negative than the ice wedges. None of the other samples collected along the Yukon coast have been analysed for hydrogen isotope ratios and, thus, no further discussion of these three samples is possible at this time.

Table 2.2 Isotope data for 1983 samples from Yukon Coast - J.S. Vincent

	δ^2H (°/oo SMOW)
Shingle Pt. Gravel Pit Ice wedge in upper till	-170
Shingle Pt. Gravel Pit Massive ice, 30 cm below upper till	-211
East of King Pt., Ice wedge	-178
East of King Pt., Massive ice	-204
Kay Pt., Ice wedge	-179
Stokes Pt., Segregated ice in lower marine sequence	-192

2.4 Sabine Point

2.4.1 Site Description

Sabine Point is located 24 kilometres northwest of the Shingle Point D.E.W. Line station (Figure 2.1). The site is characterized by a large hill adjacent to the coast with low-lying polygonal ground surrounding it on the remaining three sides.

On the northeast side of the hill, the outline of an earlier retrogressive thaw slide is still visible (Figure 2.3). Within the boundary of this old slide, a newly activated thaw slide is growing with a lower base level. The backwall of this slide is approximately two metres in height.

A second active thaw slide is located on the northwest side of the hill. The headwall of this slide is variable in height, ranging from zero to ten metres. Most of the work at this site focussed on this slide area. A large unstable overhang of organic material above the highest portion of the headwall prevented work along that section.

2.4.2 Work Completed

Work was undertaken at this location during the first half of June when both thaw slides were active. Two sections (E1 and E2) were sampled across a massive ice unit exposed in the face of the northwest thaw slide. A block of ice from this unit was collected by Pollard and French adjacent to section E1. In order to evaluate the extent of this ice body, four boreholes were drilled along the backwall of the

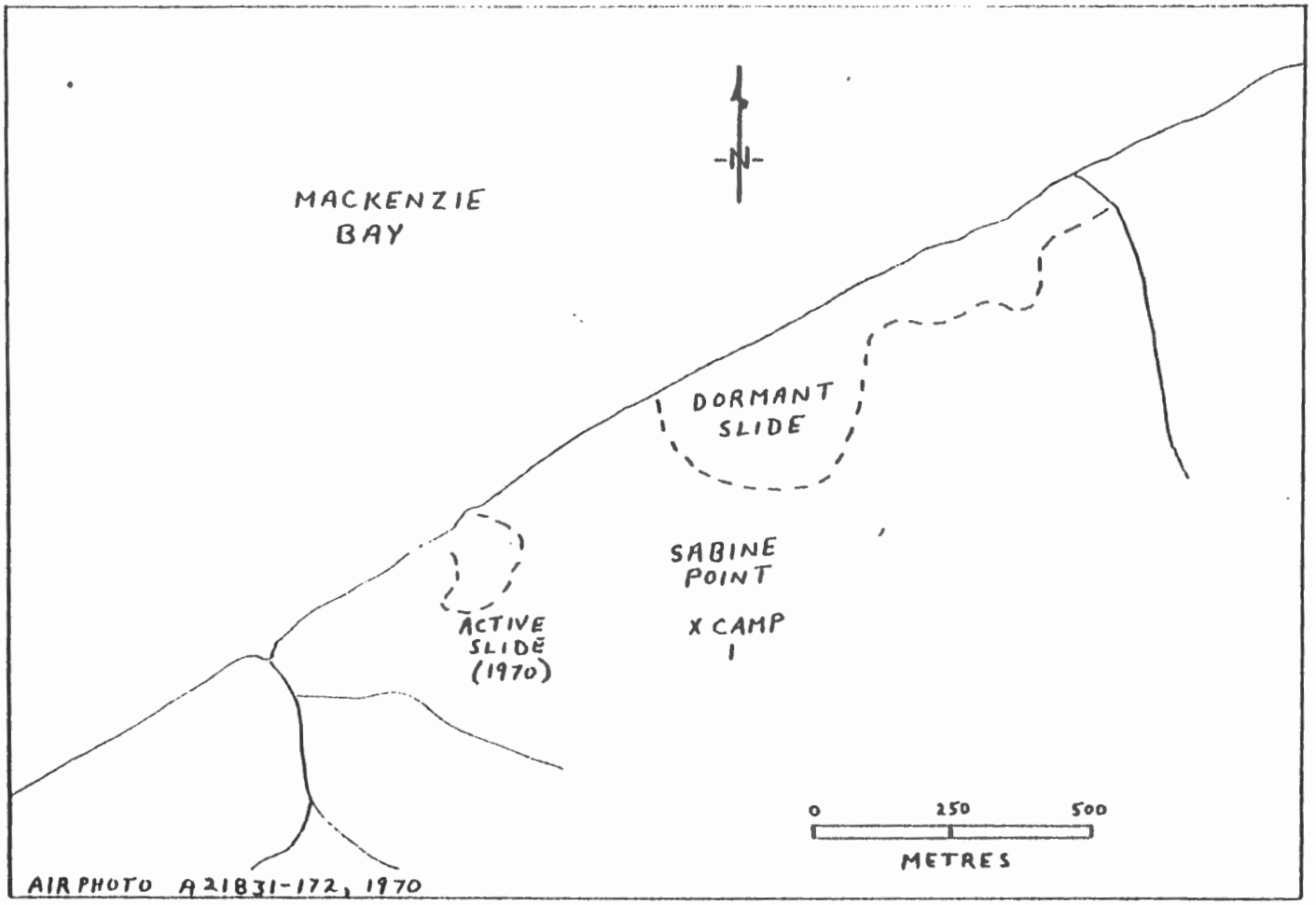

Figure 2.3 Location of thaw slides at Sabine Point site.

thaw slide. Due to various problems encountered during drilling, depth of penetration for these boreholes ranges from 28 cm (DH1) to 505 cm (DH3).

Adjacent to the northeast thaw slide an exposure was located in which two generations of ice wedges were visible. A vertical section across these wedges was sampled as E3. Other work at the site involved the drilling of four shallow boreholes (63 to 98 cm) at various locations in order to sample active layer material.

2.4.3 Stratigraphy

Rampton (1982) classifies the surficial sediments of the Sabine Point area as lacustrine plain, containing interbedded peat and lacustrine silts and clays. The hill forming Sabine Point rises well above the general level of this plain.

Within the headwall of the northwest thaw slide and adjacent coastal bluffs, the stratigraphy consists of a surficial layer of interbedded peat and organic silts (over 3 metres thick in places) overlying a 1 to 1.5 metres thick discontinuous stoney clay silt, which in turn overlies a grey marine silty clay. At the top of the marine clay unit, a layer of massive segregated ice 0.5 to 3 metres thick was exposed. Below the massive ice, the clay is highly fractured by ice lenses forming a boxwork pattern. The size of these ice lenses decreased with depth. The marine clay unit is approximately 1.5 metres thick and is underlain by a coarse sand layer of unknown thickness.

2.4.4 Isotopic Results

To date, ^{18}O concentrations have been determined for samples from borehole DH3 and exposure E2 (Table 2.3). These data are plotted in Figures 2.4 and 2.5 respectively.

The stratigraphy encountered in borehole DH3 can be divided into three units. Peat and silty clay, 1.5 metres thick, overlie 3 metres of massive ice which in turn overlies silty clay with randomly oriented ice lenses (boxwork). As can be seen in Figure 2.4, the upper unit contains ice with $\delta^{18}O$ values in the -18.5 to -20.5°/oo range. These values are similar to shallow permafrost waters in the Illisarvik area (Michel 1982) and probably represent recharge during the period of present climatic conditions.

Within an 11 cm interval (146 to 157 cm), the ^{18}O profile shifts more than 6°/oo to -26.3°/oo, marking the top of the massive ice unit. Over the 3 metre interval of ice the ^{18}O concentration gradually decreases by an additional 2.5°/oo.

A similar pattern is evident in section E2 (Figure 2.5). In this figure the depth scale has been expanded, since the massive ice is only 1.5 metres thick (2.5 to 4.0 metres) at this location. Above the ice unit, the ^{18}O concentration increases upwards toward -20°/oo, as in DH3, but the shift is not nearly as rapid. The reason for this difference is unknown.

Table 2.3 Isotope data for Sabine Point site

	SAMPLE NUMBER	DEPTH (CM)	TYPE OF MATERIAL	$\delta^{18}O$ (°/oo SMOW)
E2	1	200-210	peat & ice	-21.1
	2	210-220	clay with peat	
	3	220-230	"	-25.2
	4	230-240	org. clay with pebbles	
	5	240-250	"	-26.2
	6	250-260	ice	-26.8
	7	260-270	"	-27.3
	8	270-280	"	-26.7
	9	280-290	"	-26.9
	10	290-300	"	-26.8
	11	300-310	"	-27.1
	12	310-320	"	-27.3
	13	320-330	"	-27.3
	14	330-340	"	-27.7
	15	340-350	"	-27.8
	16	350-360	"	-27.8
	17	360-370	"	-28.0
	18	370-380	"	-27.7
	19	380-390	"	-27.9
	20	390-400	"	-29.1
	21	400-410	ice & clay	-28.4
	22	410-420	"	-29.5
	23	420-430	"	-29.2
	24	430-440	"	-29.3
	25	440-450	"	-28.9
	26	450-460	"	-28.4
	27	460-470	"	-28.6
	28	470-480	"	-28.7
	29	480-490	"	-29.0
	30	490-500	clay & ice	-28.7
	31	500-510	"	
	32	510-520	"	-28.3
	33	520-530	"	-28.3
	34	530-540	"	-28.6
	35	540-550	"	-27.8
	36	550-560	"	-28.4
	37	560-570	"	-27.0

Table 2.3 Isotope data for Sabine Point site (cont'd)

	DEPTH (CM)	TYPE OF MATERIAL	$\delta^{18}O$ (°/oo SMOW)
SABINE DH3	29-35	peat & clay	-18.9
	42-50	"	-18.7
	50-60	clay & peat	-19.3
	60-70	"	-20.2
	70-80	silty clay & ice	-19.9
	85-95	"	-19.6
	95-104	silty clay & peat	-19.4
	104-113	peat	-19.3
	136-146	peat & silty clay	-19.8
	157-165	ice	-26.3
	165-173	"	-26.6
	173-181	"	-26.7
	181-189	"	-26.8
	189-200	"	-26.5
	200-211	"	-26.5
	211-220	"	-26.5
	220-230	"	-27.0
	230-245	"	-27.2
	245-252	"	-27.0
	252-260	"	-27.2
	260-264	"	-27.2
	264-274	"	-27.2
	274-283	"	-27.4
	283-292	"	-27.4
	292-298	"	-27.1
	298-310	"	-26.3
	310-319	"	-27.4
	319-327	"	-26.9
	327-336	"	-27.4
	336-345	"	-27.5
	345-353	"	-27.5
	353-360	"	-27.8
	360-368	"	-28.0
	368-374	"	-28.2
	374-380	"	-27.8
	388-395	"	-28.4
	395-402	"	-28.3
	402-409	"	-28.0
	409-417	"	-28.5
	417-429	"	-28.1
	429-437	"	-27.6
	437-443	"	-28.4
	443-450	"	-28.7
	465-473	ice & clay	-29.5
	473-480	"	-29.9
	480-487	"	-29.3

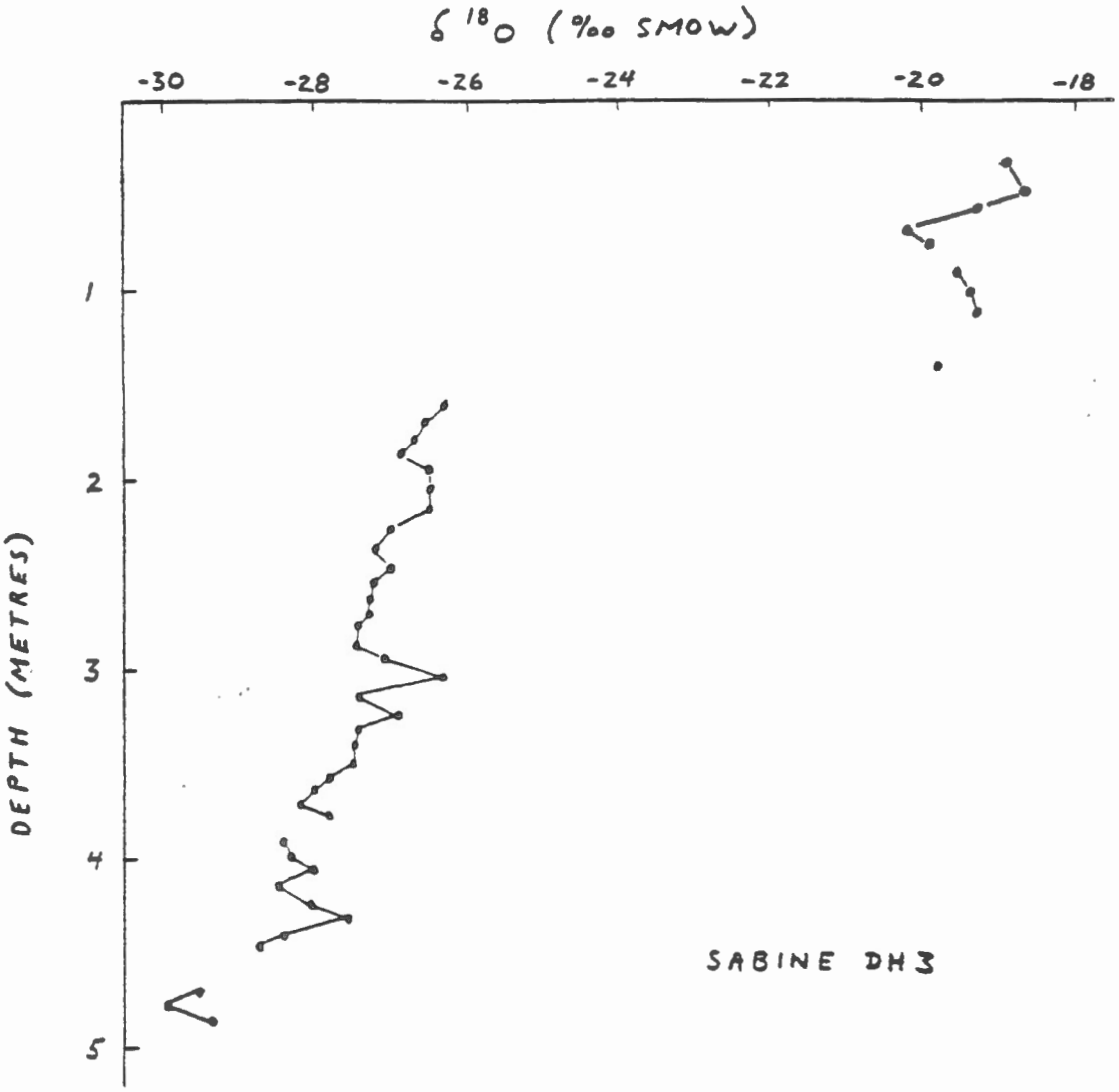

Figure 2.4 Variation in ^{18}O content with depth for core DH3 at Sabine Point.

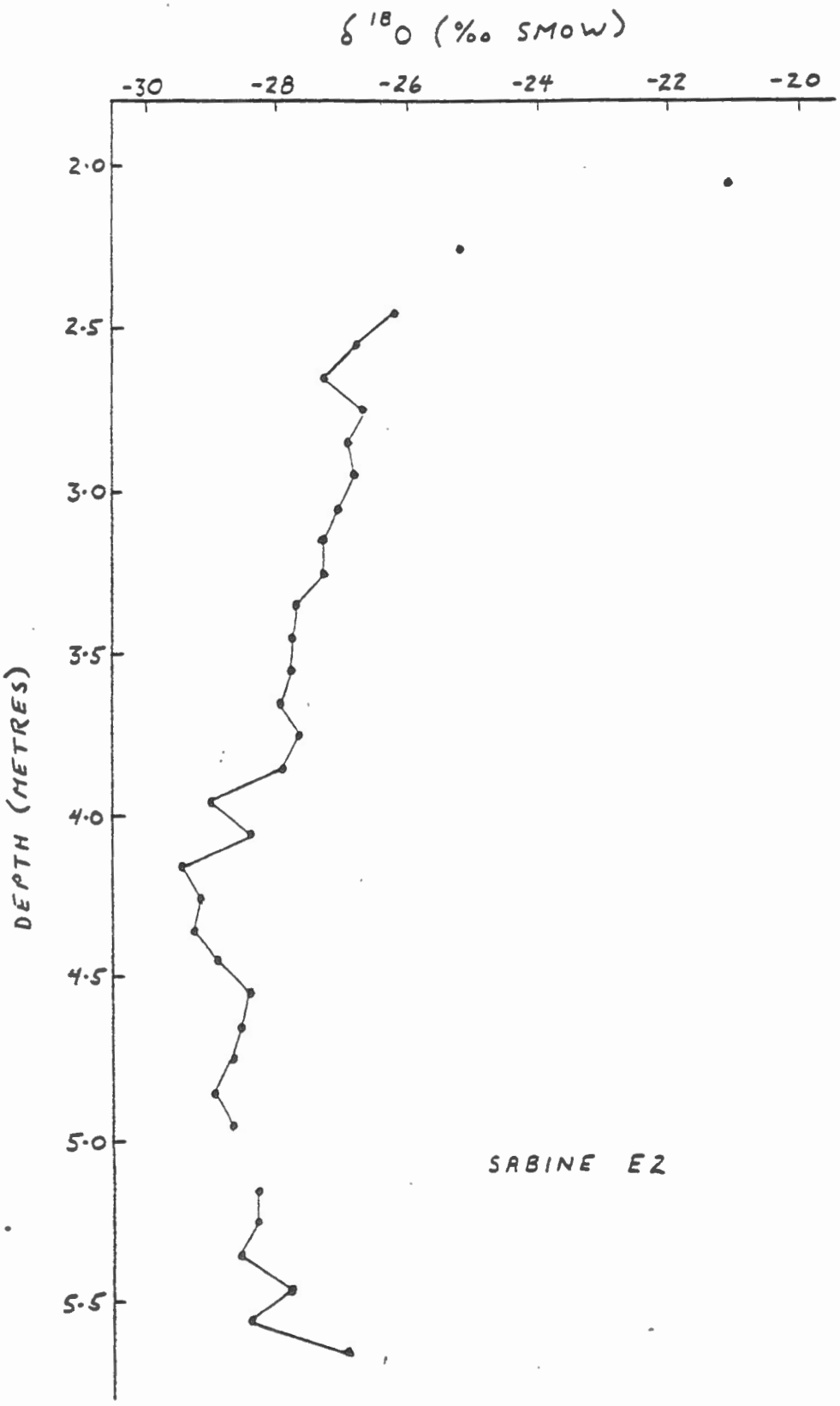

Figure 2.5 Variation in ^{18}O content with depth for section E2 at Sabine Point.

Although the ice unit in E2 is only half the thickness of DH3, the isotopic profile is identical. The uppermost ice in both sections has a $\delta^{18}O$ value of -26.3 ± 0.2°/oo. At the base of the ice the ^{18}O composition has shifted to -28.9 ± 0.2°/oo. This is interpreted as indicating that the original thickness of ice at both locations has been preserved.

The stratigraphic relationship between the massive ice and enclosing sediments is suggestive of a segregational origin for the ice. The formation of a large segregated ice body involves the migration of water to the freezing front from the underlying unfrozen sediments. The first ice to form will be isotopically enriched in the heavy isotope (^{18}O) while the adjacent residual water becomes depleted. As freezing continues, the ^{18}O composition of the ice and residual water will gradually shift to lower concentrations of oxygen-18. Unless the residual water is completely removed and replaced by water which has not previously been subjected to fractionation, the gradual shift in ^{18}O composition should continue throughout the thickness of the ice lens and underlying frozen sediments.

The ^{18}O profiles (Figures 2.4 and 2.5) for the massive ice lens display exactly this pattern of gradual ^{18}O depletion. The ice lens formed by downward advancement of the freezing front and upward migration of water through the underlying unfrozen clay. The small fluctuations in the

profiles are interpreted as representing minor variations in the rate of advancement of the freezing front, which should correspond to the rate of ice formation.

In both profiles, the ^{18}O concentration of ice within clay immediately below the base of the massive ice is lower than the basal massive ice. However, with increasing depth, the oxygen isotope ratios reverse this trend and shift toward less negative values (Figure 2.5). The cause of this reversal in trend is not understood at present, but may involve a decrease in the rate of upward water migration. $\delta^{18}O$ values at the bottom of the profile should be approaching the original composition of water in the clay before the massive ice unit began forming. Immediately below the bottom sample, the top of a sand unit was visible. This sand may have supplied water for the system during formation of the massive ice lens.

2.5 King Point

2.5.1 Site Description

The King Point site is located 10 kilometres west of Sabine Point and 4 kilometres east of the base of King Point (Figure 2.1). The site (Figure 2.6) is dominated by a large retrogressive thaw slide 0.6 kilometres in length, parallel to the coast. Extensive banded massive ice is exposed in the headwall (Rampton 1982). The currently active thaw slide is superimposed on an earlier episode of thaw activity. South

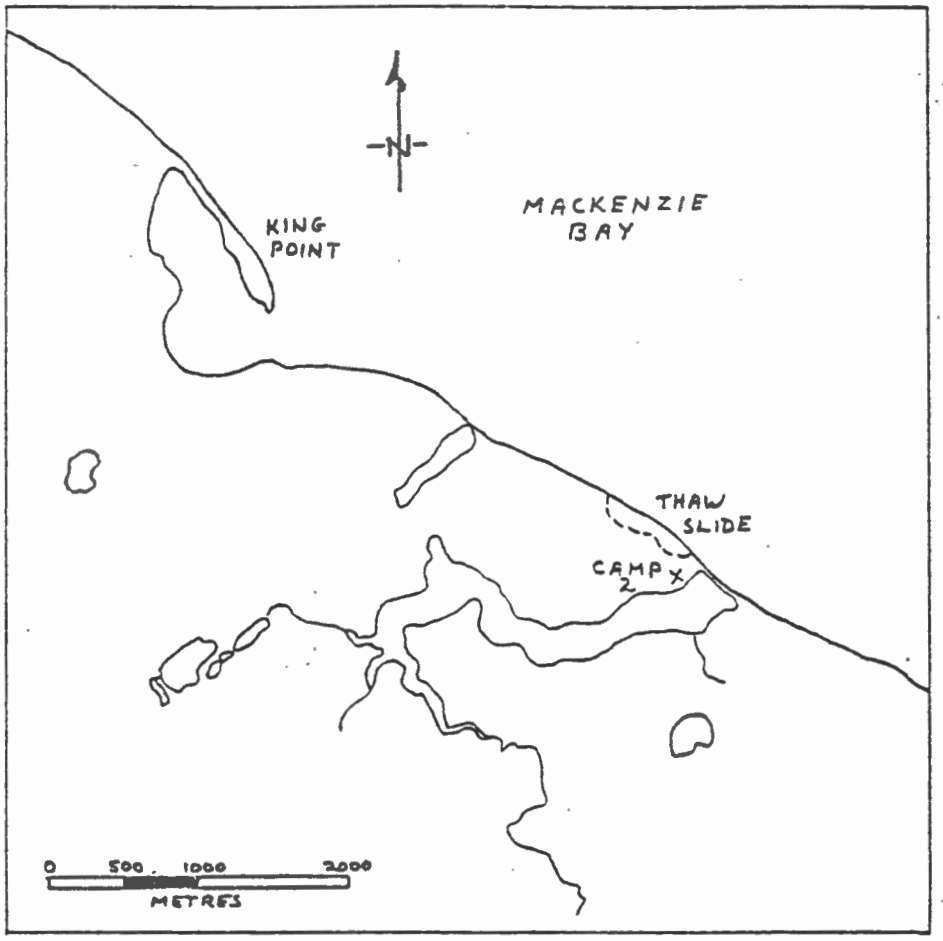

Figure 2.6 Location of thaw slide near King Point.

of the headwall, extensive patterned ground has developed. Ice wedges exposed in the headwall have been described by Harry et al. (1985).

2.5.2 Work Completed

Work was undertaken at this location during the last two weeks of June. During this time most of the massive ice was covered by snow and was inaccessible for sampling. As a result, considerable time was spent measuring and sampling ice wedges exposed along the top of the headwall. Of 65 ice wedges mapped, single grab samples were collected from 38 while an additional 14 were sampled in detail.

Four boreholes (AL5-8) were drilled behind the headwall to provide samples from the active layer. Borehole AL7 was completed to a depth of 3.33 metres to provide continuous samples of the sediments overlying the massive ice. A fifth borehole was attempted on top of an isolated uneroded block in the thaw slide, however, drilling was abandoned at a depth of 98 cm due to stoney material.

At the base of this section, a 3 metre exposure of massive ice was sampled near the end of the visit. Nine grab samples of ice were also collected at this location. In late July the site was briefly revisited. At the east end of the slide area a 12 metre section containing 10 metres of massive ice was sampled at 0.5 to 1.0 metre intervals.

2.5.3 Stratigraphy

Surficial sediments at this site are part of the same lacustrine plain sequence as at Sabine Point. Interbedded peat and organic clay silts up to 1.6 metres thick overlie 1.5 metres of silty clay. Below the silty clay is a stoney clay unit which immediately overlies the banded massive ice.

Approximately 10 metres of this banded ice was exposed at the time of sampling. The upper 2.5 metres of ice contains 10 to 15% soil inclusions which are up to 1 cm in diameter. From 2.5 to 10 metres the ice contains 20 to 30% soil inclusions consisting of silty clay. The soil inclusions form distinct soil-rich bands containing 30 to 80% soil fragments. Throughout the massive ice bubbles are rare. The bands appear to be dipping at 60 to 70% toward the coast (NE).

2.5.4 Isotopic Results

Oxygen isotope ratios have been measured for the banded massive ice section sampled in late July. These data (Table 2.4) are plotted in Figure 2.7.

Although continuous samples were not collected from this section, a pattern of oscillations is clearly visible in the ^{18}O profile. The profile can be subdivided into two zones which correspond to the ice contents. The upper zone, 2 to 4.5 metres, with an 85 to 90% ice content, displays almost a

Table 2.4 Isotope data for King Point thaw slide site

	SAMPLE NUMBER	DEPTH (CM)	TYPE OF MATERIAL	^{18}O (°/oo SMOW)
East end section	1	170-180	clay & ice	-25.0
	2	185-195	silty clay & pebbles	
	3	200-210	banded ice & 10-15% sediment	-28.9
	4	250-260	"	-27.9
	5	300-310	"	-27.4
	6	350-360	"	-28.2
	7	400-410	"	-28.6
	8	450-460	"	-28.3
	9	550-560	banded ice & silty clay	-26.3
	10	650-660	"	-26.4
	11	750-760	"	-27.2
	12	850-860	"	-27.4
	13	950-960	"	-27.1
	14	1050-1060	"	-26.6
	15	1150-1160	"	-25.7
	16	1190-1200	"	-26.2

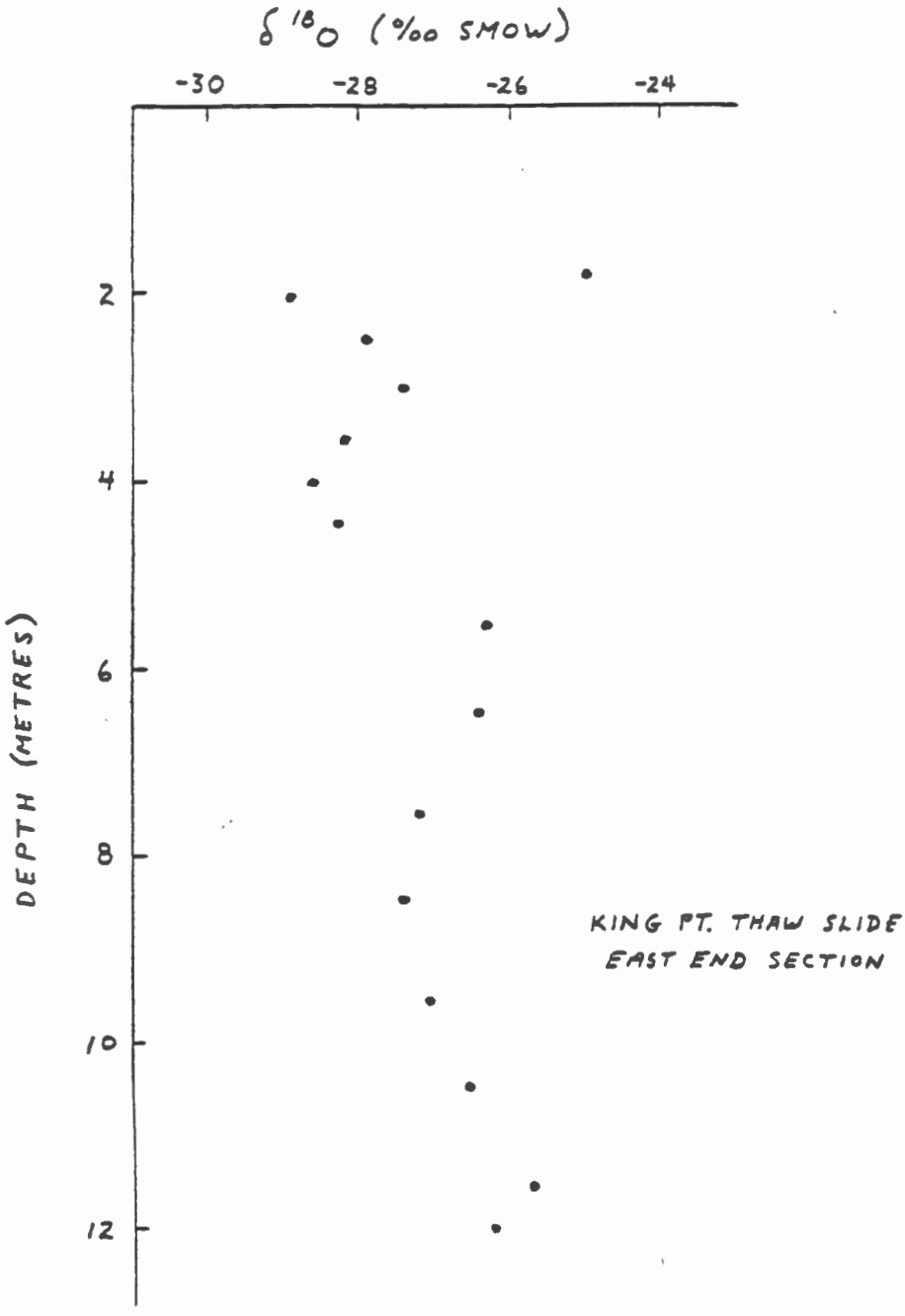

Figure 2.7 Variation in ^{18}O content with depth for the east end section of King Point thaw slide.

full oscillation with $\delta^{18}O$ values in a 1.5°/oo range (-27.4 to -28.9°/oo). The lower zone, 4.5 to 12 metres, contains 70 to 80% ice with $\delta^{18}O$ values between -25.7°/oo and -27.4°/oo.

This ^{18}O profile is very different from the two ^{18}O profiles for segregated ice at Sabine Point, described in section 2.4.4. It is possible, therefore, to state that the banded massive ice exposed in the headwall of this thaw slide is not of a segregational origin. Although there is a minor resemblance to profiles composed of sequential water injections, such as pingo ice reported by Michel and Fritz (1980), the variation in $\delta^{18}O$ values is too small.

Comparison with the ^{18}O data for banded massive ice exposed on Herschel Island (see section 2.7.4) reveals a definite similarity in ^{18}O profiles. On the basis of this similarity, the banded massive ice at this site is assigned a similar origin to the Herschel Island ice; buried glacier ice (see Herschel Island discussion in section 2.7.4).

If this interpretation is correct, then the oscillations in $\delta^{18}O$ values represent differences in summer and winter precipitation. Molecular diffusion has probably decreased the magnitude of these variations. The large thickness of ice for a single oscillation cycle is interpreted as being due to sampling of an apparent section. Since both the banding and the slope of the face dip towards the coast, a section oblique to the true thickness was sampled.

2.6 Kay Point

2.6.1 Site Descriptions

The third camp was established 6 kilometres southeast of Kay Point near the shore of Mackenzie Bay (Figure 2.1). A high ridge parallels the coast from King Point to Kay Point and is bounded by Mackenzie Bay to the northeast and the Babbage River flood plain to the southwest. Along this ridge, streams have cut small canyons which dissect the terrain, exposing good stratigraphic sections. Several active retrogressive thaw slides occur between the camp site and Kay Point.

2.6.2 Work Completed

Camp 3 was occupied for a period of 10 days during the first half of July. Poor weather during this period limited the amount of work accomplished. Adjacent to the camp site (Figure 2.8), four boreholes were drilled to depths of 15 to 64 cm for samples of the active layer. Numerous stones in the surficial sediments prevented deeper penetration.

Within 3 kilometres of the camp, in the direction of Kay Point, three retrogressive thaw slides were investigated. Banded massive ice was exposed in the headwalls of all three slides. Two sections (7.55 and 9.05 metres) were sampled at thaw slide MI1, 2.66 kilometres northwest of camp. At MI2, 2.58 kilometres from camp, a vertical section (5.1 metres) was sampled. Within the banded ice a 9.5 metre horizontal section was sampled at 0.5 metre intervals. Two sections of

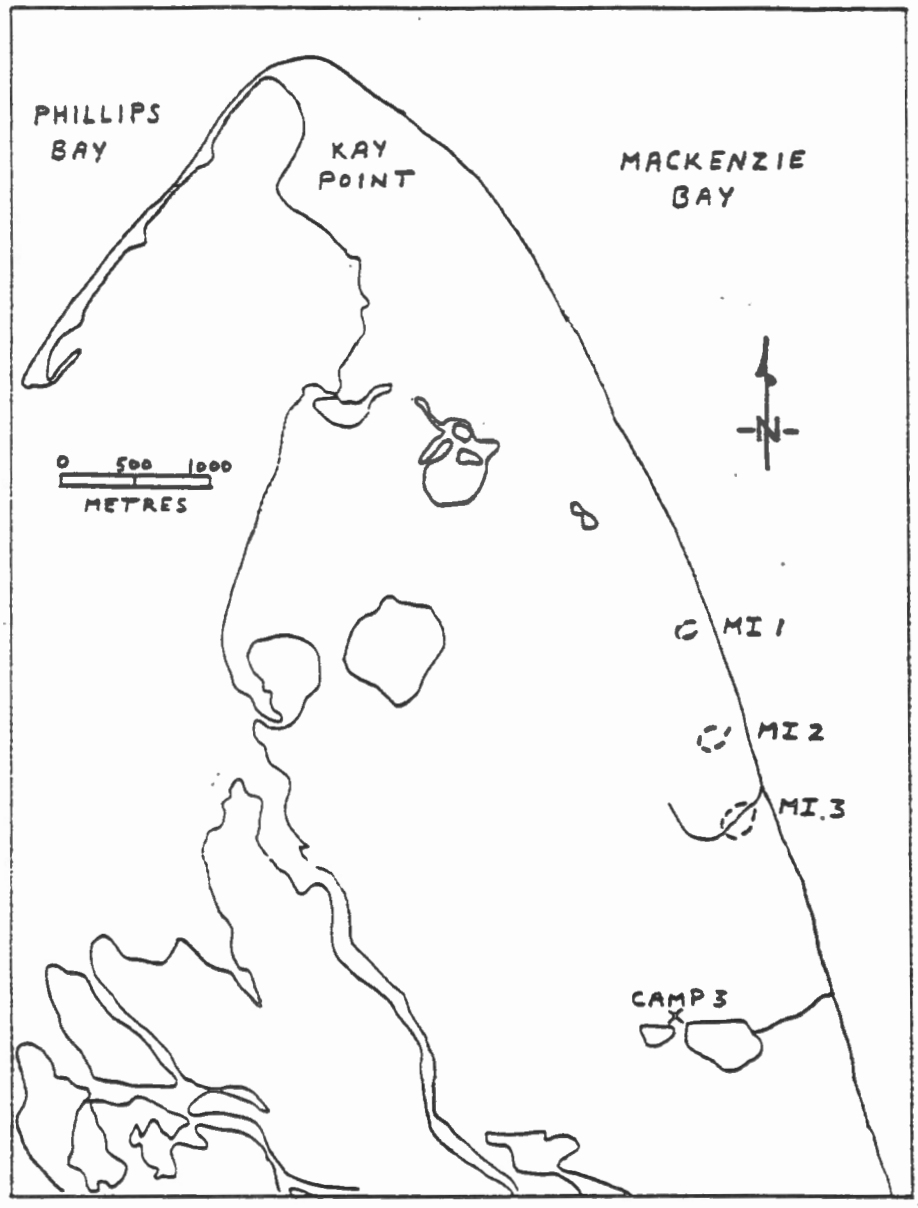

Figure 2.8 Location of thaw slides near Kay Point.

massive ice (2.8 and 4.0 metres thick) were sampled at MI3, located 1.2 kilometres northwest of camp. Material was also collected at two small exposures, 75 and 300 metres northwest of MI3.

At the time of writing no isotopic results are available for this area.

2.6.3 Stratigraphy

Rampton (1982) has mapped this ridge as deformed, ice thrust pre-Buckland sediments. The surficial sediments are composed of stoney sands and clays. Within the banded ice material, the sediment is primarily silty clay with occasional pebbles, especially in the upper portions. Ice content for the banded material varies from 30 to 95% and averages 60 to 70%. Ice at sites MI1 and MI2 contain very few bubbles, while bubbles 1 to 3 mm in diameter form 5 to 25% of the ice volume at MI3.

2.7 Herschel Island

2.7.1 Site Description

Herschel Island (Figure 2.1) has been described by Rampton (1982) as an ice-thrust moraine, similar in origin to the ridge between Kay Point and King Point referred to in the previous section. The island rises to almost 180 metres above sea level. It is bounded by steep coastal bluffs and dissected by deep stream valleys.

Along the southeast coast of the island, adjacent to Thetis Bay, a number of recently activated retrogressive thaw slides occur (Figure 2.9). Examination of aerial photographs for this area reveals that most of these thaw slides have become active since 1976 and are experiencing headwall retreat rates of 10 to 15 metres per year. Figure 2.10 depicts the position of the headwall in various years for the largest thaw slide (HER 5) which became active in the early 1950s.

2.7.2 Work Completed

Work on Herschel Island was conducted during the last two weeks of July and focussed on the thaw slides of the southeast coast. Six major thaw slides occur along a 2 kilometre section of this coast. The four largest slide areas were examined using ropes and climbing equipment.

Samples from two vertical sections (4.0 and 2.4 metres in length) were collected from the north wall of the largest thaw slide (HER 5). In addition, 19 grab samples from various ice-rich intervals within the headwall were taken. At HER 4, the furthest south of the group, a series of 17 samples were collected from four ice wedges, massive ice, ice-rich sediments and surficial organic deposits. At HER 3, the second largest thaw slide, two vertical sections (7.0 and 8.4 metres long) 19 metres apart were sampled in 10 cm intervals. Individual sediment-rich horizons could be traced between sections.

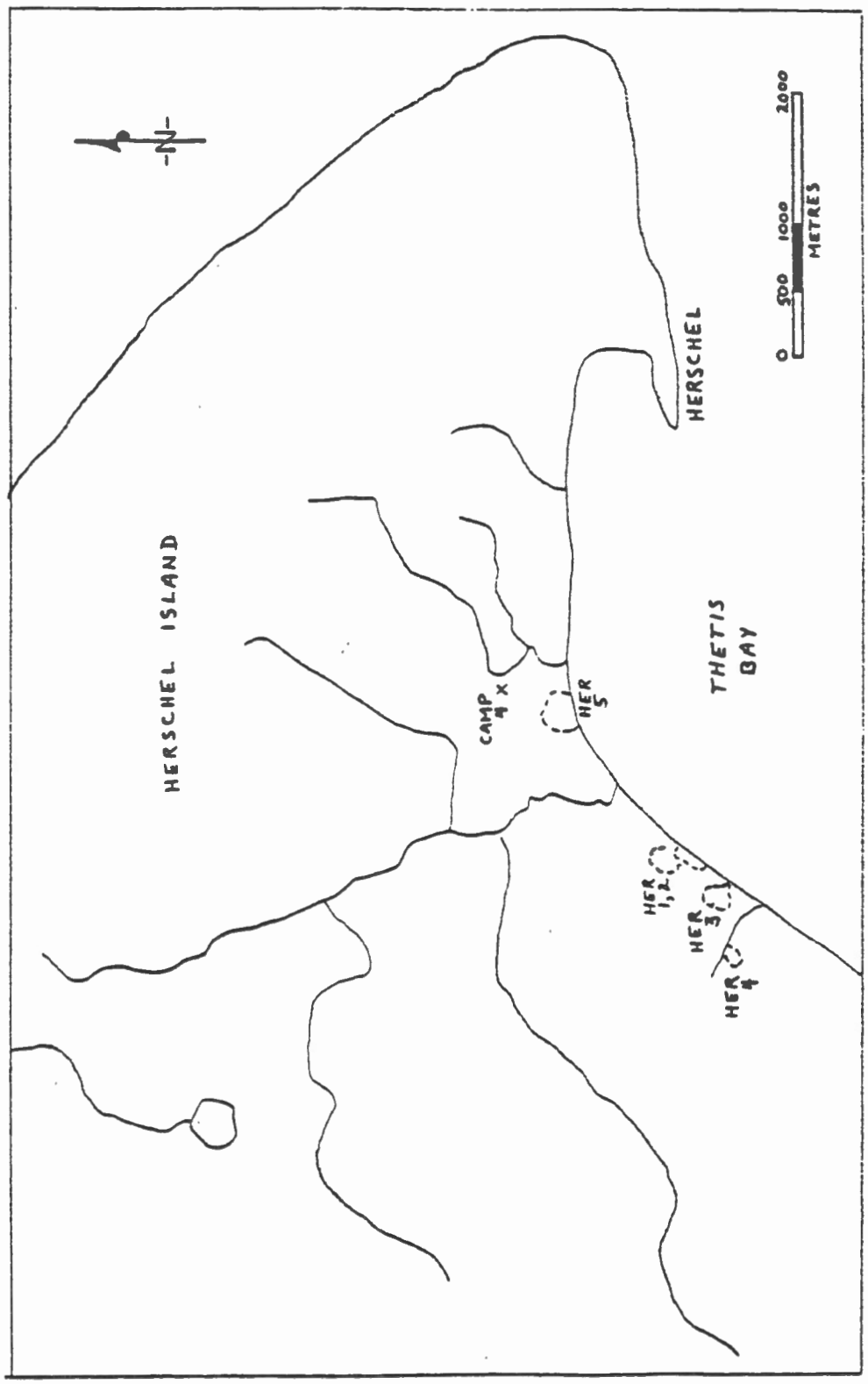

Figure 2.9 Location of study area thaw slides on Herschel Island.

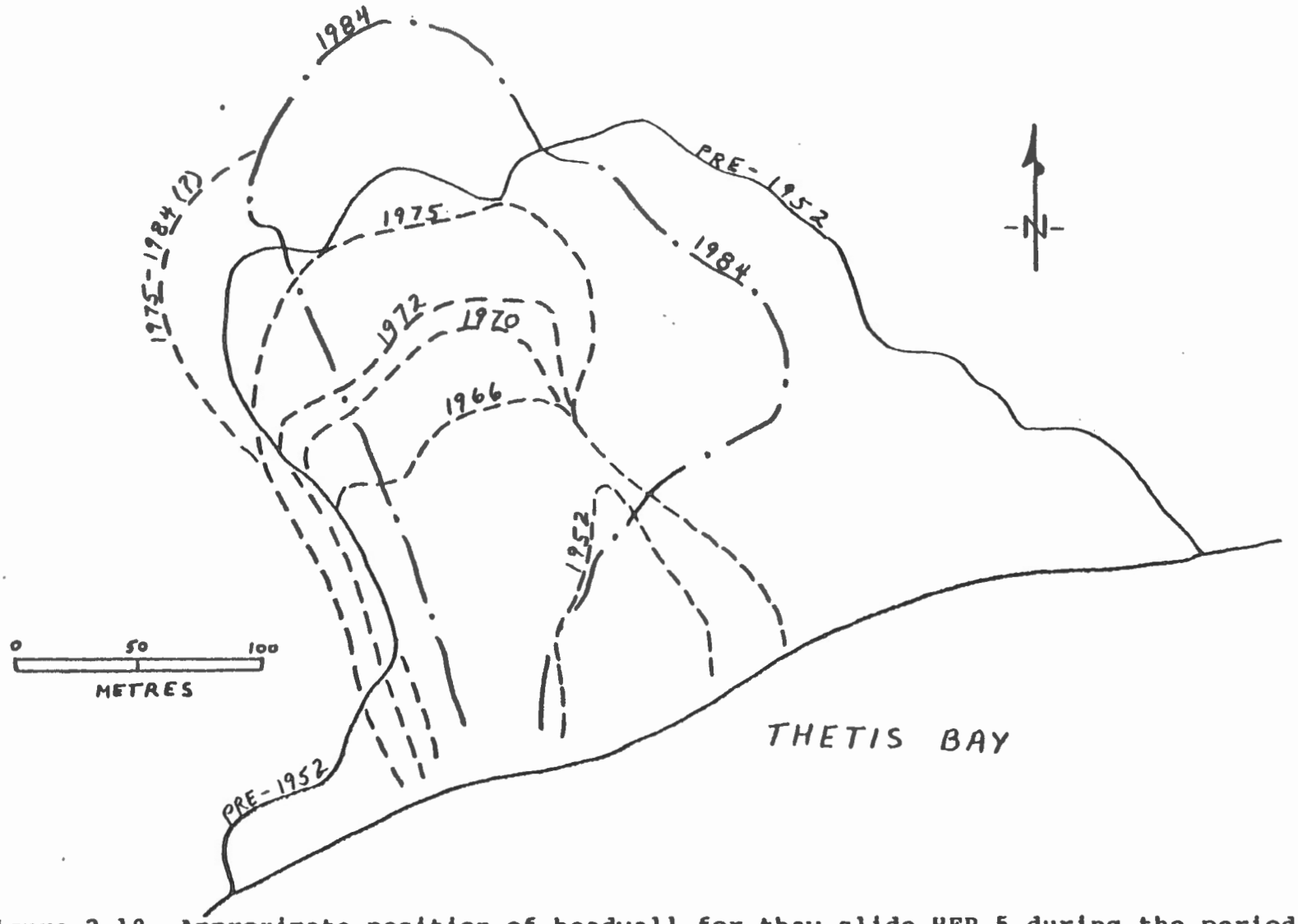

Figure 2.10 Approximate position of headwall for thaw slide HER 5 during the period 1952-84. Headwall positions are based on air photos for the years shown.

Work at the fourth thaw slide, HER 1 and 2, consisted of a 6.0 metre section of banded ice (HER 2) and a vertical and horizontal section of an ice wedge (HER 1), 22 metres to the east of HER 2. Several samples of ice-rich material adjacent to the ice wedge were also collected.

2.7.3 Stratigraphy

Detailed work on the stratigraphy of Herschel Island has been undertaken by Bouchard (1974). The stratigraphy is complex due to severe deformation, but appears to contain two marine silty clay units separated by a 'mixed' sediments unit containing silt, sand, gravel and organic layers. Covering the ground surface is a stoney clay silt containing boulders with exotic compositions.

In the vicinity of the thaw slides investigated during this study, modern organics were underlain by a stoney sand to clay-silt unit containing scattered organic fragments; stones ranged from pebble to cobble size and decreased in number with depth. Below this unit, banded ice-rich sediments in excess of 10 metres in thickness were exposed. The sediments varied from silty clay in most sections to medium sand in parts of HER 5. The sand-rich intervals contain less ice than other sediment types, which causes the formation of resistant rilled blocks. An extensive exposure of this material in the southwest portion of thaw slide HER 5 is believed to be responsible for the northward shift in headwall retreat since 1976 (see Figure 2.10).

The ice content of these banded sediments generally ranges from 40 to 100%, however, in some sediment-rich intervals the ice content can be as low as 10%. Bubbles in the ice are generally less than 1 mm in diameter and make up less than 15% of the ice volume. Bubble shapes are predominantly spherical but include flattened, tear, vertically elongated and ring types.

The banded ice-sediment unit is highly deformed with well-developed fold structures and occasional shear planes. The northeast and northwest walls of the largest thaw slide (HER 5) are shown schematically in Figure 2.11. Several tightly folded sequences visible in the figure contain axial planes which indicate that movement during deformation occurred approximately from the southeast toward the northwest.

Within the eastern most portion of Figure 2.11, the banded unit is overlain unconformably by a thin veneer of sediments up to 2 metres thick. The contact is a thaw unconformity formed during an earlier episode of retrogressive thaw slide activity (pre-1952). The depth of this thaw unconformity decreases to the northwest, toward the headwall of the earlier pre-1952 slide.

Beyond the edge of the earlier thaw slide, a considerably thicker sequence of sediments is exposed in the headwall. Due to the angle at which the section was photographed (from which Figure 2.11 is drawn), the height of the upper portion of the sequence is somewhat compressed.

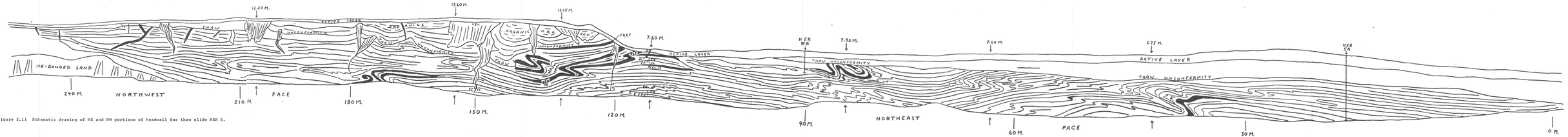

Figure 2.11 Schematic drawing of NE and NW portions of headwall for thaw slide HER 5.

Nevertheless, at least 3 generations of ice wedges and 2 thaw unconformities are well exposed. The two oldest sets of ice wedges penetrate much deeper and are thinner than the modern ice wedges. This is considered to reflect an extremely cold environment (glacial?) during their time of growth.

The oldest ice wedges are truncated by the deepest thaw unconformity. This thaw unconformity is believed to be related to ponding of water at the site and development of the thick surficial organic sequence visible in this part of the headwall (110 to 180 metre interval in Figure 2.11). One sample of wood fragments from these organics has been submitted for radiocarbon dating.

2.7.4 Isotopic Results

Oxygen isotope ratios have been measured for HER 3A, HER 4A to Q, HER 5A to U and several miscellaneous samples. All of these data are listed in Table 2.5.

The three precipitation samples all have $\delta^{18}O$ values which are slightly less negative than the average $\delta^{18}O$ values for Inuvik precipitation during this period. Although this may be due to variations in single precipitation events, it could also reflect a coastal influence. Collection of all precipitation for at least one year would be necessary before an unequivocal answer could be obtained.

Samples from several ice wedges and the upper permafrost zone were collected from the various thaw slides. $\delta^{18}O$ values for most of these samples are in the -18 to -21°/oo

Table 2.5 Isotope data for Herschel Island sites

Precipitation	$\delta^{18}O$ (°/oo SMOW)
15/07/84	-17.9
26/07/84	-13.1
27/07/84	-14.8
Sea Ice	-5.8

SECTION	DEPTH (CM)	TYPE OF MATERIAL	$\delta^{18}O$ (°/oo SMOW)
HER 3A	82-105	grey clay silt	-27.1
	105-111	" (brecciated)	-28.4
		Zero point for following samples from this section is at 111 cm depth which is the top of banded ice-clay silt material.	
	0-10	banded ice-sediment	-27.9
	10-20	"	-29.4
	20-30	"	-29.3
	30-40	"	-28.7
	40-50	"	-29.0
	50-60	"	-29.0
	60-70	"	-28.5
	70-80	"	-29.8
	80-90	"	-30.1
	90-100	"	-30.2
	100-110	"	-29.2
	110-120	"	-28.4
	120-130	"	-28.3
	130-140	"	-27.9
	140-150	"	-28.0
	150-160	"	-27.2
	160-170	"	-27.6
	170-180	"	-27.3
	180-190	"	-27.5
	190-200	"	-28.3
	200-210	"	-28.3
	210-220	"	-27.7
	220-230	"	-28.3
	230-240	"	-28.1
	240-250	"	-28.0
	250-260	"	-27.9
	260-270	"	-27.2
	270-280	"	-28.1
	280-290	"	-27.6

Table 2.5 Isotope data for Herschel Island sites (cont'd)

SECTION	DEPTH (CM)	TYPE OF MATERIAL	$\delta^{18}O$ (°/oo SMOW)
HER 3A	290-300	banded ice-sediment	-28.2
	300-310	"	-27.8
	310-320	"	-27.7
	320-330	"	-27.6
	330-340	"	-27.4
	340-350	"	-27.6
	350-360	"	-26.9
	360-370	"	-26.8
	370-380	"	-27.3
	380-390	"	-27.7
	390-400	"	-27.9
	400-410	"	-28.7
	410-420	"	-29.2
	420-430	"	-29.4
	430-440	"	-29.6
	440-450	"	-29.5
	450-460	"	-29.5
	460-470	"	-28.8
	470-480	"	-29.2
	480-490	"	-29.5
	490-500	"	-27.5
	500-510	"	-27.4
	510-520	"	-27.2
	520-530	"	-27.2
	530-540	"	-26.6
	540-550	"	-27.1
	550-560	"	-27.2
	560-570	"	-27.3
	570-580	"	-27.1
	580-590	"	-28.3
	590-600	"	-28.1
	600-610	"	-28.1
	610-620	"	-28.3
	620-630	"	-29.2
	630-640	"	-29.2
	640-650	"	-29.1
	650-660	"	-29.1
	660-670	"	-28.7
	670-680	"	-28.1
	680-690	"	-28.8
	690-700	"	-28.7

Table 2.5 Isotope data for Herschel Island sites (cont'd)

SECTION	SAMPLE	DEPTH (CM)	TYPE OF MATERIAL	$\delta^{18}O$ (°/oo SMOW)
HER 4	A	40-50	ice wedge	-21.3
	B	75	"	-20.8
	C	75	"	-21.1
	D	75	"	-22.4
	E	75	"	-21.7
	F Right	360	"	-22.0
	F Left	360	"	-23.7
	F Centre	360	"	-22.5
	F Oblique	360	"	-22.1
	G	200	ice & clay silt	-23.7
	H	300	" (& pebbles)	-24.6
	I	410	ice	-33.2
	J	480	"	-35.2
	K	540	"	-33.7
	L	600	silty sand & ice	-33.4
	M	700	"	-30.6
	N	~120	ice wedge	-23.7
	O	~200	"	-18.5
	P	260	peat	-19.6
	Q	~ 60	"	-18.7

SECTION	DEPTH (CM)	TYPE OF MATERIAL	$\delta^{18}O$ (°/oo SMOW)
HER 5A	Zero point is at base of unfrozen ground (50 cm thick)		
	0-10	stoney silty clay & ice	-18.7
	10-20	"	-18.4
	20-30	"	-18.7
	30-40	"	-18.6
	40-50	"	-18.7
	50-60	"	-19.3
	60-70	"	-20.1
	70-80	"	
	80-90	"	-21.8
	90-100	"	-23.2
	100-110	"	-25.6
	110-120	"	-25.7
	120-130	"	-24.4
	130-140	"	-25.9
	140-150	"	-27.3

Table 2.5 Isotope data for Herschel Island sites (cont'd)

SECTION	DEPTH (CM)	TYPE OF MATERIAL	$\delta^{18}O$ (°/oo SMOW)
HER 5A	150-160	banded sediment & ice	-27.5
	160-170	"	-28.2
	170-180	"	-27.9
	180-190	"	-28.3
	190-200	"	-28.7
	200-210	"	-28.6
	210-220	"	-29.4
	220-230	"	-29.6
	230-240	"	-30.4
	240-250	"	-30.4
	250-260	"	-29.6
	260-270	"	-29.5
	270-280	"	-29.6
	280-290	"	-28.6
	290-300	"	-29.1
	300-310	"	-29.5
	310-320	"	-29.5
	320-330	"	-29.6
	330-340	"	-29.2
	340-350	banded ice & sediment	-29.8
	350-360	"	-30.6
	360-370	"	-30.1
	370-380	"	-30.7
	380-390	"	-31.3
	390-400	"	-32.1

SECTION	DEPTH (CM)	TYPE OF MATERIAL	$\delta^{18}O$ (°/oo SMOW)
HER 5B	Zero point is at base of unfrozen ground (65 cm thick)		
	0-10	silty clay & ice	
	10-20	"	-19.6
	20-30	"	-20.2
	30-40	"	
	40-50	"	
	50-60	"	-24.2
	60-70	"	
	70-80	banded ice	-29.4
	80-90	"	-27.9
	90-95	"	-28.1
	95-100	"	-28.3

Table 2.5 Isotope data for Herschel Island sites (cont'd)

SECTION	DEPTH (CM)	TYPE OF MATERIAL	$\delta^{18}O$ (°/oo SMOW)
HER 5B	100-110	ice	-28.4
	110-120	"	-28.7
	120-130	"	-29.9
	130-140	"	-29.9
	140-150	"	-29.9
	150-160	"	-29.9
	160-170	"	-29.7
	170-180	"	-29.7
	180-190	"	-28.9
	190-200	"	-27.0
	200-210	banded sediment & ice	-26.0
	210-220	"	-26.5
	220-230	"	-27.0
	230-240	"	-26.6

SECTION	SAMPLE NUMBER	TYPE OF MATERIAL	$\delta^{18}O$ (°/oo SMOW)
HER 5 GRAB SAMPLES	C	ice	-29.7
	D	ice & minor sandy silt	-25.4
	E	ice (adjacent to D)	-26.2
	F	ice & sandy silt (adjacent to E)	-26.1
	G	clay silt & ice	-30.9
	H	ice	-29.1
	I	sand (below H)	-28.0
	J	ice (below I)	-28.3
	K	sand (below J)	-28.3
	L	ice (depth 265 cm)	-28.9
	M	ice (30 cm below L)	-31.8
	N	ice & sandy silt (depth 560 cm)	-27.7
	O	clay silt (100 cm below N)	-28.3
	P	ice & clay silt (50 cm below O)	-31.6
	Q	ice (same as C)	-31.2
	R	ice (adjacent to Q)	-29.6
	S	ice wedge (depth 1200 cm)	-27.9
	T	sand (adjacent to S)	-27.1
	U	ice wedge (depth 70 cm)	-20.4

range. Ice wedges exposed at HER 4 have $\delta^{18}O$ values which vary from -18.5°/oo, for a small very young wedge, to -23.7°/oo, for an adjacent larger ice wedge. At HER 5, a basal sample from one of the deeply penetrating second generation ice wedges (HER 5S) yielded a $\delta^{18}O$ value of -27.9°/oo, which is considerably more negative than currently active ice wedges. Further systematic sampling of ice wedges of different ages is required before the significance of this one value can be determined.

The isotopic composition of the banded ice-sediment material is considerably different than the upper permafrost zone. Oxygen-18 concentrations as low as -35.2°/oo have been determined for banded ice exposed in thaw slide HER 4, which is stratigraphically the highest of all the thaw slide exposures. Figure 2.12, a sketch of the HER 4 exposure (SE wall), shows the large difference in isotope composition between proximal ice-wedge ice and banded massive ice. The massive ice is folded, with the trace of the axial plane nearly parallel to the upper and lower contacts of the unit. The lower contact of the ice and underlying ice-rich sediment coincides with a shear plane. Above the massive ice, the sediment-rich ice (20 to 50% silty clay sediment) is not part of the banded sequence.

The rapid shift in isotope composition between the upper permafrost sediments and the banded ice is clearly evident in Figures 2.13 and 2.14; sections 5A and 5B. In sections 5A and 5B, the top of the banded ice unit is 2.0 and 1.35

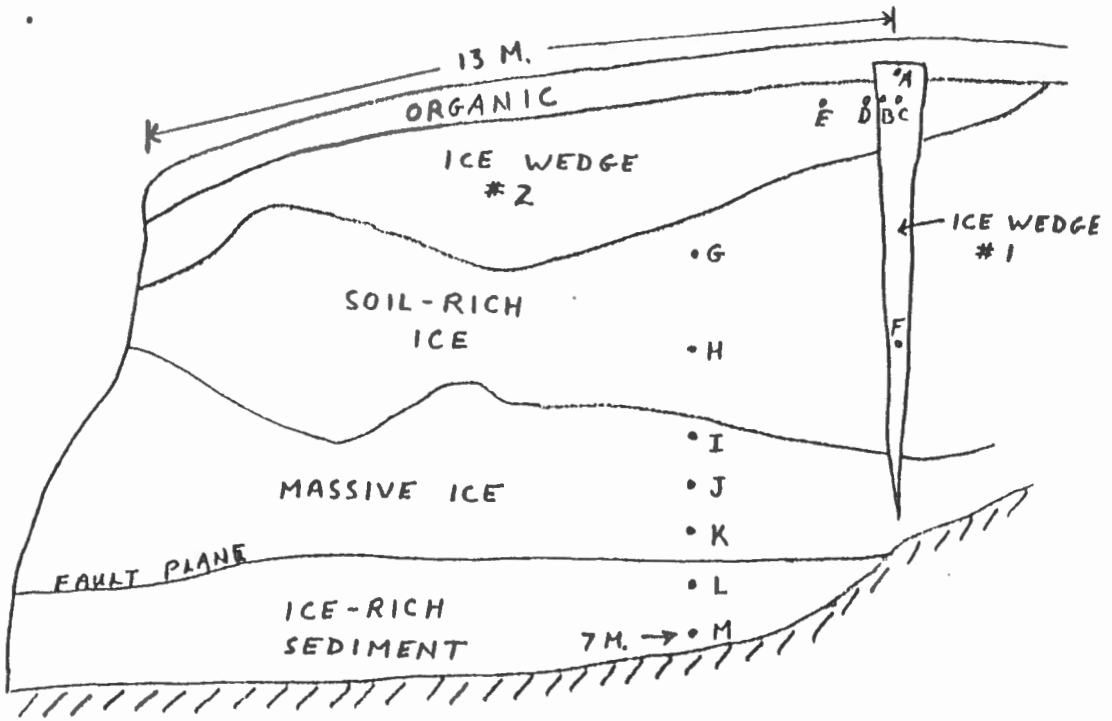

Figure 2.12 Schematic drawing of SE portion of headwall for thaw slide HER 4.

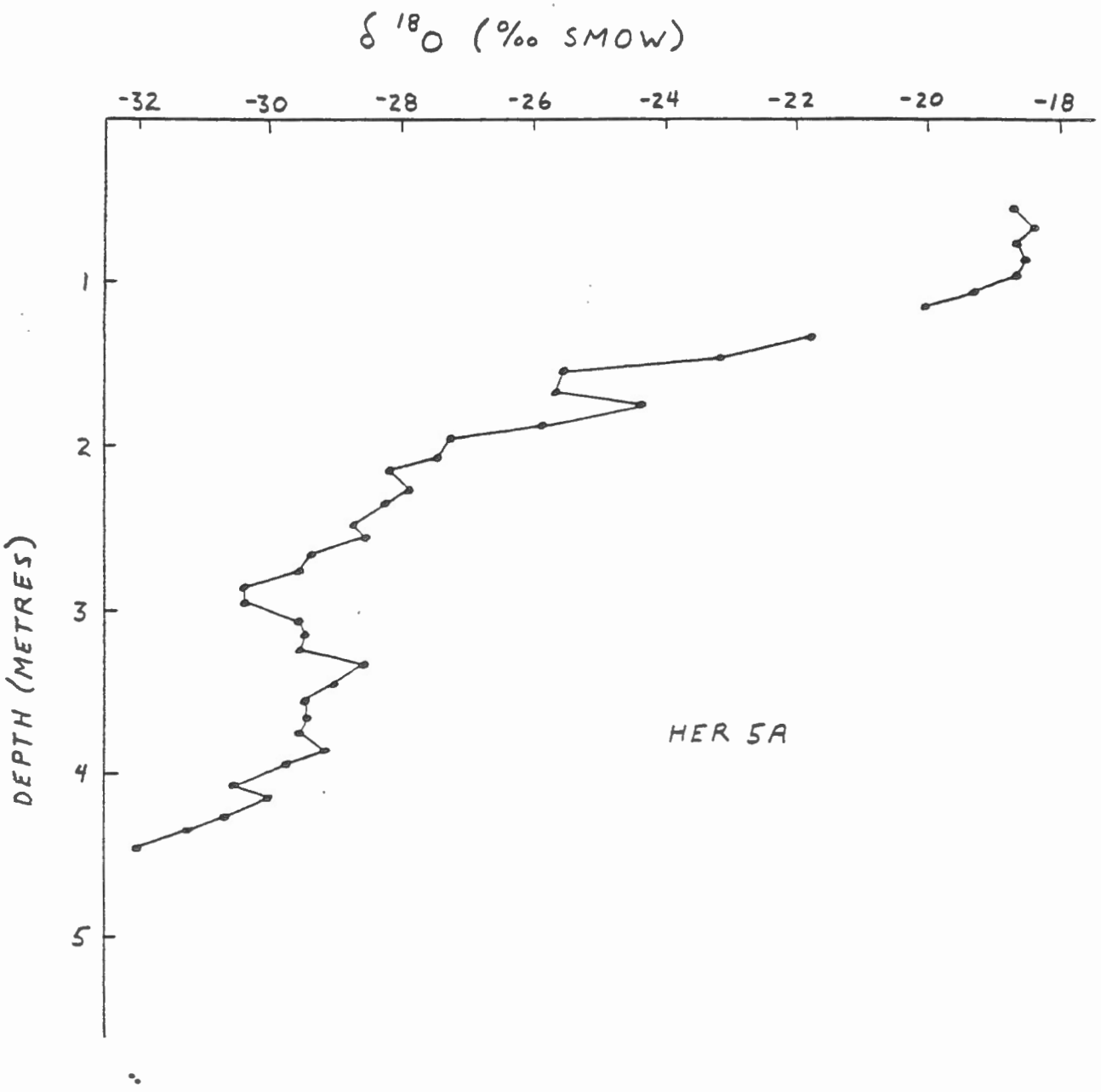

Figure 2.13 Variation in ^{18}O content with depth for section HER 5A.

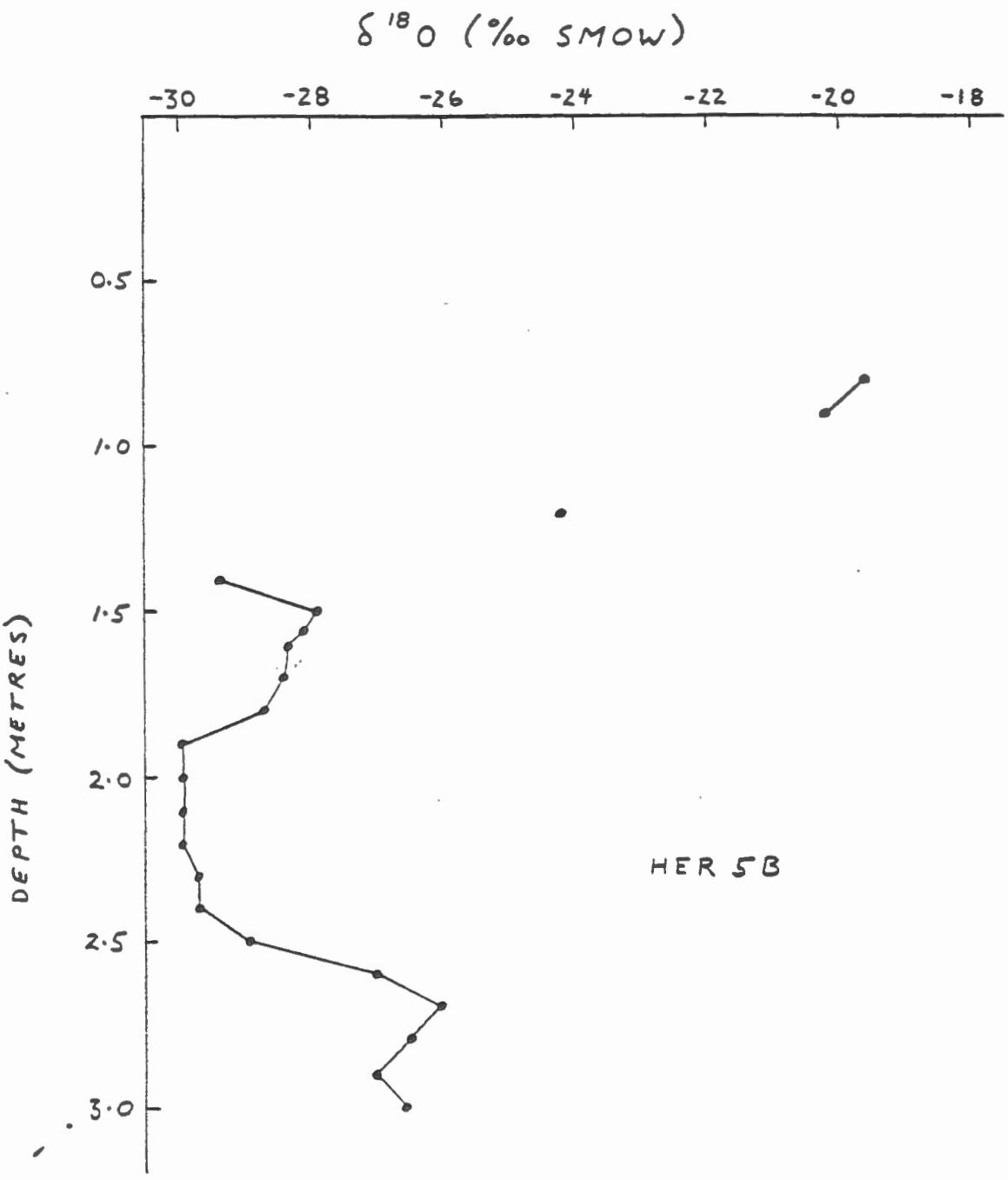

Figure 2.14 Variation in ^{18}O content with depth for section HER 5B.

metres, respectively, below surface. As noted earlier, ice lenses in the uppermost permafrost have $\delta^{18}O$ values in the -18 to -21°/oo range. With increasing depth, the $\delta^{18}O$ values within the clayey silt sediments approach those of the banded ice; -27 to -32°/oo.

Within the banded ice, the oxygen isotope composition oscillates systematically with an amplitude of 2 to 4°/oo. The oscillations are similar to the ^{18}O profile determined for banded ice exposed at the King Point thaw slide (Figure 2.7). These oscillations are interpreted as representing seasonal variations preserved in buried glacier ice.

The repetitiveness of these oscillations is best displayed in section HER 3A (Figure 2.15). In the 7 metres of banded ice sampled, there are six oscillations visible. The variation in magnitude of the $\delta^{18}O$ values ranges from 1 to 3°/oo.

The pattern of isotope variations present in this profile is completely different from those for closed system freezing of a confined reservoir (North Fork Pass frost blister, see section 3.4), segregated ice (Sabine Point), or ice-wedge ice (Illisarvik and Eagle River). There is a vague similarity to multiple injection ice, such as for a pingo, however, the differences are much greater.

Comparison of the ^{18}O profile in Figure 2.15 with a typical ^{18}O profile for a portion of the Camp Century, Greenland ice cap core (Figure 2.16) reveals a striking similarity. On the basis of this similarity in ^{18}O profiles,

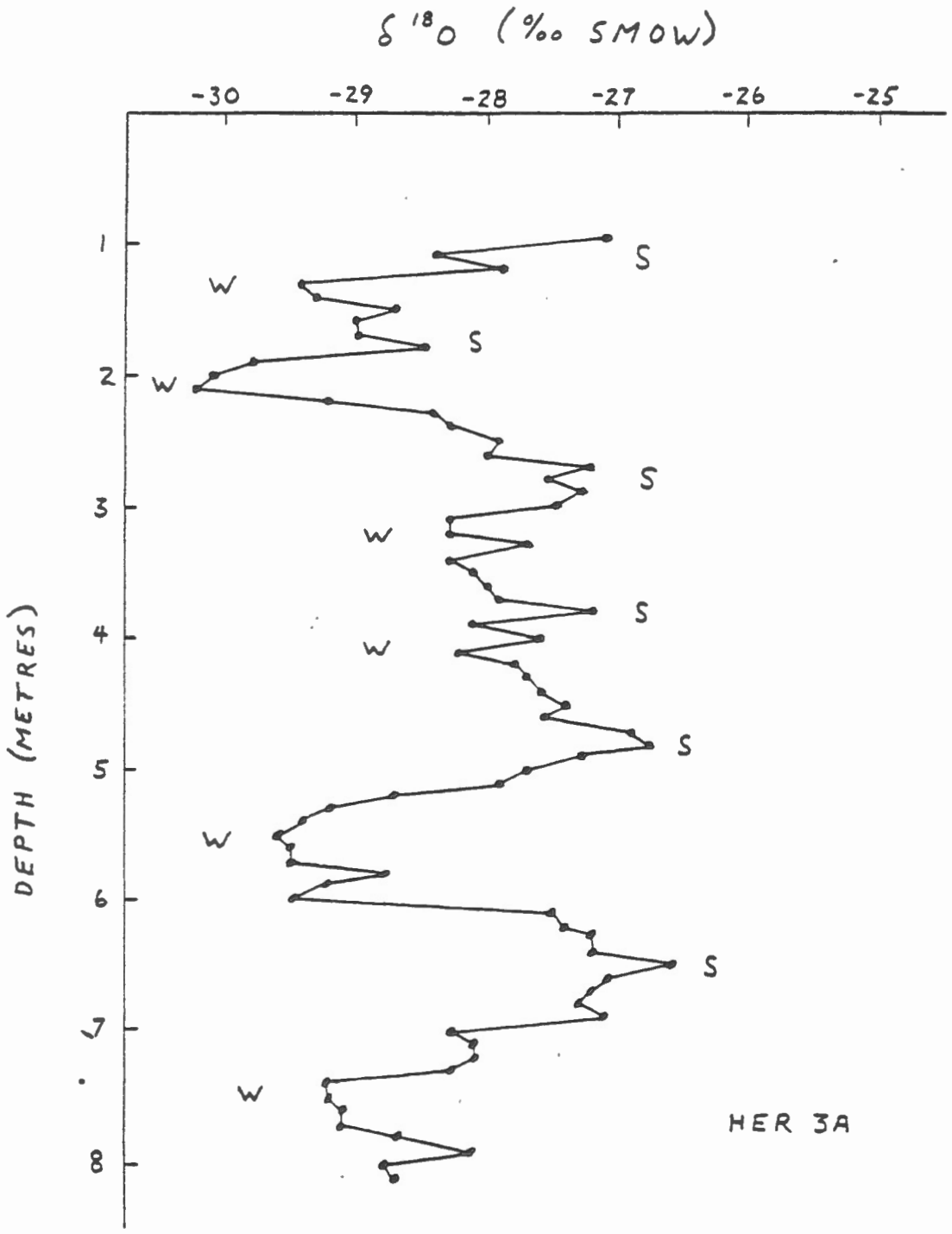

Figure 2.15 Variation in ^{18}O content with depth for section HER 3A. S=summer, w=winter.

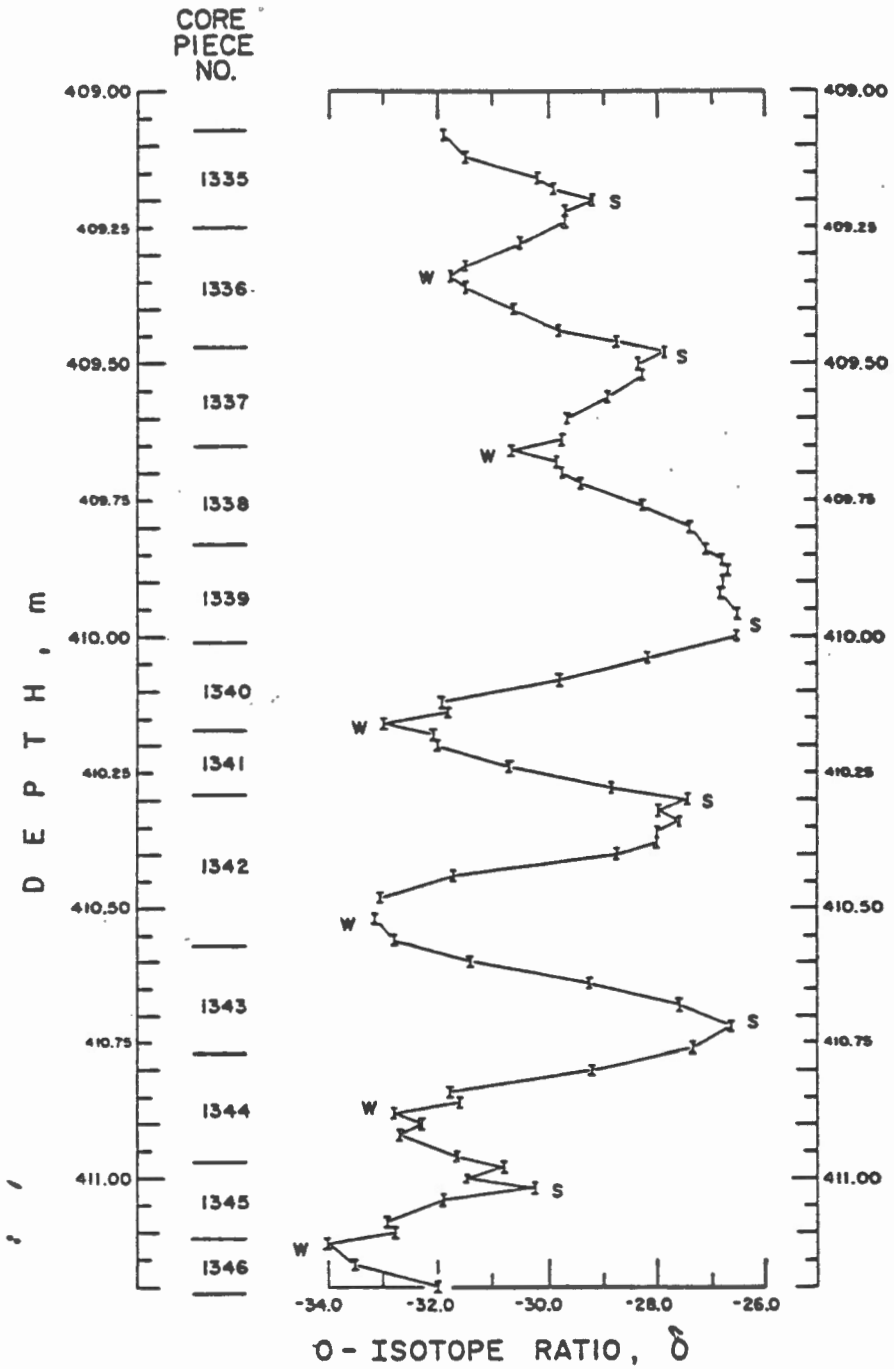

Figure 2.16 Variation in ^{18}O content with depth for Greenland ice core, 490 to 411 metre interval. (from Figure 8 of Langway 1970).

bubble content and modern glacier ice characteristics, this banded ice-sediment unit is interpreted as buried glacier ice. This ice is most likely from the basal portion of the ice sheet, probably within 100 metres of the bottom.

According to Rampton (1982), Herschel Island was last glaciated during or prior to the early Wisconsinan. This would suggest that the ice exposed in the thaw slides is at least of early Wisconsinan age. All deformation structures present in the banded unit are considered to have formed as the ice sheet was advancing. Preliminary structural data on the axial planes of folds and the orientation of shear planes indicate movement of the ice sheet from the southeast toward the northwest. At present, the aerial extent of this ice unit is unknown. However, the similarity in ^{18}O profiles with banded ice at the King Point thaw slide and the occurrence of banded ice in thaw slides near Kay Point suggest that it may originally have been very extensive.

Burial of detached ice blocks is known to occur in the end moraines of glaciers (see Hambrey 1984). Subsequent melting under a moderating climate is thought to lead to the formation of kettle lakes. In a cold polar climate, ablation of the upper ice sheet may lead to an accumulation of debris (ablation till) burying the basal ice. With the maintenance of extremely low air temperatures, permafrost conditions would develop and help to preserve the buried ice.

The preservation of seasonal isotope variations in this ice, plus bubble characteristics, suggest that the thickness of the ice sheet was no more than a few hundred metres thick and possibly much less. Isotope diffusion over time has probably reduced the magnitude of seasonal variations in the ^{18}O profile. Nevertheless, the average ^{18}O composition of the banded ice samples collected is approximately -28 ± 1°/oo, which suggests formation under significantly colder climatic conditions than currently exist.

3. CENTRAL YUKON

3.1 Introduction

On the basis of borehole logs provided by Foothills Pipe Lines (Yukon) Ltd. (1978), two sites were chosen for investigation in 1983 along the Dempster Highway. These sites, located in Figure 3.1 as the Ogilvie River and Eagle River sites, represent very different settings in terms of topography, geomorphology and Quaternary history. In addition, isotopic investigations have been conducted on frost blisters in North Fork Pass, ice-rich sediments exposed in Klondike placer operations near Dawson and ice-rich glaciolacustrine sediments near Mayo.

3.2 Ogilvie River Site

3.2.1 Site Description

The drill site is located on a colluvial terrace overlooking the Ogilvie River. The terrace, which is easily recognizable on air photographs, is buttressed by pillars of limestone bedrock adjacent to the side of the river. Bedrock is also exposed on the mountainside above the terrace. The terrace slopes southwest toward the river with a gradient of

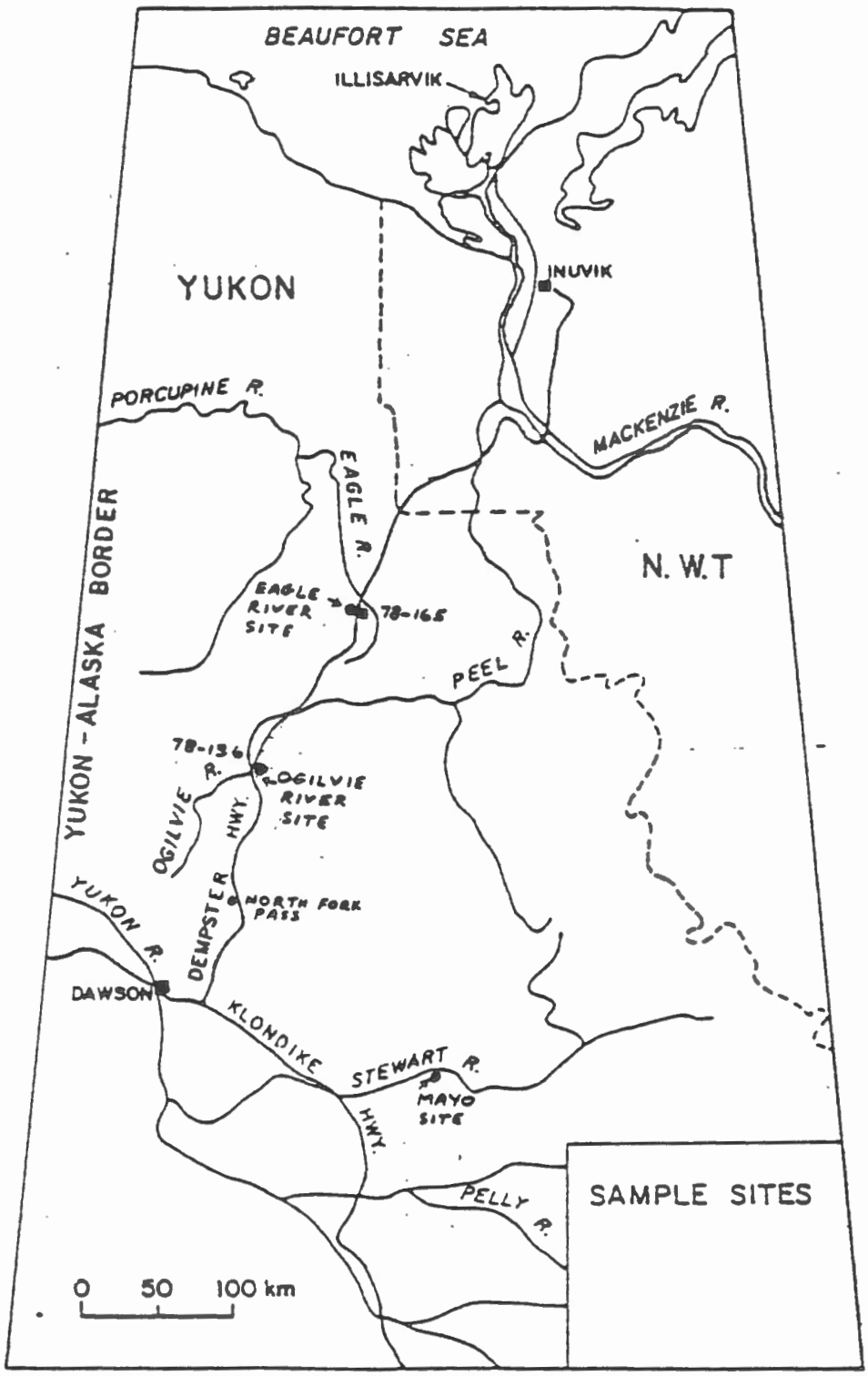

Figure 3.1 Location map of study sites along the Dempster Highway.

5 to 8%. Vegetation consists of black spruce 4 to 12 metres tall and a ground cover of moss and peat hummocks. The centre of the terrace was cleared of all trees during the Foothills' program when hole 78-136 was drilled. The exact location of this borehole within the clearing could not be determined.

3.2.2 Work Completed

Drilling at this site proved to be more difficult than expected. As a result of the numerous stones encountered, a single hole 3.3 metres deep was drilled. Upon reaching this depth, a rod sheared and the core barrel and lower two metres of rod were lost. To continue with the program it was decided to recover the lost drilling equipment by digging a pit. This pit required three days to excavate, but provided a much clearer picture of the stratigraphic complexities at this site. It was necessary to sink the pit the full 3.3 metres in order to recover the core barrel. Groundwater seepage (a spring) entering the river was located and sampled at the base of the terrace.

3.2.3 Stratigraphy

Although it was impossible to locate the exact position of 78-136, it is believed that borehole O.R. 83-1 was within

5 to 10 metres of the original borehole. The log for 78-136 (Figure 3.2) indicates that the site contains organic silt with massive ice 0.5 to 3.5 metres thick. In addition, there were sand and "gravel pockets" containing some fine to medium gravel within the organic silt units. The first massive ice zone was encountered at a depth of 2.4 metres.

In contrast, the log for borehole O.R. 83-1 (Figure 3.2) describes sandy silt containing large quantities of medium to coarse-grained gravel. The gravel consists of broken limestone fragments up to 5 cm in length. Only a minor amount of massive ice was encountered in the 3.3 metres drilled.

During excavation of the pit, the gravel was found to be subangular limestone blocks up to 30 cm in diameter which had been broken into finer material during the drilling operation. In the excavation, a rock-debris wedge was exposed which started at the base of the active layer and widened with depth. At a depth of 2.5 metres the pit was entirely within the rock-debris wedge (Figure 3.3). Adjacent to the rock-debris wedge was ice-rich material that may correspond to some of the massive ice reported in 78-136.

Comparison of the logs for 78-136 and O.R. 83-1 with the stratigraphy exposed in the pit clearly demonstrates that the massive ice is not a simple tabular body. The ice-rich material is of very local extent and it is impossible to

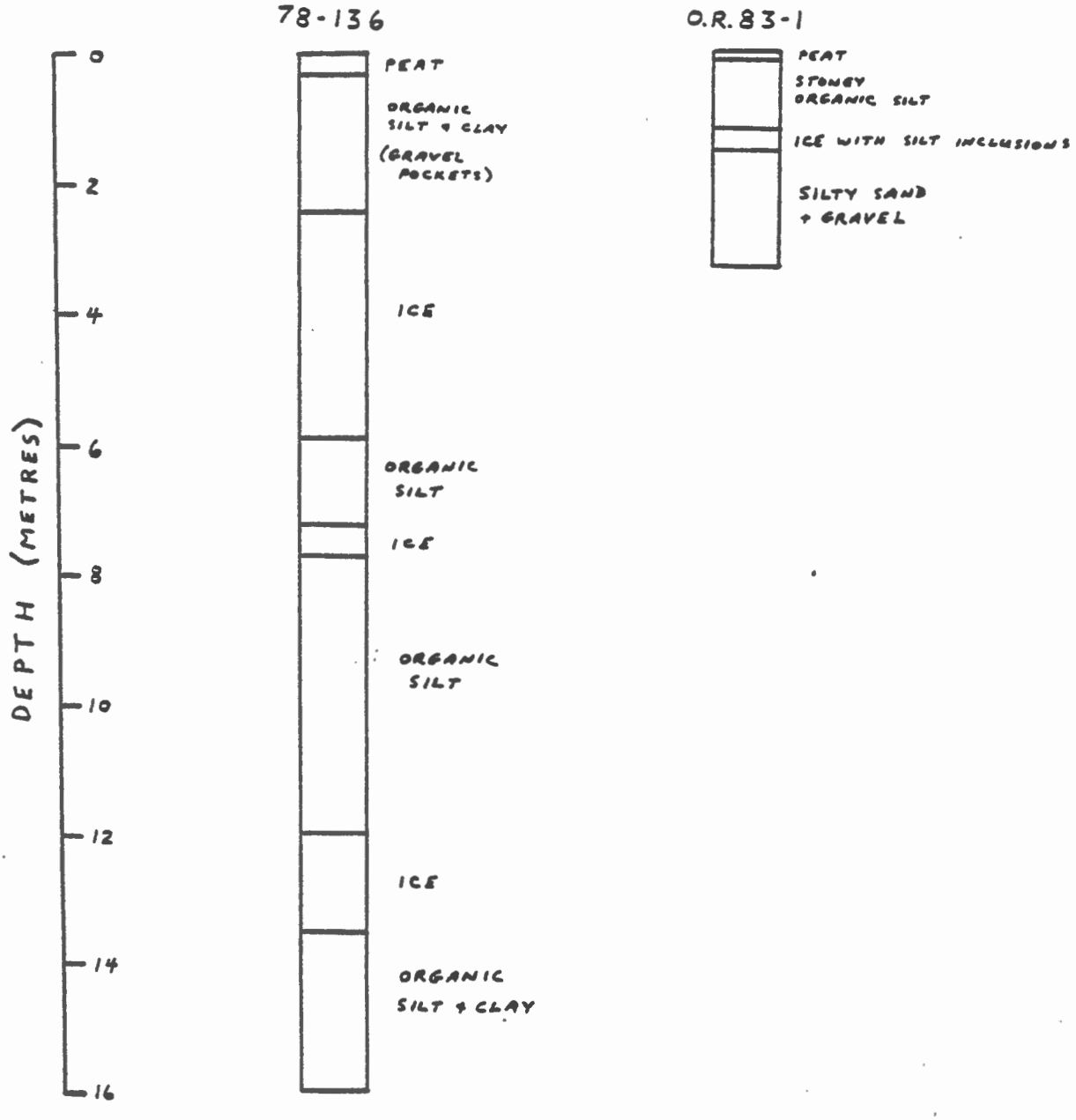

Figure 3.2. Borehole logs for O.R. 83-1 and Foothills' 78-136. In O.R. 83-1 the gravel is actually limestone talus blocks. Boreholes are approximately 5 to 10 metres apart.

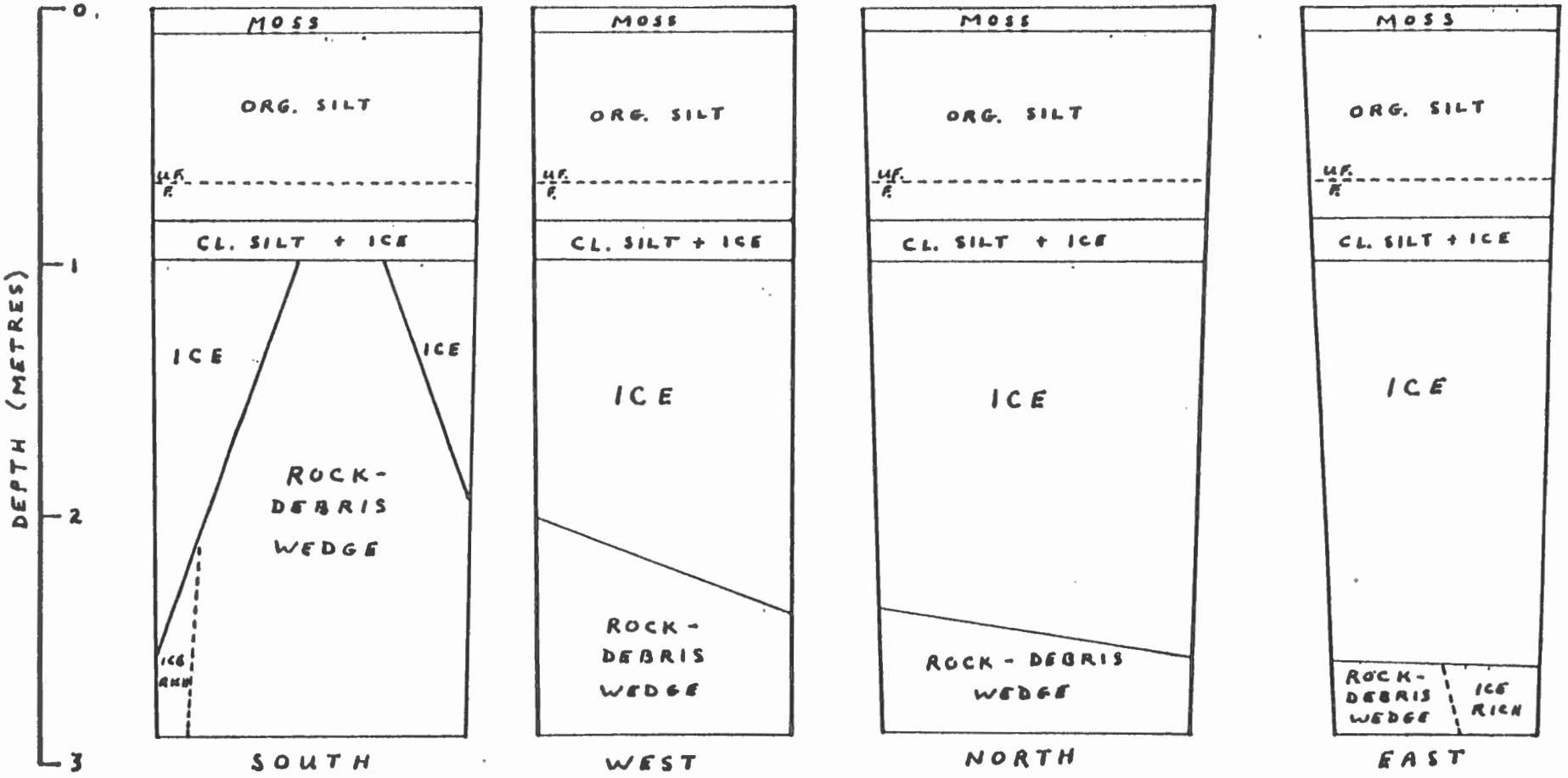

Figure 3.3. Stratigraphy exposed in pit at O.R. 83-1 site. Bottom 40 cm of pit filled with mud. Directions refer to pit wall. UF./F. = unfrozen - frozen boundary.

predict where the ice will occur. Therefore, single boreholes such as 78-136 cannot be expected to accurately reflect the ground-ice conditions for the terrace area.

3.2.4 Isotopic Results

Continuous channel samples (19 in all) were collected in 10 cm intervals from the ice face of the eastern pit wall, while a single sample of water from the floor of the pit was also collected. In addition, core material was subsampled and packaged in the field. Isotopic results are tabulated in Table 3.1.

Groundwater discharging from the spring at the base of the terrace is modern unaltered precipitation. With a tritium concentration of 140 T.U., this groundwater was recharged less than 20 years ago. Since groundwaters are usually isotopically representative of average annual precipitation, this sample can be used for comparison with the isotopic composition of ground ice samples. Water collected from the pit floor is a mixture of active layer water and melting ground ice, and thus has a composition intermediate to the spring water and the ground ice.

The ground ice can be subdivided into two types; massive ice and ice in ice-rich sediments. Ice contained within the sand and gravel (talus) has δ^2H values between -201 and -212 °/oo, which is on average, 40 °/oo more negative than the modern groundwater. Since the ice is segregational, it

Table 3.1 Isotope data for Ogilvie River site

	DEPTH (CM)	TYPE OF MATERIAL	$\delta^{18}O$ (°/oo SMOW)
Borehole O.R. 83-1			
	90-100	stoney silt	-195
	117-130	ice	-213
	137-145	ice	-218
	145-150	sand & gravel	-212
	155-165	"	-209
	170-180	"	-210
	190-197	"	-207
	212-220	"	-206
	240-250	"	-201
	250-260	"	-206
	270-279	"	-202
	297-305	"	-203
	312-325	"	-202

	SAMPLE NUMBER	TYPE OF MATERIAL	$\delta^{2}H$ (°/oo SMOW)
Pit O.R. 83-1			
	1	ice	-218
	5	ice	-218
	10	ice	-216
	15	ice	-216
	18	ice & rock	-208
	20	pit water	-185

	$\delta^{18}O$ (°/oo SMOW)	$\delta^{2}H$ (°/oo SMOW)	^{3}H (T.U.)
O.R. 83-1 Spring	-22.3	-165	140

represents an average groundwater composition different than today and probably reflects recharge during a period of colder climatic conditions.

The massive ice is bubble-rich with large spherical to vertically elongate bubbles 2 to 3 mm in diameter. No fabric, other than vertical bubble trains, was noted in the ice. Isotopically, the massive ice is more negative ($\delta^{2}H$ = -216 to 218 °/oo) than the talus ice, which suggests a different water source for each ice type. The geometry of the 'rock wedge', as shown in Figure 3.3, suggests that the massive ice may be ice-wedge ice. Such an interpretation is consistent with the isotope data since ice wedges are formed from snow melt, which has a lower heavy isotope concentration than the average annual precipitation. Thus, both ice types may have formed at approximately the same time, with the massive ice representing selective recharge of snow melt water. There is no evidence to suggest that ice wedges are currently forming at the site.

3.3 Eagle River Site

3.3.1 Site Description

The Eagle River site is located on the Eagle Plain between the Richardson and Ogilvie Mountains. The Eagle Plain was not glaciated during the late Wisconsinan, however, the Eagle River did serve as a major glacial spillway. The area of interest is a 2 kilometre section of the Dempster Highway between 2 and 4 kilometres south of the Eagle River

crossing. This section of the highway is situated on a high-level terrace overlooking the river which is 80 to 100 metres below in the valley. Due to the fine-grained sediments present on the terrace, Harris et al. (1983) have suggested that glacial-lake waters were impounded in the area during late Pleistocene time.

A series of boreholes was drilled along this section of the highway during the construction period (Johnston 1980). Between KM 368 and 370 the terrace was found to be underlain by ice-rich organic silt and clay containing massive ice. The thickness of massive ice encountered during drilling ranged from not present to approximately 6.5 metres. Six of the nine holes were terminated in the ice. In addition to these nine holes, Foothills drilled one hole (78-165) on the opposite side of the roadway and encountered 0.55 metres of ice.

3.3.2 Work Completed

From the logs available for the original drill program, it was decided to drill one hole at each end of the ice-rich section (Figure 3.4). The first borehole, ER 83-1, was situated 6 metres from the original borehole #2 where 6.5 metres of massive ice was encountered. A total depth of 8.05 metres was attained at this location for ER 83-1. The second borehole was sited 600 metres further south near the original borehole #8. A depth of 5.75 metres was attained before shearing of a rod forced abandonment of this borehole and

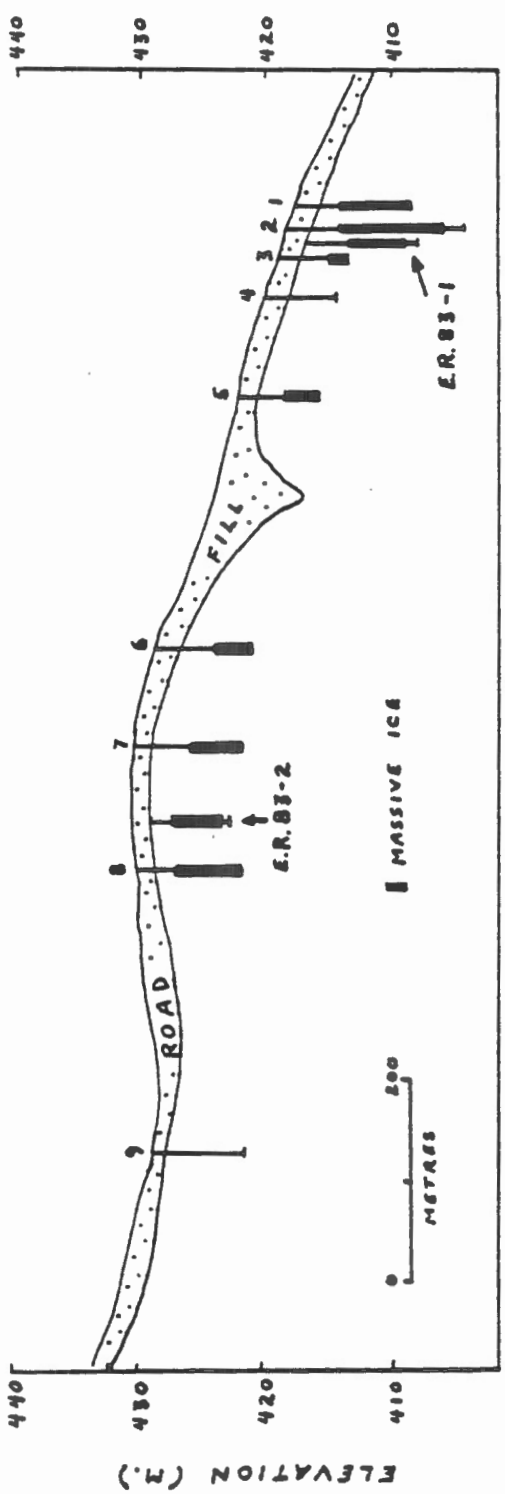

Figure 3.4. Surficial deposits underlying Dempster Highway, KM 368-370, near Eagle River bridge. Modified after Harris et al. 1983. (Source: G.H. Johnston, Division of Building Research, National Research Council of Canada, Ottawa)

termination of the drilling program for the 1983 field season. Continuous core was recovered from both holes. In addition, material has been made available from Foothills Pipe Lines (Yukon) Ltd. (1978) for borehole 78-165.

3.3.3 Stratigraphy

Massive ice was encountered in both of the boreholes drilled during the program, however, the thickness of ice present does not agree with the reported thicknesses in the original program. This was especially noteable in ER 83-1 where the top of the ice was at a greater depth than anticipated (3.05 metres) and the total thickness was only 60% of that expected on the basis of the original borehole #2. This indicates that either the ice occurs as very localized lenticular masses, with large variations in thickness over short distances, or there is some error in the originally reported thicknesses because the stratigraphy was based on flight auger cuttings. In the latter instance, ice-rich sediments may in fact appear as massive ice when viewed as cuttings.

Evidence to support the former hypothesis can be found in the actual variations in ice thickness reported for these two boreholes and the reported variations between other boreholes in the section drilled using the same technique. From the original drilling program, borehole #8 encountered approximately 5 metres of massive ice while at borehole #9, 200 metres away, there was no massive ice reported. Within

the middle of the section, borehole #2 encountered approximately 6.5 metres, borehole #3 (80 metres away) 1.5 metres and borehole #4 (140 metres beyond #3) encountered no massive ice. In addition, at Foothills' borehole 78-165 only 0.55 metres of ice was reported.

Borehole ER 83-1 encountered 4 metres of massive ice (3.05 to 7.05 metres) containing 1 to 3 mm diameter bubbles (20 to 30% of volume) and thin silt bands, both of which were vertically oriented. Above the massive ice, horizontal to sub-horizontal ice lenses, 1 to 5 mm thick, occur within a brown sandy silt and constitute 50 to 70% of the total volume. Below the massive ice, the brown sandy silt changes to a grey clayey silt with horizontal ice lenses 1 to 15 mm thick. Ice content decreases from 70% immediately below the massive ice to less than 10% at the bottom of the core.

In borehole ER 83-2, a total of 3.1 metres of massive ice was recovered. Throughout the ice interval (2.3 to 5.4 metres), vertically oriented silt bands and large 2 to 3 mm air bubbles were noted. The bubbles often represented 20 to 30% of the sample volume and elongate bubbles were oriented either vertically or inclined toward the horizontal. At the bottom of the ice zone, the ice formed a steeply dipping contact with the enclosing sandy silt, which was well-oxidized. Ice lenses 1 mm thick were oriented parallel to this contact.

3.3.4 Isotopic Results

Selected samples from both ER 83-1 and ER 83-2 have been analysed for their oxygen and/or hydrogen isotope ratios. These data are listed in Table 3.2.

The original isotope data (oxygen ratios) for this locality were measured on samples from borehole DH 78-165, which was drilled by Foothills Pipe Lines (Yukon) Ltd. in 1978 (Michel 1983). As noted earlier, borehole 78-165 encountered only 0.55 metres of massive ice within a 9.5 metre thick organic silt unit. Although no samples of the ice were available for analysis, it can be seen in Figure 3.5 that the ice separates isotopically distinct sections of the organic silt. Above the ice layer, the ^{18}O concentration (-22.5 °/oo) is within the range of modern precipitation and shallow permafrost waters. Below the ice layer, the ^{18}O concentrations (-26.0 to -27.3 °/oo) are considerably more negative than the upper unit. Throughout the lower unit the range in $\delta^{18}O$ values remains small.

In boreholes ER 83-1 and ER 83-2 (Figure 3.6), the organic silts overlying the massive ice have $\delta^{18}O$ values which are similar to the upper silt of 78-165, as well as modern precipitation and shallow permafrost in the central Yukon (-20 to -23 °/oo). Within the massive ice, the $\delta^{18}O$ values shift to -30 °/oo, which is 3 to 4 °/oo more negative than the lower organic silt unit of 78-165. There are no isotope data for the ice unit encountered in 78-165, however, it is possible that this ice would have an isotopic

Table 3.2 Isotope data for Eagle River site

	DEPTH (CM)	TYPE OF MATERIAL	$\delta^{18}O$ (°/oo SMOW)	$\delta^{2}H$ (°/oo SMOW)
ER 83-1	65-73	organic silt		-160
	81-90	"		-162
	99-108	"	-20.2	-161
	115-122	ice & org. silt		-162
	130-140	clay silt		-164
	150-155	ice & clay silt		-164
	163-171	ice & sandy silt	-22.6	-170
	180-190	"		-176
	200-210	sandy silt		-183
	220-230	"	-24.0	-191
	247-255	"		-201
	255-263	"		-201
	303-308	ice	-27.2	-212
	317-324	"	-27.7	-227
	332-340	"		-231
	350-360	"		-233
	368-375	"		-234
	383-390	"		-232
	400-410	"		-234
	420-430	"	-30.1	-236
	440-445	"		-234
	445-465	"		-233
	480-490	"		-225
	500-510	"	-29.2	-234
	520-530	"	-25.4	-218
	530-540	"		-223
	547-555	"		-227
	570-578	"		-212
	578-588	"	-27.3	-213
	595-602	"		-220
	602-635	"		-224
	642-650	"		-219
	655-665	"		-222
	665-675	"		-222
	685-695	"	-27.1	-211
	780-790	clay silt		-197
ER 83-2	70-80	organic silt		-174
	90-100	"	-22.6	-175
	110-119	ice & silt		-178
	128-137	"		-178
	147-156	"		-178
	164-172	"		-179
	194-204	"	-23.0	-180

Table 3.2 Isotope data for Eagle River site

	DEPTH (CM)	TYPE OF MATERIAL	$\delta^{18}O$ (°/oo SMOW)	$\delta^{2}H$ (°/oo SMOW)
ER 83-2	218-224	ice & silt		-186
	234-244	"	-25.0	-193
	244-255	ice	-28.4	-221
	265-275	"		-229
	285-295	"		-228
	305-315	"	-29.8	-230
	325-335	"		-227
	345-355	"		-231
	363-371	"		-232
	380-386	"	-29.7	-233
	404-412	"		-231
	420-430	"		-231
	440-448	"		-230
	464-472	"	-26.1	-221
	481-490	"		-218
	499-508	ice & sandy silt	-26.5	-206
	525-532	"		-200
	540-549	"	-25.0	-199
	558-567	"		-199
	567-575	sandy silt	-23.4	-192

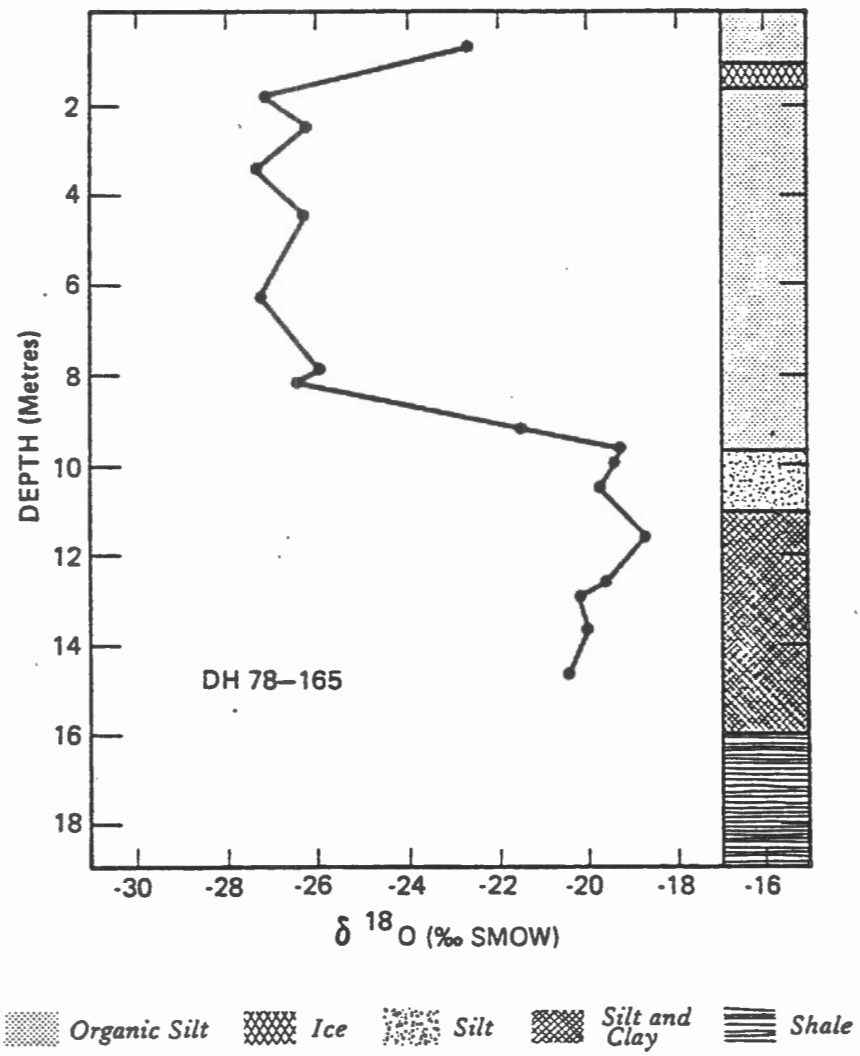

Figure 3.5 Variation in ^{18}O content with depth for core 78-165.

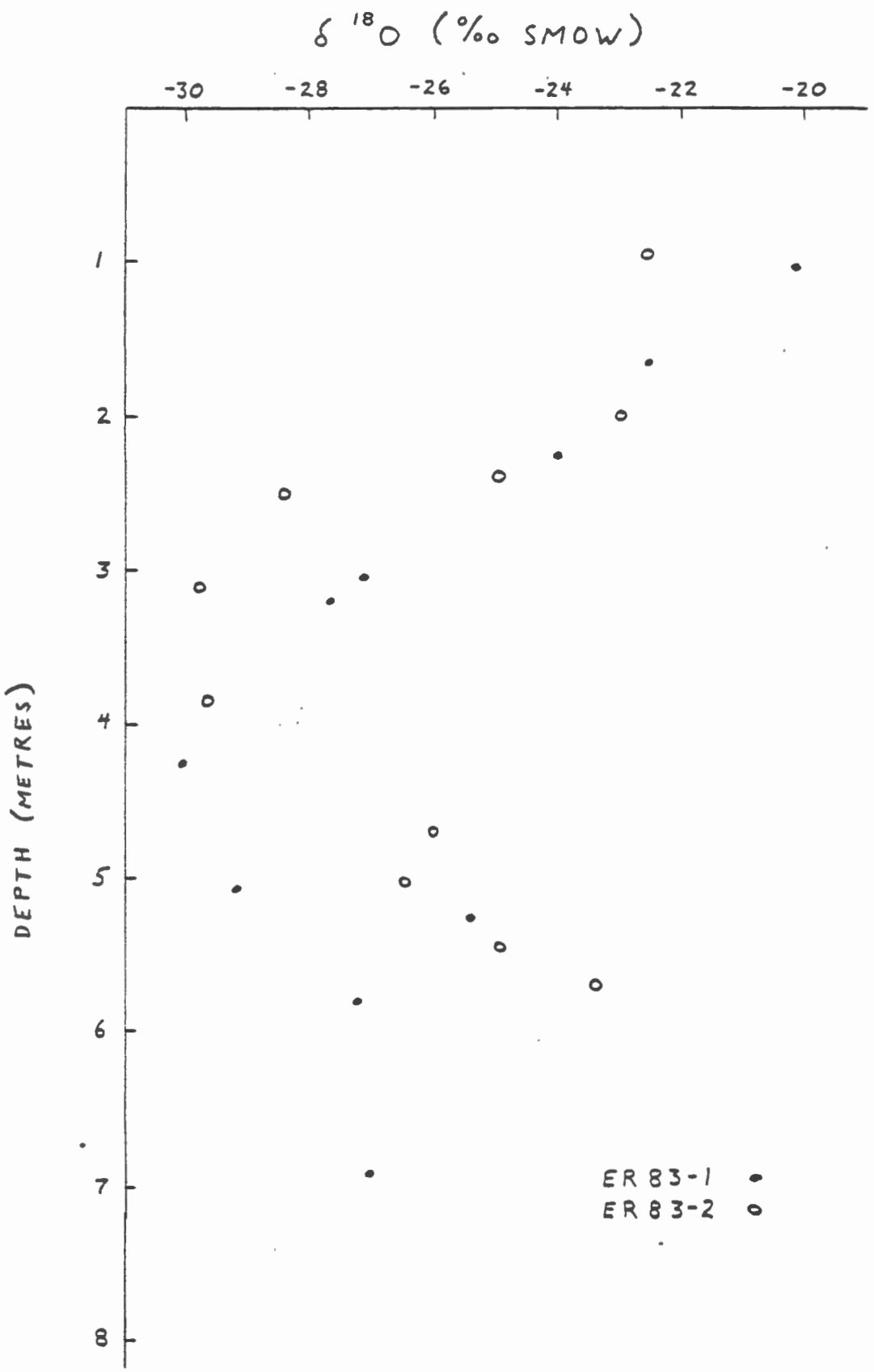

Figure 3.6 Variation in ^{18}O content with depth for cores ER 83-1 and ER 83-2.

composition similar to the massive ice in the two new boreholes. Below the massive ice unit in boreholes ER 83-1 and ER 83-2, the oxygen isotope composition does shift to values which are similar to the lower organic silt unit of 78-165 and justifies a correlation of these units.

The more extensive hydrogen isotope data, plotted in Figure 3.7, display a profile similar to the oxygen isotope data. The organic silts overlying the massive ice have $\delta^{2}H$ values which are indicative of modern precipitation, while the massive ice has $\delta^{2}H$ values which are considerably more negative (-225 to -235 °/oo). The transition between isotopic units is gradual, occurring over an interval of 1.5 metres for ER 83-1 and 0.25 metres for ER 83-2. For both cores, most of the transition occurs within the overlying organic silts.

Within the massive ice of ER 83-2, the $\delta^{2}H$ values remain constant, while in core ER 83-1 only the upper half of the ice section has a constant isotopic composition. In the lower half of the ice in ER 83-1, a number of small but distinct fluctuations occur with an average $\delta^{2}H$ value of approximately -220 °/oo. During drilling, it was noted that beginning at approximately 5 metres (the start of the fluctuations), the ice became brownish in colour due to an increase in silt content and the bubbles became smaller. At the same time, there is no further record of thin vertical silt bands in the ice.

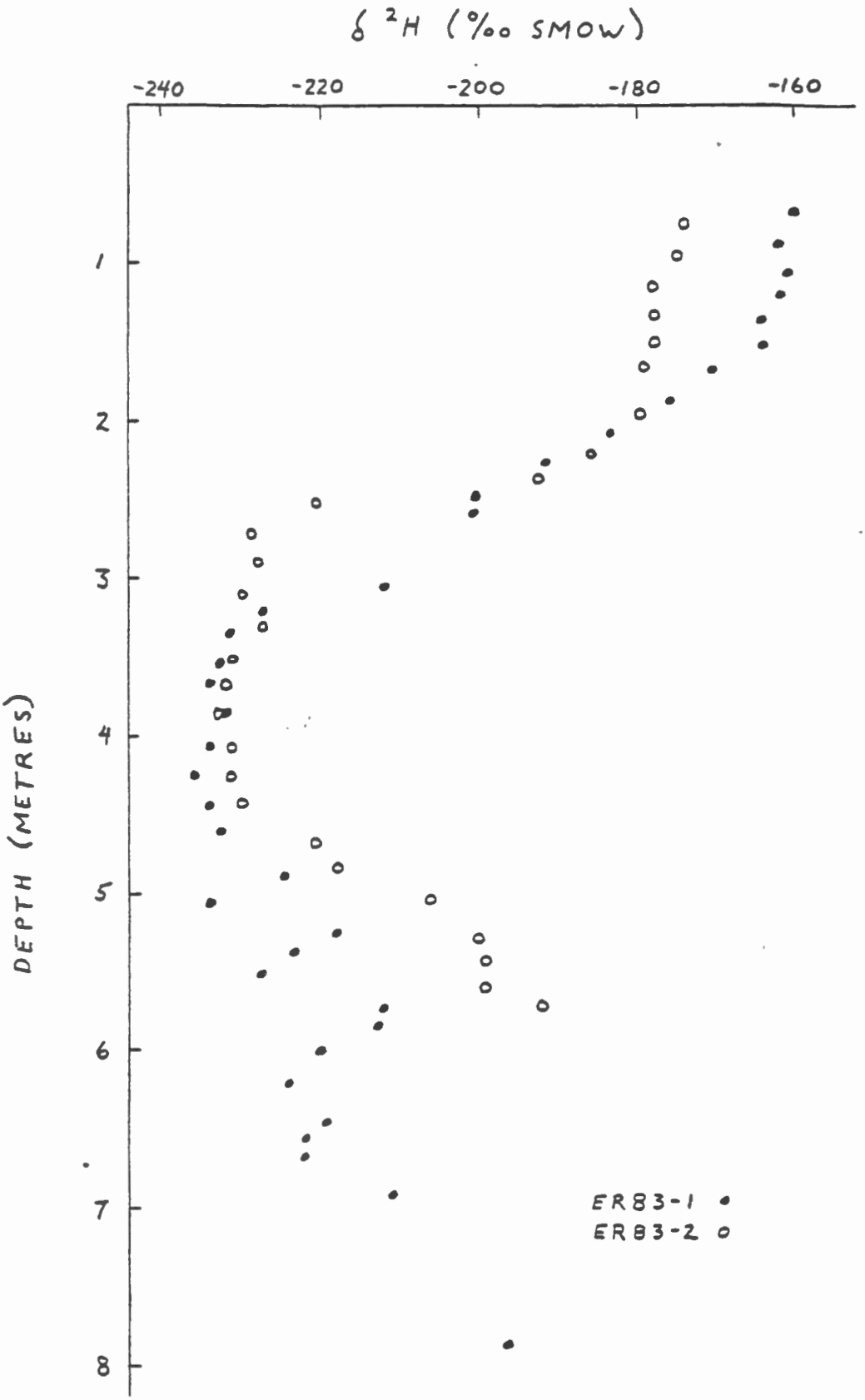

Figure 3.7 Variation in ^{2}H content with depth for cores ER 83-1 and ER 83-2.

The massive ice in ER 83-2 and the upper ice unit in ER 83-1 are interpreted as ice-wedge ice, on the basis of the physical characteristics and the uniform isotopic composition. The physical characteristics include the vertical silt bands, larger bubble size and the oxidized, near vertical contact between the ice and adjacent silt in the lower portion of ER 83-2. The isotopic composition of this ice ($\delta^{18}O$ = -30 °/oo, $\delta^{2}H$ = -230 °/oo) is indicative of colder climatic conditions than exist at present in this area.

The lower ice unit in ER 83-1 is different in appearance than the overlying ice. Although the origin of this ice cannot be stated with absolute certainty at this time, the fluctuations in isotopic composition are suggestive of slow freezing with possibly periodic stabilizations in the freezing front. If this is the case, then this ice would have a segregational origin.

Below the massive ice, the soils are predominantly silt with varying clay and sand fractions. Ice, which occurs primarily as 1 to 2 mm thick subhorizontal lenses, makes up 10 to 30% of the soil volume. Isotopically, these silts are less negative than the overlying ice and the ice lenses are definitely of a segregational origin.

Examination of the ^{2}H versus ^{18}O plot in Figure 3.8 reveals that none of the ground ice samples are altered from their original relationship by fractionation processes. Although shifted slightly to the right, the samples generally

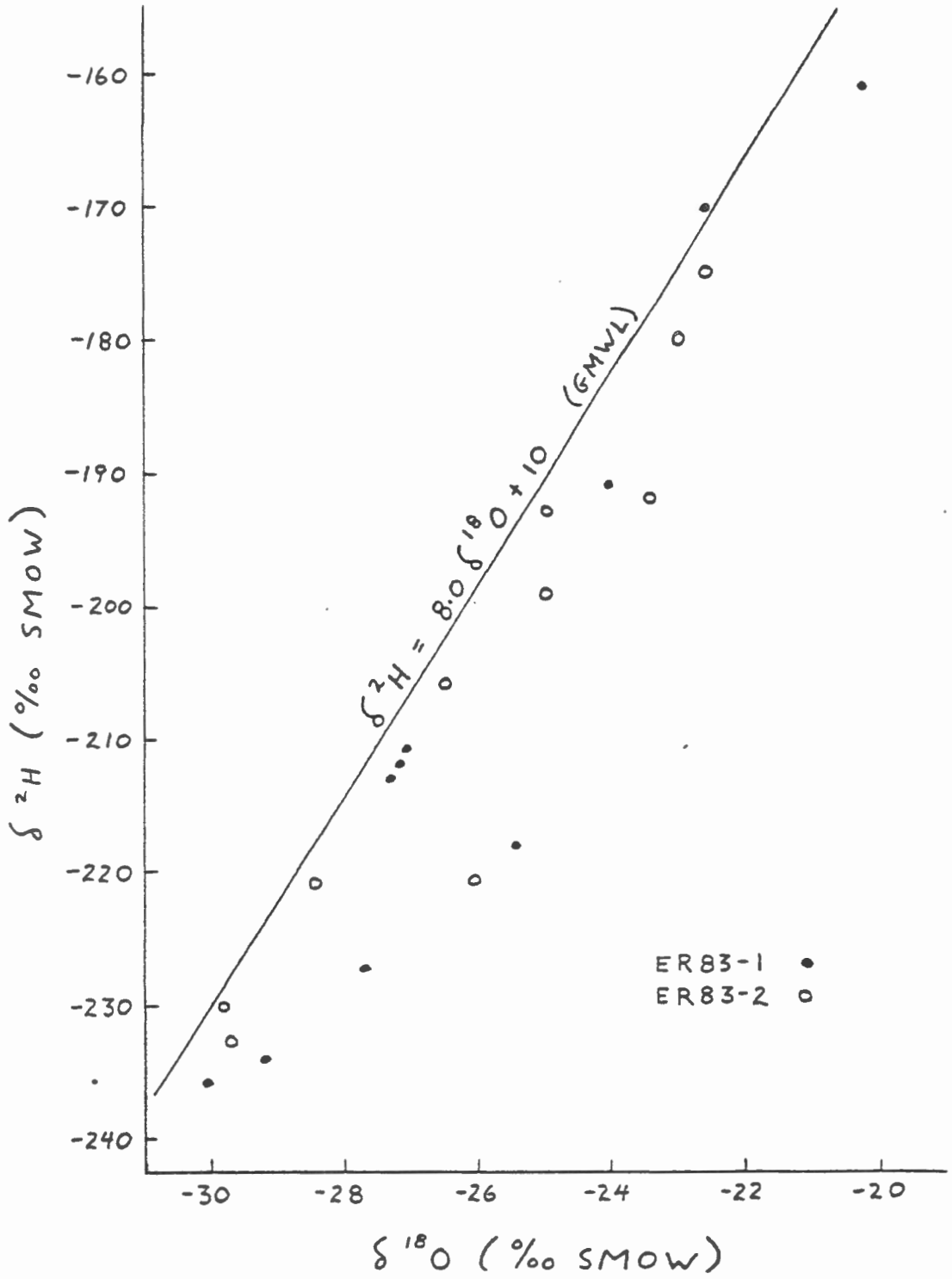

Figure 3.8 Relationship between ^{2}H and ^{18}O contents for cores ER 83-1 and ER 83-2. GMWL = global meteoric water line.

parallel the global meteoric water line drawn in the figure. This indicates that either freezing was very rapid, with no fractionation, or freezing was slow enough to permit fractionation under equilibrium conditions for both the oxygen and hydrogen isotopes. In the case of ice-wedge ice, freezing would be relatively rapid and yield a slope near 8, as demonstrated by Michel and Fritz (1982b) for ice wedges at Illisarvik, N.W.T. For the lower segregational (?) ice, slow freezing would also yield a slope approaching 8, although deviations from the normal trend may occur where the freezing rate was somewhat faster. This type of very slow freezing is probably indicative of water-saturated sediments at the time of freezing.

3.4 North Fork Pass Frost Blisters

At North Fork Pass, a large cluster of frost blisters, studied in detail by Pollard (1983), occurs near the Dempster Highway. From the work by Pollard, the formation and growth of these features are well understood. In order to examine the isotope profile which develops during the freezing of an enclosed body of water under natural conditions, one of these frost blisters was cored in September 1981. This work has been submitted as a paper to Canadian Journal of Earth Sciences and is reproduced below for this report.

ISOTOPE GEOCHEMISTRY OF FROST-BLISTER ICE, NORTH FORK PASS, YUKON, CANADA

by

Frederick A. Michel
Ottawa-Carleton Centre for Geoscience Studies
Carleton University
Ottawa, Ontario K1S 5B6

Abstract

Oxygen-18 and deuterium abundances vary with depth in ice from a frost blister at a spring site near North Fork Pass, Yukon. They indicate that the ice was formed by continuous downward freezing under nearly ideal, closed-system conditions in a water-filled cavity. Weighted mean values of $\delta^{18}O$ and $\delta^{2}H$ for the ice samples indicate that the frost-blister ice was formed from groundwater similar to that of nearby springs. The slope of the regression line (5.1) for the ^{18}O and ^{2}H data of the frost-blister ice suggests that equilibrium fractionation conditions are reached slightly faster for the oxygen isotopes than the hydrogen isotopes. Tritium concentrations in the ice show irregular variations with depth; the weighted mean ^{3}H concentration for the ice is, however, similar to that of the spring water.

Introduction

Frost blisters are short-term periglacial phenomena that form each winter in permafrost regions where groundwater discharges into valleys along the major break in slope at the valley floor. They were first described in detail by Muller (1945) and have since been reported by numerous investigators (Bogomolov and Sklyarevskaya 1969, Sloane et al. 1976, Froehlich and Slupik 1978, Michel and Fritz 1978, van Everdingen 1978, Pollard and French 1983). An idealized formational model for these features was proposed by van Everdingen (1982).

The formation of a frost blister often occurs as a two stage process. In the first stage, the ground heaves rapidly as the hydrostatic pressure of groundwater in the active layer exceeds the overburden pressure. van Everdingen (1982) reported growth rates as high as 0.55 metres per day.

During the second stage, growth is much slower because it is characterized by the gradual freezing of water contained in the core of the blister. Unless additional water is added during freezing, further growth is limited to the 9% expansion in volume as water changes to ice. During this stage, the frost blister can rupture, subside and subsequently reform if ice seals the fracture and additional water is injected into the blister.

Unless continuous monitoring or observation is undertaken, it is difficult to determine the growth history of a frost blister. Furthermore, the rate at which water in the

core freezes cannot be readily determined by monitoring the growth rate. During freezing, however, the oxygen and hydrogen atoms of the water molecules are fractionated between the liquid (water) and solid (ice) phases. A preliminary study by Fritz and Michel (1977) of frost blisters at Bear Rock, N.W.T. indicated that the determination of stable isotope compositions for the ice core could be useful in understanding the latter stage of growth.

In September of 1980, a frost blister in the North Fork Pass area was cored and sampled for isotope analysis of the ^{18}O, ^{2}H and ^{3}H contents. The aim of this study was three fold: (1) to determine whether the ice in a North Fork Pass frost blister formed under closed-system conditions, with water inflow only during the initial development of the blister or under open-system or leaky conditions with water added or lost intermittently during freezing; (2) to establish the source of water for the frost blisters; and (3) to investigate the potential usefulness of tritium analyses in similar ground-ice studies.

Site Description

The North Fork Pass area (Fig. 1) is located in the Southern Ogilvie Mountains, 76 kilometres northeast of Dawson City in the interior Yukon Territory. The study area is mapped as widespread discontinuous permafrost (Brown 1978), however, with elevations ranging from 1200 to greater than

2100 m, the entire area of interest is underlain by continuous permafrost.

Several groups of springs discharge into the headwaters of the East Blackstone River just north of North Fork Pass. One of the spring groups (No. 2, Fig. 1) is located at the break in slope between the valley floor and the west-facing side of the valley, and is situated immediately downslope from the Dempster Highway near kilometre 86 (64° 35' 39"N, 138° 18' 34"W). The perennial discharge from these springs and widespread seepage feeds a small pond and maintains saturated active-layer conditions in the poorly drained alpine tundra. During winter, discharging groundwater freezes to form extensive icings. Frost blisters develop in the vicinity of these perennial spring discharges as the saturated active layer freezes back each fall (see Fig. 2).

During the period 1980-82, more than 65 frost blisters were observed in the North Fork Pass area (Pollard and French 1983). The distribution, morphology and hydrostatic potentials of these frost blisters have been studied in detail by Pollard (1983). The internal structure of a typical blister is shown in Figure 3.

Sampling and Analytical Procedures

Water samples from springs in the area were collected in 125 ml glass bottles on two occasions; in September 1980 and in March 1981. A sample of the snowpack at the site was collected in March 1981. Core samples (7.5 cm diameter),

collected from a typical frost blister, were cut into 4 cm sections, sealed in heavy-duty plastic bags and transported to the isotope laboratory at the University of Waterloo in a frozen condition.

Samples were analysed for their ^{18}O and ^{2}H concentrations using standard preparation techniques. Results are expressed in the δ °/oo notation and are referenced to standard mean ocean water (SMOW). Reproducibility of results is ±0.2°/oo for ^{18}O and ±2.0°/oo for ^{2}H analyses.

Samples for tritium analysis were totally distilled prior to liquid scintillation counting. Results are reported in tritium units (T.U.), where 1 T.U. represents a concentration of 1 tritium atom in 10^{18} atoms of hydrogen. Analytical error for individual samples is ± 10 T.U.

Isotope Fractionation during Freezing

The relative abundance of the various stable isotopes of oxygen and hydrogen in precipitation fluctuates with the seasons due to a variety of factors (Dansgaard 1964). Summer precipitation is generally enriched in the heavier isotopes (^{18}O and ^{2}H) relative to winter precipitation. Within a groundwater flow system, however, isotopic differences are smoothed out and the groundwater will usually possess an isotopic composition which closely reflects the average annual precipitation input.

The heavy isotopes, ^{18}O and ^{2}H, are preferentially incorporated into the solid ice phase during freezing, while the residual liquid becomes depleted. The $\delta^{18}O$ and $\delta^{2}H$ values of ice in isotopic equilibrium with water are 2.8°/oo and 20.6°/oo more positive, respectively, than the water (Suzuoki and Kimura 1973).

If the frost-blister ice formed in an open system, with a continuous subsurface replenishment of water with a constant isotopic composition, then the δ values for the ice would be relatively constant throughout the thickness of the ice body.On the other hand, frost-blister ice formed in equilibrium with water in a closed system, during continued slow freezing of a diminishing reservoir, would result in progressive depletion of the remaining water with respect to the heavy isotopes.

The closed-system freezing process can be described by the Rayleigh distillation equation (cf. Broecker and Oversby 1971, p. 166) as

$$\delta_R = (\delta_o + 1000)\, f^{(\alpha-1)} - 1000 \qquad (1)$$

where δ_R is the isotopic content of the ice being formed relative to the standard,

δ_0 is the original isotopic content of the water before freezing begins,

f is the fraction of water remaining, and

α is the isotope fractionation constant.

Although fractionation of the oxygen and hydrogen isotopes occurs during freezing of the water mass, the bulk isotopic composition of the ice formed in a closed system will still reflect the composition of the source water.

Tritium, as a radioactive isotope of hydrogen with a half-life of 12.43 years, can be employed for the dating of relatively young groundwaters. Large concentrations of tritium were released into the atmosphere in the early 1960's during the testing of nuclear devices. By measuring the tritium levels in precipitation since nuclear testing began, it is possible to determine the approximate age of groundwaters which have been recharged since 1953, the year of the first major atmospheric nuclear test. Groundwaters which are older than 1953 do not contain tritium.

The tritium atom has three times the mass of a hydrogen atom and one and a half times the mass of a deuterium atom. Therefore, the magnitude of fractionation for tritium in the ice-water system should be considerably larger than the deuterium fractionation. Due to the low concentration of tritium in most waters, however, this fractionation may not be detectable.

Results and Interpretation

Springs

The $\delta^{18}O$ and $\delta^{2}H$ values for spring waters and snowpack (Fig. 4) correlate reasonably well with the global meteoric water line (GMWL) described by Craig (1961). Local precipi-

tation is regarded, therefore, as the source of water in spring groups 1 and 2.

The tritium concentrations found in these spring waters (110 to 161 T.U.) were considerably higher than those found in precipitation samples collected periodically during the study period (0 to 30 T.U.). The high ^{3}H values suggest that the spring waters represent precipitation that fell between 10 and 15 years earlier (latter half of 1960's).

Frost-blister ice

The $\delta^{18}O$, $\delta^{2}H$ and ^{3}H values for the frost blister samples are plotted against depth in Figure 5. The thaw boundary (active layer base) in the frost blister was within the overlying peat at the time of sampling and, therefore, the entire thickness of massive ice was available for study.

Weighted mean values of $\delta^{18}O$, $\delta^{2}H$ and ^{3}H for the ice samples (No. 4 to 20) are -22.5°/oo, -171°/oo and 149 T.U., respectively, and are similar to values obtained for local spring waters (labelled S in Figure 5). Since these springs represent a single zone of concentrated discharge for the groundwater flow system, it is reasonable to conclude that groundwater similar to that discharging from these springs provided water for the development of the frost blister examined.

^{3}H Data

Tritium data for the massive ice core (Fig. 5) show an irregular scatter in a range between 128 and 200 T.U. Fractionation effects similar to those shown by ^{18}O and ^{2}H are not apparent in these tritium data. Since the ice contains on average only 149 T.U., or 149 tritium atoms per 10^{18} atoms of hydrogen, and the analytical error is ±10 T.U., it is possible that any fractionation effects which might be present are masked. It is also possible, however, that the freezing rate was too rapid to permit significant fractionation to occur. Nevertheless, the tritium contents of the ice samples do indicate that the water feeding the frost blisters at North Fork Pass is similar in age to the nearby springs and that this water entered the groundwater system during the latter half of the 1960's.

In the overlying peat, the tritium concentration within the frozen portion is similar to the massive ice, but is significantly less in the upper unfrozen zone (83 to 87 T.U.). The lower tritium contents reflect more recent precipitation than the spring water, but are still higher than precipitation samples collected in 1980-81. It is suggested, therefore, that water within the unfrozen active layer of these raised mounds is a mixture of recent precipitation and groundwater seepage.

^{18}O and ^{2}H Data

In Figure 5, the overlying peat contains water with uniform $\delta^{18}O$ and $\delta^{2}H$ values which are only slightly more negative than values for the uppermost massive ice. The $\delta^{18}O$ and $\delta^{2}H$ values for the upper portion of the massive ice are more positive than those for the spring water. The differences are smaller than the equilibrium values determined by Suzuoki and Kimura (1973) and possibly result from relatively rapid freezing and/or inadequate mixing of the water reservoir. The increasingly more negative values found in the remainder of the ice core (samples No. 8 to 20) produce profiles similar to that expected from a Rayleigh distillation process as described by equation (1). Similar systematic isotope variations were reported by Michel (1982) for laboratory experiments in which confined columns of water were slowly frozen from the top downward. Thus, the ^{18}O and ^{2}H profiles are suggestive of continuous freezing of a gradually diminishing water reservoir that was progressively being depleted of the heavier isotopes.

This continuous downward depletion of the heavier isotopes, through the entire thickness of the massive ice, indicates that the fractionation process was not interrupted during freezing of the water mass. In contrast, van Everdingen (1982) reported the periodic rupture and partial loss of residual water from frost blisters at Bear Rock, N.W.T., which resulted in detectable fluctuations within the ^{18}O and ^{2}H profiles. Since the profiles through the massive

ice at North Fork Pass do not display any indication of water loss during freezing, it is concluded that the frost blister cored for this study is representative of one cycle of freezing under nearly ideal, closed-system conditions.

Below the massive ice, 26 cm of ice-rich peat was recovered. No cavity was found between the ice and the frozen peat. The lower part of the peat (samples No. 22 to 26), with $\delta^{18}O$ and $\delta^{2}H$ values similar to those of the spring water, is isotopically representative of shallow permafrost in the area as determined during investigations conducted along the Dempster Highway by Michel and Fritz (1982).

The ^{18}O and ^{2}H contents of the uppermost sample of ice-rich peat (sample No. 20) are consistent with those in the massive ice. This trend suggests that the water in this interval represents the final portion to freeze. All of the massive ice above contained large vertically-oriented columnar ice crystals indicative of a horizontal freezing front. Therefore, the ice in the core above a depth of 93 cm must have formed by freezing from the surface downward, in response to negative air temperatures. The absence of a cavity inside the blister supports the hypothesis that the core formed during a single period of continuous freezing with no loss of water. The ice-rich peat immediately below 93 cm (sample No. 21), with an intermediate isotope composition, may have frozen by upward advancement of the freezing front from the permafrost table, which would have been located between samples No. 21 and 22.

To study the isotope fractionation which has occurred during formation of the massive ice core, the data for samples No. 4 to 20 can be examined more closely in terms of the Rayleigh distillation model. By varying the fractionation factor (α) in equation 1, a family of type curves can be generated for ^{18}O and ^{2}H. Representative curves are shown in Figure 6. The largest value used in each plot is the equilibrium fractionation constant determined by Suzuoki and Kimura (1973).

By equating the residual fraction axis to the depth axis in Figure 5, the type curves can be compared directly to the frost-blister ice data. As can be seen in Figure 7a, the ^{18}O data approximate the equilibrium type curve ($\alpha = 1.0028$). This suggests that fractionation of the oxygen isotopes during freezing occurred under conditions near or at equilibrium in a closed-system environment.

The ^{2}H data, shown in Figure 7b, match a type curve with an α value (1.0130) considerably less than the ^{2}H equilibrium fractionation constant (1.0206). It is obvious that equilibrium conditions did not exist during freezing with respect to hydrogen isotope fractionation. Nevertheless, the form of the ^{2}H data curve does indicate that freezing within a closed-system environment has occurred.

The fact that the oxygen isotopes fractionated under equilibrium conditions while the hydrogen isotope fractionation was not at equilibrium is not totally unexpected. Due to the proportional differences in mass of the hydrogen (2:1)

and oxygen (18:16) isotopes being considered, different lengths of time should be required to reach a state of equilibrium. The smaller relative mass difference between the oxygen isotopes, in comparison to the hydrogen isotopes, means that equilibrium conditions should be reached sooner for the oxygen isotopes. This situation would result in a linear ^{18}O - ^{2}H relationship with a slope of less than 8; the slope of the GMWL.

Data published by Michel and Fritz (1978) and van Everdingen (1978, 1982) for frost blisters at Bear Rock, N.W.T. produce regression lines with slopes between 3.5 and 6.5. Similar slope values have also been determined by Jouzel and Souchez (1982) for meltwater which has refrozen at the base of glaciers. Least square regression applied to the frost-blister data from North Fork Pass produces a linear relationship, with a slope of 5.1, described by the equation

$$\delta^{2}H = 5.1\,\delta^{18}O - 56.4 \quad (r = 0.99) \qquad (2)$$

All of these data support the hypothesis of different fractionation rates for the oxygen and hydrogen isotopes.

In Figure 8, the average $\delta^{18}O$ and $\delta^{2}H$ values for the frost-blister ice and the local groundwater plot at the intersection of the GMWL and the data regression line. The uppermost ice (sample No. 4) plots furthest to the right and subsequent samples shift toward increasingly more negative values. It should also be noted that data points to the right of the initial groundwater composition represent the

upper 2/3 of the ice sequence (samples No. 4 to 15) and that the distance between data points gradually increases, especially in the lower half of the ice sequence.

In Figure 9, $\delta^{18}O$ and $\delta^{2}H$ values calculated using the equilibrium fractionation constants of Suzuoki and Kimura (1973) are plotted for SMOW as the initial liquid. The K values denote the frozen fraction in the system. Except for the slope of the calculated line in Figure 9, comparison of Figures 8 and 9 clearly reveals a similar form. By replacing SMOW with the local groundwater and by using the fractionation factors determined from Figure 7a and 7b for the frost-blister ice, the calculated line in Figure 9 would coincide with the regression line in Figure 8. This further supports the assumption of one cycle of freezing in a closed system with no leakage.

The range in slope values mentioned earlier (3.5 to 6.5) probably reflects variations in the amount of fractionation that the oxygen and hydrogen isotopes are undergoing during freezing. This, in turn, would be controlled by the rate at which the freezing front advances, thereby limiting the length of time that the newly-formed ice is in contact with the residual water reservoir. If the rate of advance is slow enough to permit equilibrium of both the oxygen and hydrogen isotopes between the ice and water phases, then slope values as high as the 7.06 in Figure 9 should be attainable. More

work is required on the ice-water system in order to quantify these potential relationships and to determine the rate of fractionation for both the oxygen and hydrogen isotopes.

Conclusions

The results of ^{18}O, ^{2}H and ^{3}H analyses on spring waters and frost-blister ice indicate that water, which freezes to form the massive ice cores of frost blisters in the North Fork Pass area, is supplied by local groundwater flow systems. These discharge as seepage and as several distinct spring groups in the area. The flow systems are recharged by local precipitation which takes 10 to 15 years to reach the discharge area.

The trend with depth in the ^{18}O and ^{2}H contents of the massive ice reflect the progressive depletion of heavy isotopes as the volume of residual unfrozen water decreased during freezing under nearly ideal, closed-system conditions. Ice was continuously formed as a horizontal freezing front migrated downward. Ice formed by upward freezing from the original permafrost surface may be present in peat immediately beneath the ice core.

The slope of the regression line for the ^{18}O and ^{2}H data of the frost-blister ice is 5.1, which is considerably less than the slope of 8.0 for the GMWL. Other published frost-blister data indicate that slopes can vary between at least 3.5 and 6.5. These data suggest that isotope fractionation

approaches equilibrium values faster for oxygen isotopes than for hydrogen isotopes, and that the slope is related to the freezing rate.

Natural tritium levels in the groundwater are apparently too low to detect fractionation. Tritium is still important, however, for determining the age of groundwaters and for aiding in interpretations of the frost blister water source.

Acknowledgements

The author thanks J.A. Banner, National Hydrology Research Institute, for his assistance during drilling and sample collection; and the staff of the isotope laboratory at the Univeristy of Waterloo for conducting the isotope analyses. I would also like to thank Dr. R.O. van Everdingen (NHRI), Dr. W.H. Pollard (University of Ottawa) and Dr. P. Fritz (University of Waterloo) for their encouragement and constructive criticism of this manuscript. Figures 1 to 3 were kindly provided by Dr. Pollard. The financial support provided to the author by Dr. P. Fritz is greatfully acknowledged.

References

Bogomolov, N.S., and Sklyarevskaya, A.N. 1969. On explosion of hydrolaccoliths in the southern part of Chitinskaya Oblast. In Siberian Naleds. Edited by O.N. Tolstikhin and V.M. Piguzova. U.S.S.R. Academy of Sciences, Siberian Branch, Izdatel'stvo Nauka, Moscow, pp. 127-133.

Broecker, W.S., and Oversby, V.M. 1971. Chemical Equilibria in the Earth. McGraw Hill, New York, 318 p.

Brown, R.J.E. 1978. Permafrost Map of Canada. Third International Conference on Permafrost, National Research Council of Canada.

Craig, H. 1961. Isotopic variations in meteoric waters. Science, 133, pp. 1702-1703.

Dansgaard, W. 1964. Stable isotopes in precipitation. Tellus, 16(4), pp. 436-468.

Fritz, P., and Michel, F. 1977. Environmental isotopes in permafrost-related waters along two proposed pipeline routes. Report on Project No. 606-12 for Canada Department of Energy, Mines and Resources, Contract No. 06SU-23235-6-0681, Waterloo Research Institute, University of Waterloo, 51 p.

Froehlich, W. and Slupik, J. 1978. Frost mounds as indicators of water transmission zones in the active layer of permafrost during the winter season (Khangai Mts.,

Mongolia). Proceedings, Third International Conference on Permafrost, National Research Conference on Permafrost, National Research Council of Canada 1,pp. 189-193.

Jouzel, J., and Souchez, R.A. 1982. Melting-refreezing at the glacier sole and the isotopic composition of the ice. Journal of Glaciology, 28(98), pp. 35-42.

Michel, F.A. 1982. Isotope investigations of permafrost waters in Northern Canada. Ph.D. thesis, University of Waterloo, Waterloo, Ontario, 424 p.

Michel, F.A., and Fritz, P. 1978. Laboratory studies to investigate isotope effects occurring during the formation of permafrost. Report on Project No. 606-12-02 for Canada Department of Energy, Mines and Resources, Contract No. 0SU-77-00172, Waterloo Research Institute, University of Waterloo, 43 p.

Michel, F.A., and Fritz, P. 1982. Laboratory and field studies to investigate isotope effects occurring during the formation of permafrost. Report on Project No. 606-12-06 for Canada Department of Energy, Mines and Resources, Contract No. 0SU-81 -00076, Waterloo Research Institute, University of Waterloo, 76 p.

Muller, S.W. 1945. Permafrost or permanently frozen ground and related engineering problems. U.S. Army, Office Chief of Engineers, Military Intelligence Division. Special report, Strategic Engineering Study No. 62, 231 p.

Pollard, W.H. 1983. A study of seasonal frost mounds, North Fork Pass, Northern Interior Yukon Territory. Unpublished Ph.D. Thesis, University of Ottawa, Ottawa, 236 p.

Pollard, W.H., and French, H.M. 1983. Seasonal frost mounds in the North Fork Pass area, Ogilvie Mtns., Northern Yukon, Canda. F.I.C.O.P., Fairbanks, Alaska, pp. 1000-1004.

Sloane, C.E., Zenone, C. and Mayo, L.R. 1976. Icings along the Trans-Alaska pipeline route. U.S. Geological Survey Professional Paper no. 979, 31 p.

Suzuoki, T., and Kimura, T. 1973. D/H and $^{18}O/^{16}O$ fractionation in ice-water systems. Mass Spectroscopy, 21 (3), pp. 229-233.

van Everdingen, R.O. 1978. Frost mounds at Bear Rock, near Fort Norman, Northwest Territories, 1975-1976. Canadian Journal of Earth Sciences, 15 (2), pp. 263-276.

van Everdingen, R.O. 1982. Frost blisters of the Bear Rock spring area near Fort Norman, N.W.T. Arctic, 35 (2), pp. 243-265.

Illustration Captions

Figure 1. Location of the North Fork Pass area, Yukon and locations of springs and frost blisters.

Figure 2. View looking south into North Fork Pass from the Dempster Highway near km 86 (mile 53), showing spring location No. 2 (S), the small pond (P) and a partly collapsed frost blister (F). A small portion of the Dempster Highway is visible at extreme left of photo.

Figure 3. View of ice core in a frost blister in the North Fork Pass area.

Figure 4. Plot of $\delta^{2}H$ vs. $\delta^{18}O$ for samples of spring water and snowpack from the North Fork Pass area; points for snow at Little Fox Lake and for rain at Whitehorse, and the global meteoric water line (GMWL, Craig 1961) are included for comparison.

Figure 5. Plots of ^{18}O, ^{2}H and ^{3}H concentration vs. depth for core samples from a 1980 frost blister in the North Fork Pass area. S indicates isotope values for spring group No. 2.

Figure 6. Representative fractionation curves for ^{18}O (a) and ^{2}H (b) generated by employing various α values in equation (1). Initial composition of the ice is assumed to be 0 $^{o}/_{oo}$ for both ^{18}O and ^{2}H.

Figure 7. Comparison of type curves in Figure 6 to ^{18}O data (a) and ^{2}H data (b) for the massive ice of the frost blister.

Figure 8. Plot of $\delta^{2}H$ vs. $\delta^{18}O$ for frost-blister ice. Correlation factor for the regression line is 0.99.

Figure 9. Plot of δ values for successive ice fractions (K) calculated using the equilibrium fractionation constants of Suzuoki and Kimura (1973). Modified from Jouzel and Souchez (1982).

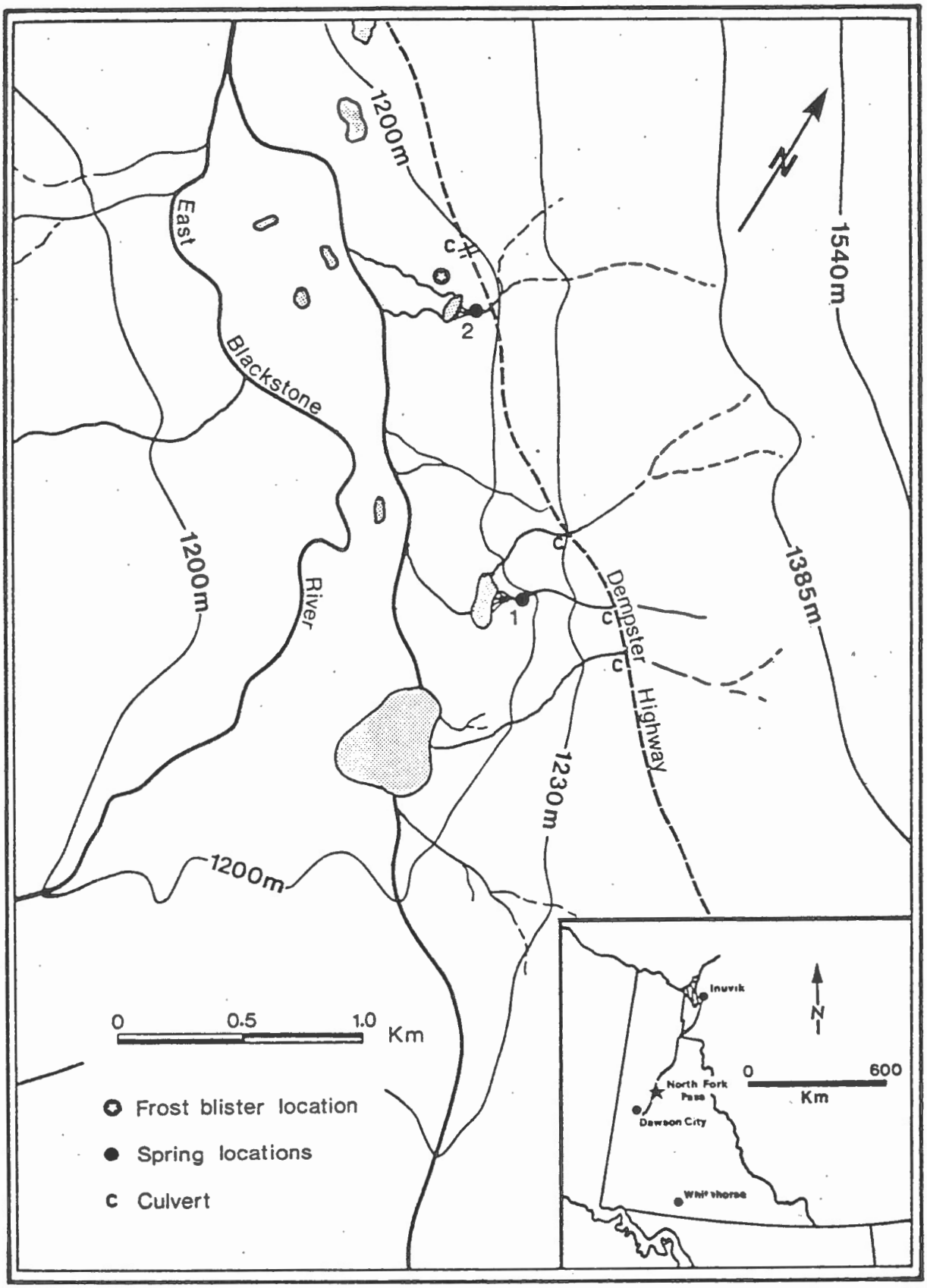
East
Blackstone
River
1200m
1200m
1200m
1230m
1385m
1540m
Dempster Highway
1
2
C
C
C
C
0
0.5
1.0
Km
Frost blister location
Spring locations
C Culvert
Inuvik
N
0
600
Km
North Fork Pass
Dawson City
Whitehorse

Figure 1

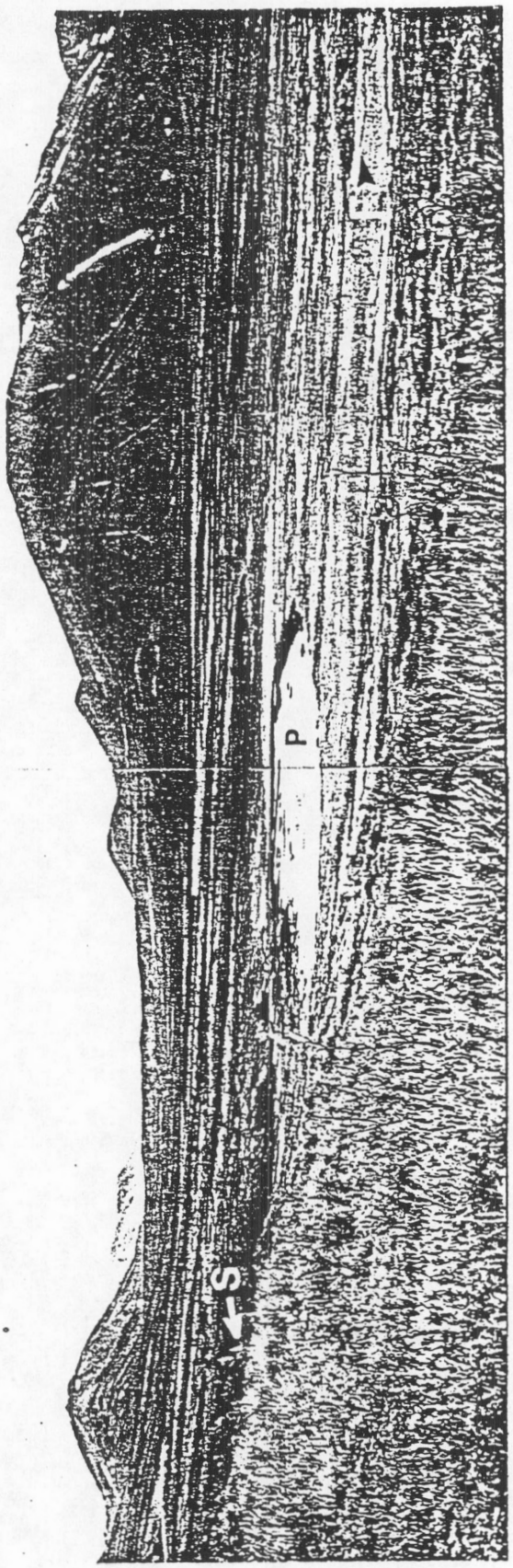

Figure 2

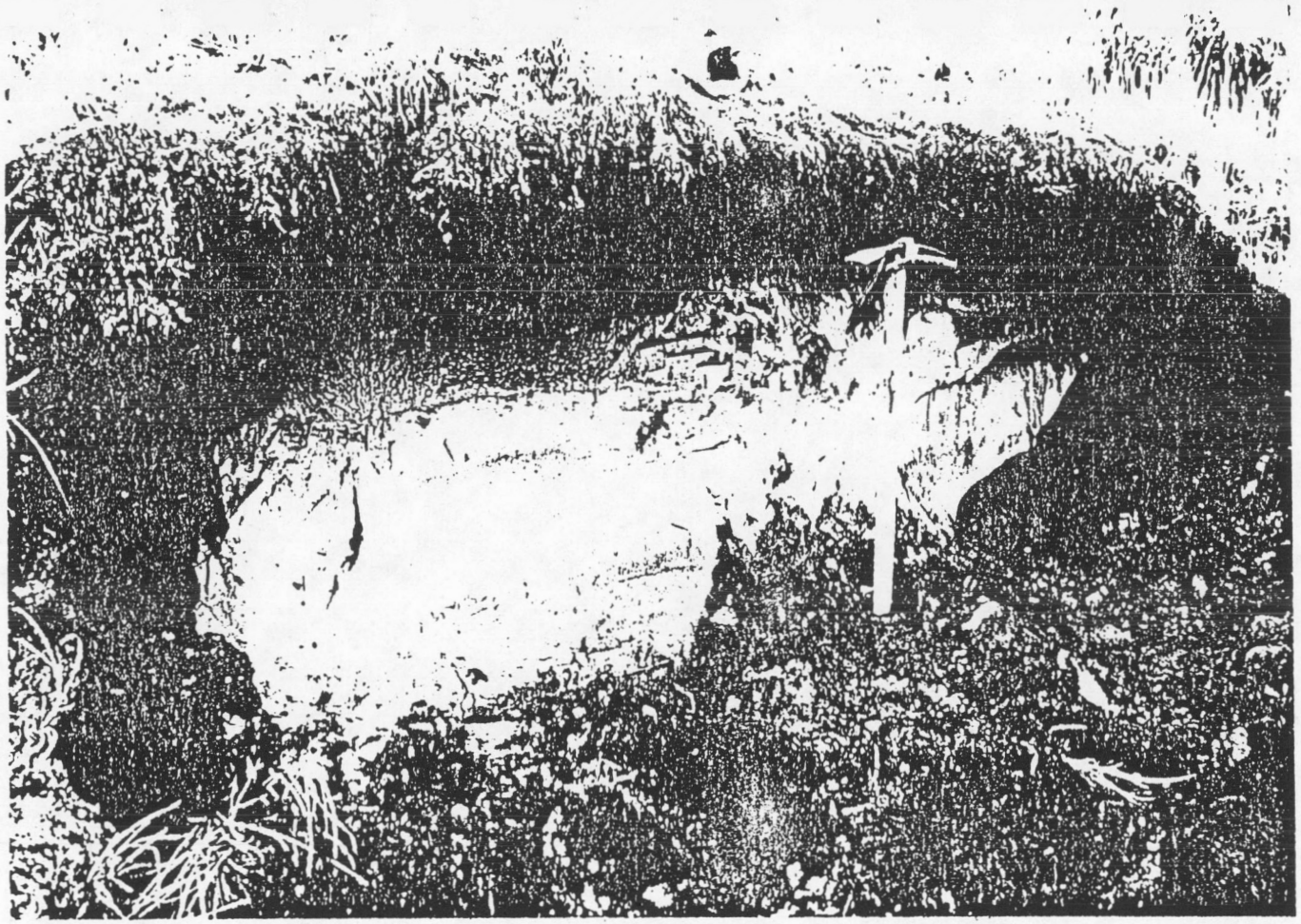

Figure 3

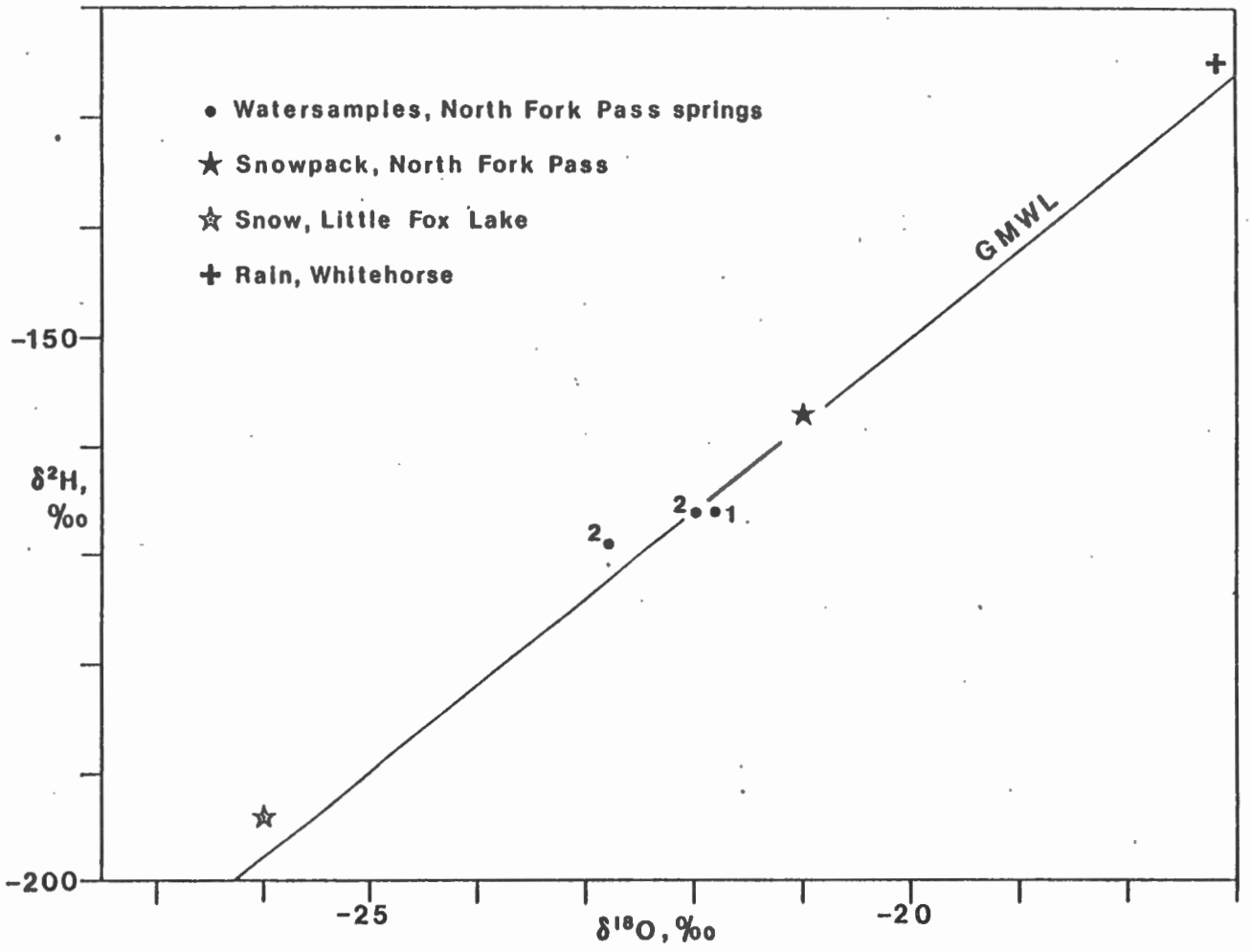
• Watersamples, North Fork Pass springs
★ Snowpack, North Fork Pass
☆ Snow, Little Fox Lake
+ Rain, Whitehorse
GMWL
-150
-200
δ²H, ‰
2
2
1
-25
-20
δ¹⁸O, ‰

Figure 4

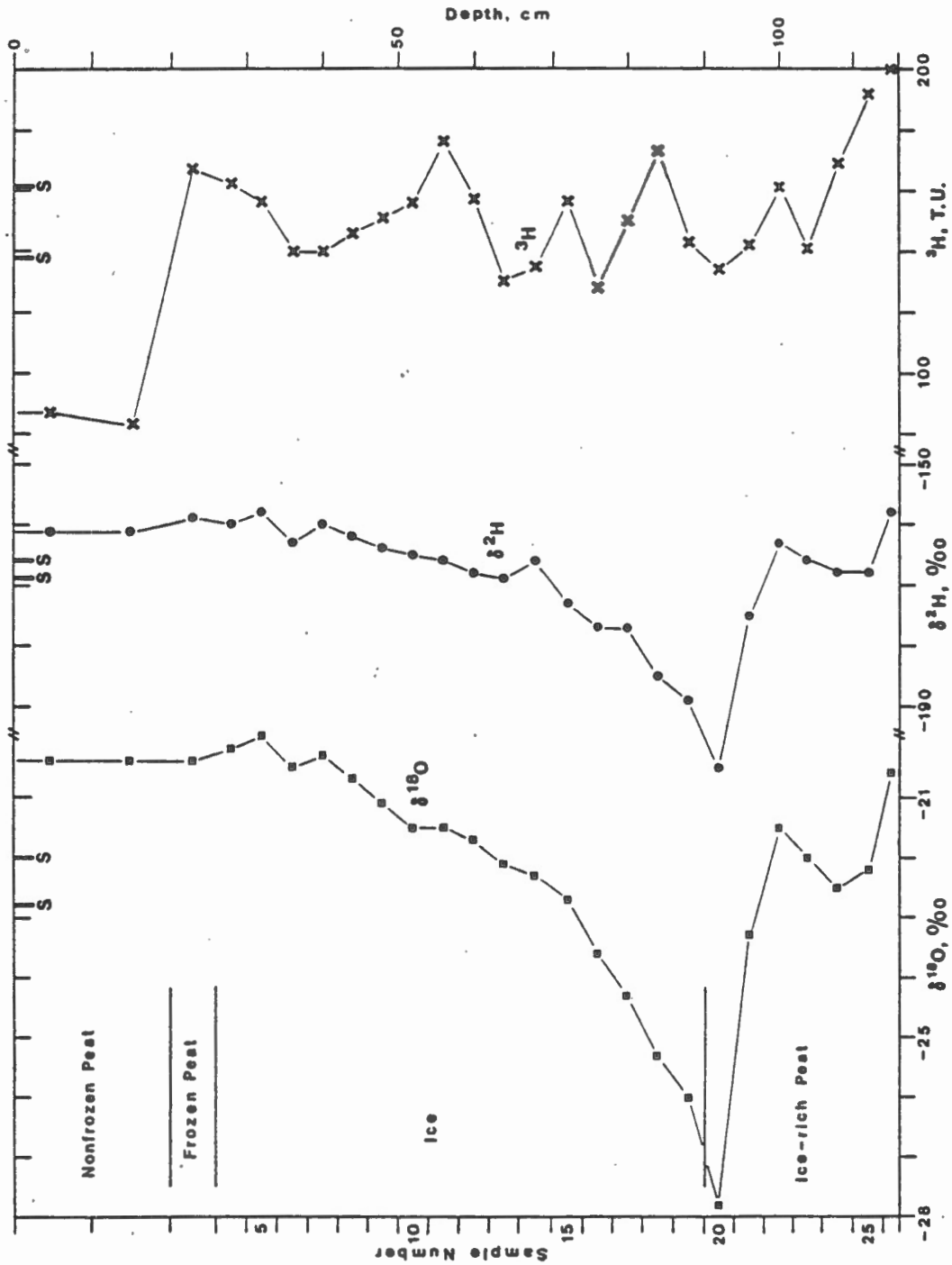
Depth, cm
0
50
100
200
^{3}H
^{3}H, T.U.
100
-150
δ^2H
δ^2H, ‰
-190
-21
δ^{18}O
δ^{18}O, ‰
-25
-28
Nonfrozen Peat
Frozen Peat
Ice
Ice-rich Peat
Sample Number
5
10
15
20
25

Figure 5

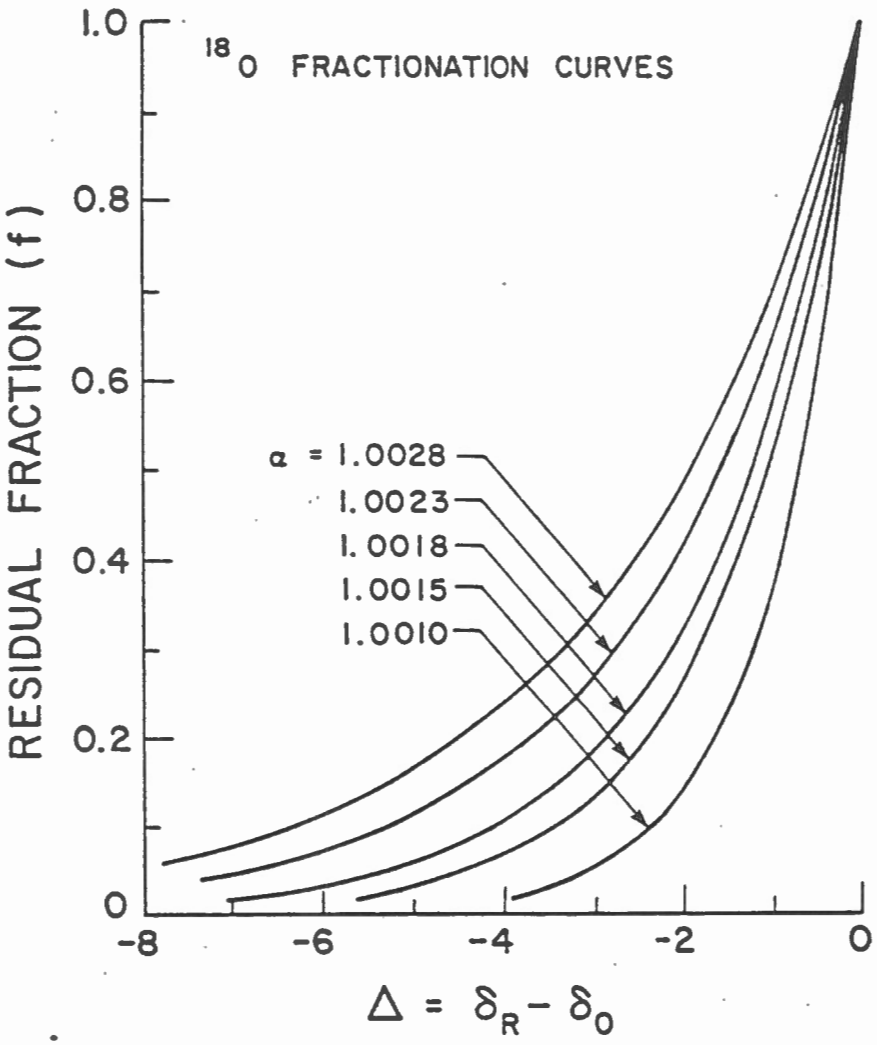
^{18}O FRACTIONATION CURVES
RESIDUAL FRACTION (f)
1.0
0.8
0.6
0.4
0.2
0
α = 1.0028
1.0023
1.0018
1.0015
1.0010
-8
-6
-4
-2
0
Δ = $\delta_R - \delta_0$

Figure 6a.

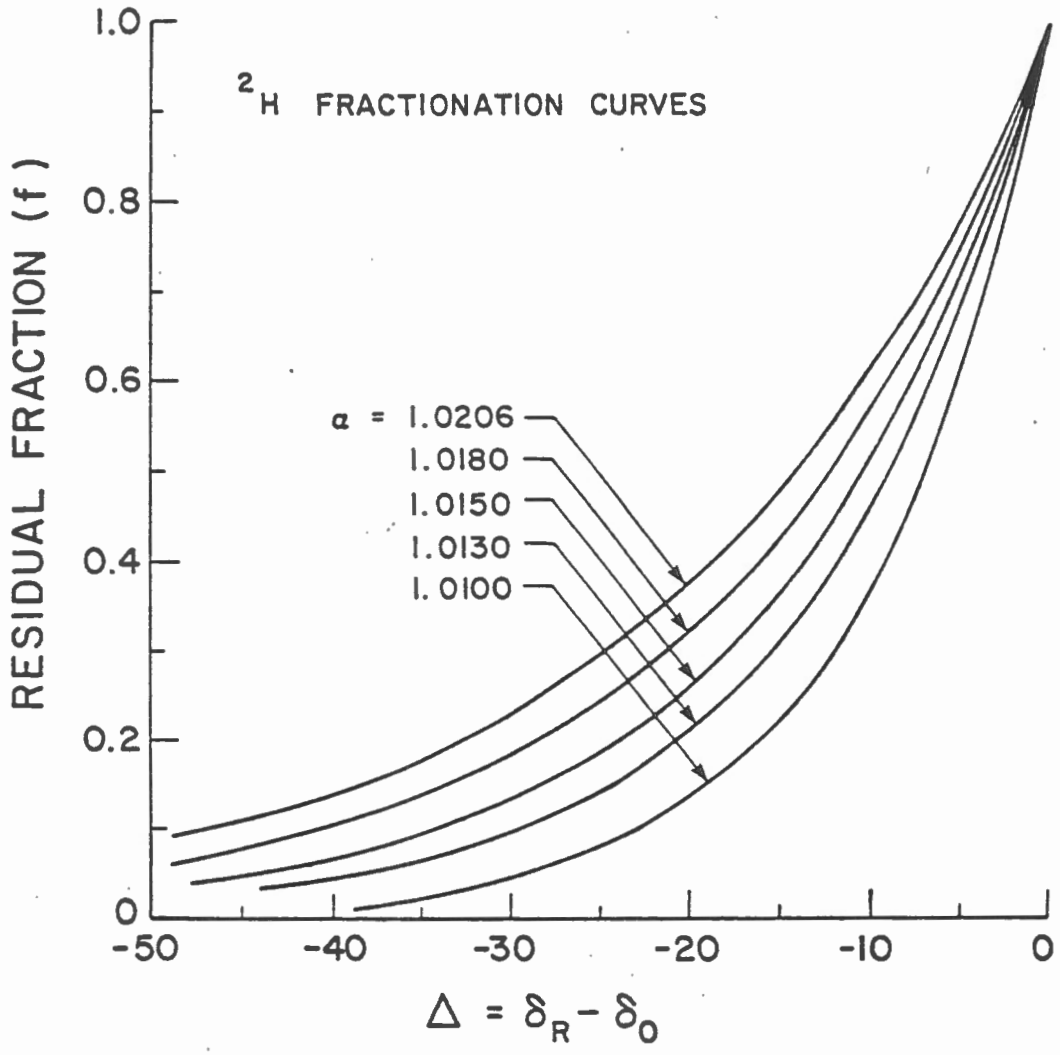
^{2}H FRACTIONATION CURVES
RESIDUAL FRACTION (f)
1.0
0.8
0.6
0.4
0.2
0
α = 1.0206
1.0180
1.0150
1.0130
1.0100
-50
-40
-30
-20
-10
0
Δ = δR - δ0

Figure 6b.

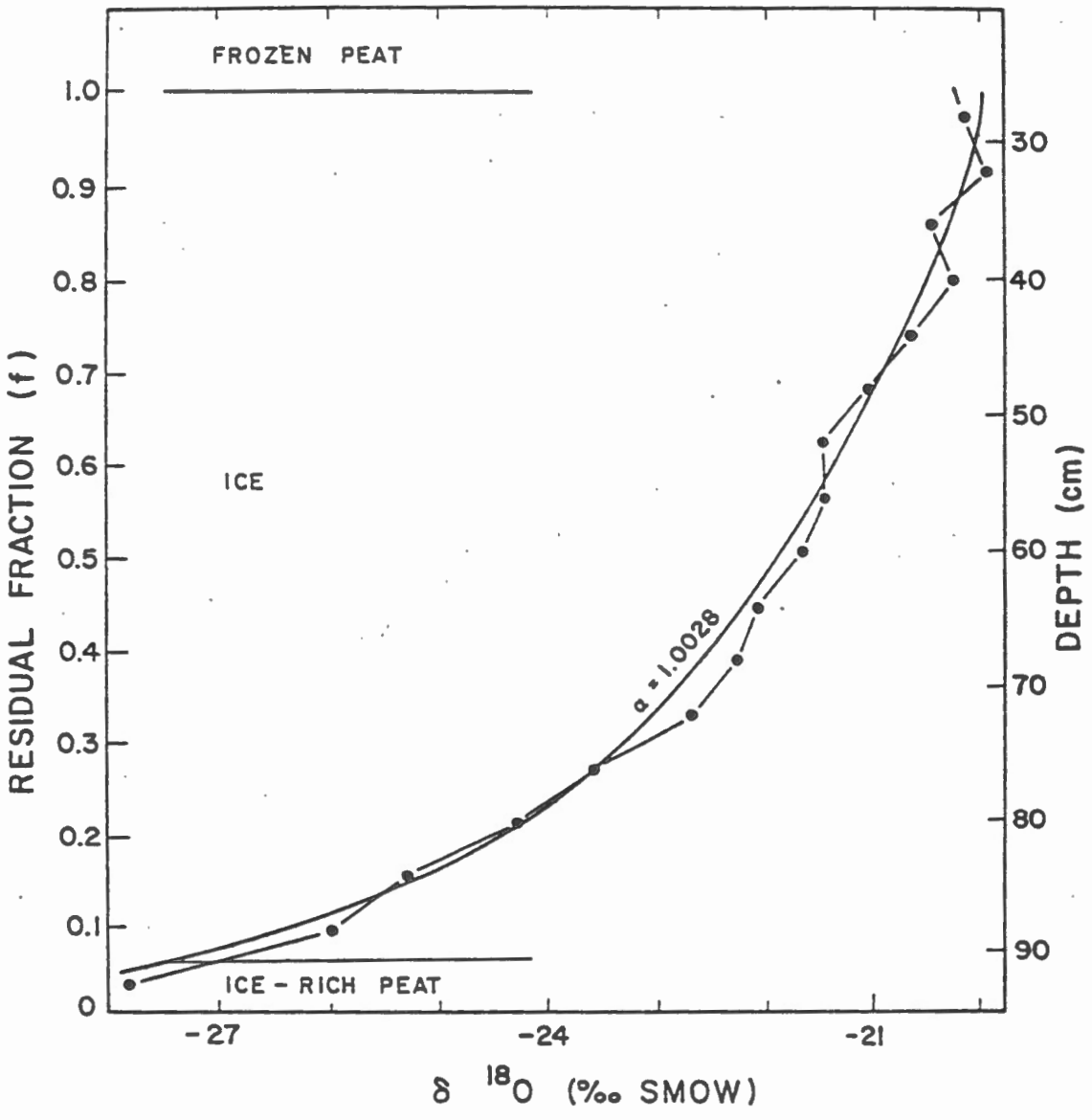
FROZEN PEAT
ICE
ICE - RICH PEAT
α = 1.0028
RESIDUAL FRACTION (f)
DEPTH (cm)
δ 18O (‰ SMOW)
1.0
0.9
0.8
0.7
0.6
0.5
0.4
0.3
0.2
0.1
0
30
40
50
60
70
80
90
-27
-24
-21

Figure 7a.

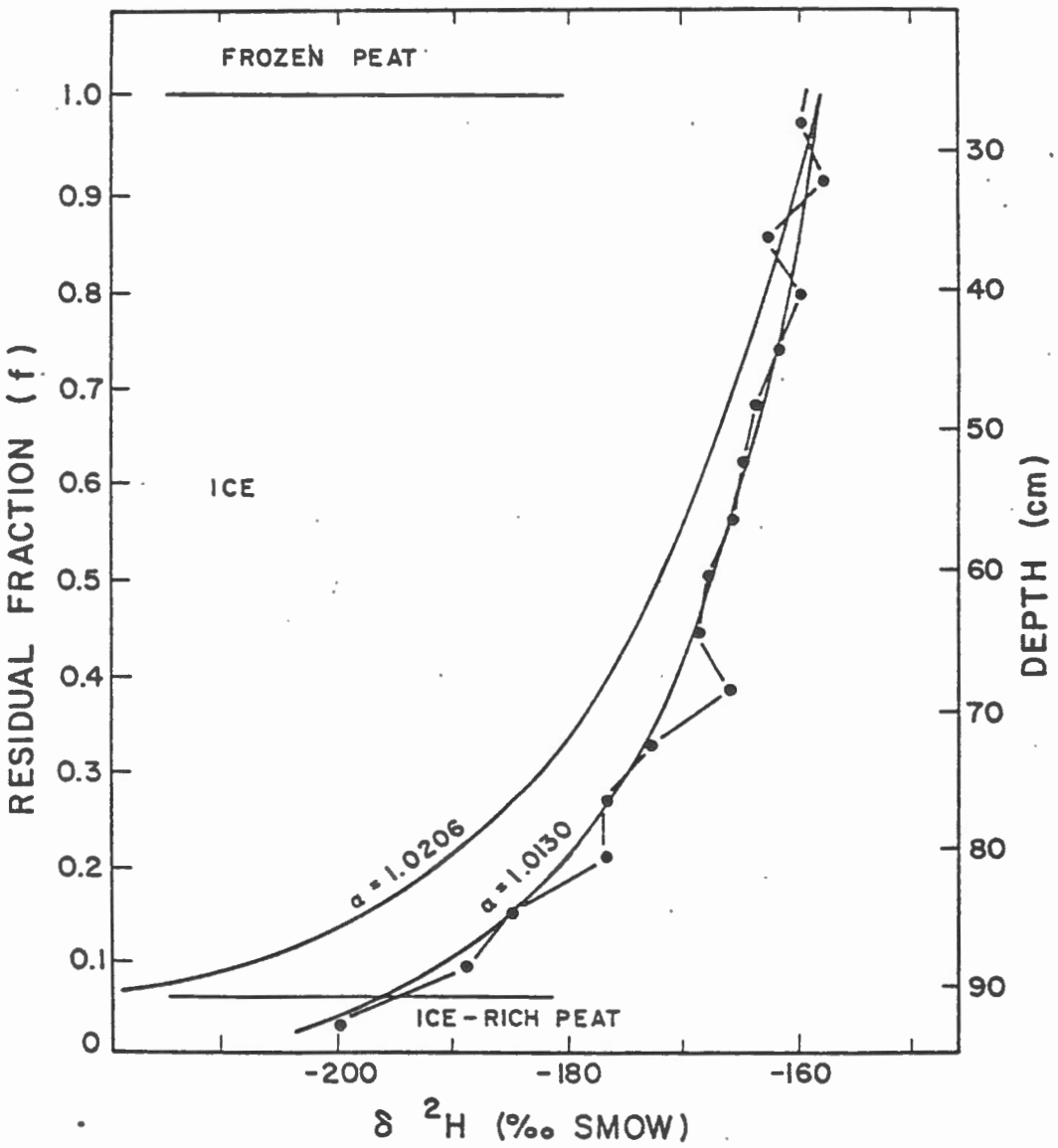
FROZEN PEAT
ICE
ICE-RICH PEAT
α = 1.0206
α = 1.0130
RESIDUAL FRACTION (f)
DEPTH (cm)
δ ²H (‰ SMOW)
1.0
0.9
0.8
0.7
0.6
0.5
0.4
0.3
0.2
0.1
0
30
40
50
60
70
80
90
-200
-180
-160

Figure 7b.

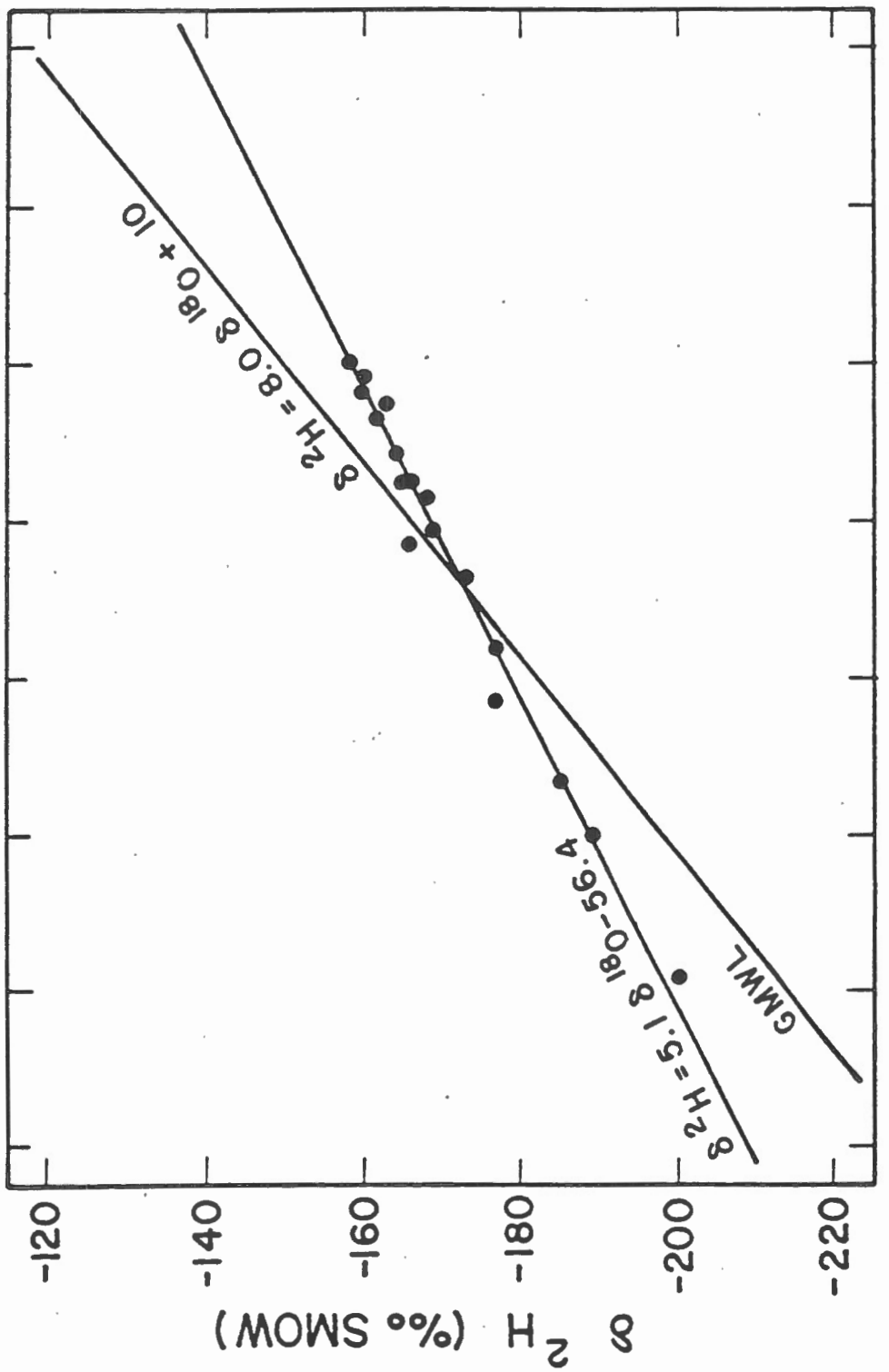
δ 2H = 8.0 δ 18O + 10
δ 2H = 5.1 δ 18O - 5.4
GMWL
δ 18O (‰ SMOW)
δ 2H (‰ SMOW)
-16
-18
-20
-22
-24
-26
-28
-30
-120
-140
-160
-180
-200
-220

Figure 8

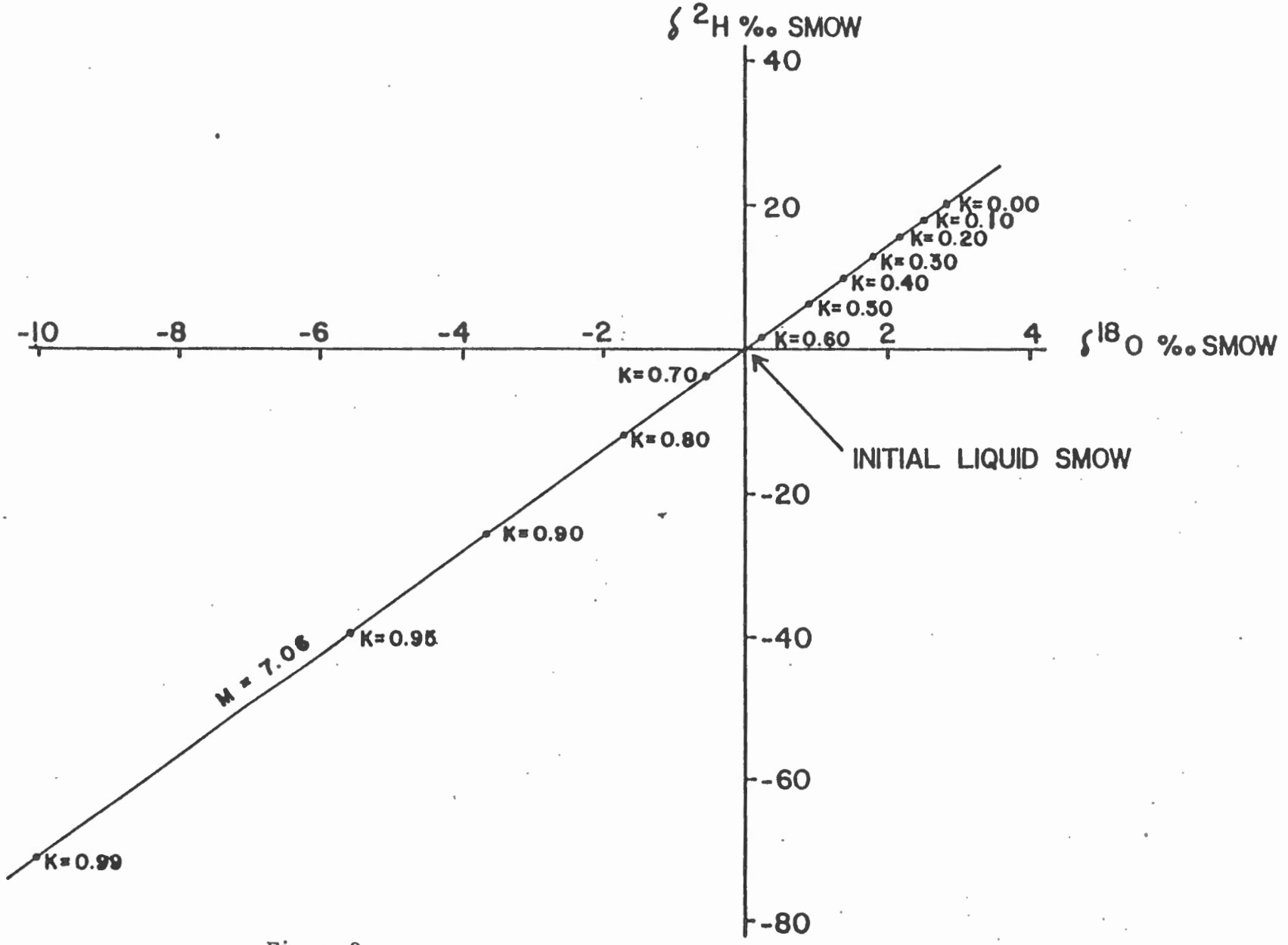
δ 2H ‰ SMOW
40
20
-20
-40
-60
-80
-10
-8
-6
-4
-2
2
4
δ 18O ‰ SMOW
K=0.00
K=0.10
K=0.20
K=0.30
K=0.40
K=0.50
K=0.60
K=0.70
K=0.80
K=0.90
K=0.95
K=0.99
M = 7.06
INITIAL LIQUID SMOW

Figure 9

3.5 Dawson Area

Ice-rich material, exposed during placer mining operations on Hunker Creek near Dawson, was sampled in 1984 by W. Pollard. Twenty samples were collected for stable isotope analysis. Oxygen and hydrogen isotope data for these samples are presented in Table 3.3. Since no information is available on the location of these samples, relative to one another, no discussion of the isotope data is possible at this time.

3.6 MAYO SITE

3.6.1 Site Description

This site is located on the south bank of the Stewart River, 3 km upstream from Mayo (Figure 3.9). The study area is underlain by glaciolacustrine clays and silts with varying ice contents. From the river, the ground rises gradually with an average slope of 1.5%. Ground cover is generally mature black spruce forest.

The study area contains numerous small thermokarst lakes and two active retrogressive thaw slides. Burn (1982) estimated that the thermokarst lakes started to form around 1880 while the thaw slides became active prior to 1949 in one instance and between 1961 and 1965 for the other. Work for this project has been confined to the larger slide at the east end of the study area.

Table 3.3 Isotope data for Pollard 1984 Klondike site

SAMPLE NUMBER	$\delta^{18}O$ (°/oo SMOW)	$\delta^{2}H$ (°/oo SMOW)
1	-27.1	-210
2	-28.2	-219
3	-28.4	-219
4	-28.7	-220
5	-28.3	-221
6	-28.6	-222
7	-28.3	-219
8	-27.5	-219
9	-28.4	-218
10	-27.7	-218
11	-28.2	-216
12	-27.7	-217
13	-27.9	-218
14	-27.5	-216
15	-27.8	-216
16	-27.6	-217
17	-27.9	-217
18	-28.1	-216
19	-27.4	-215
20	-27.6	-214

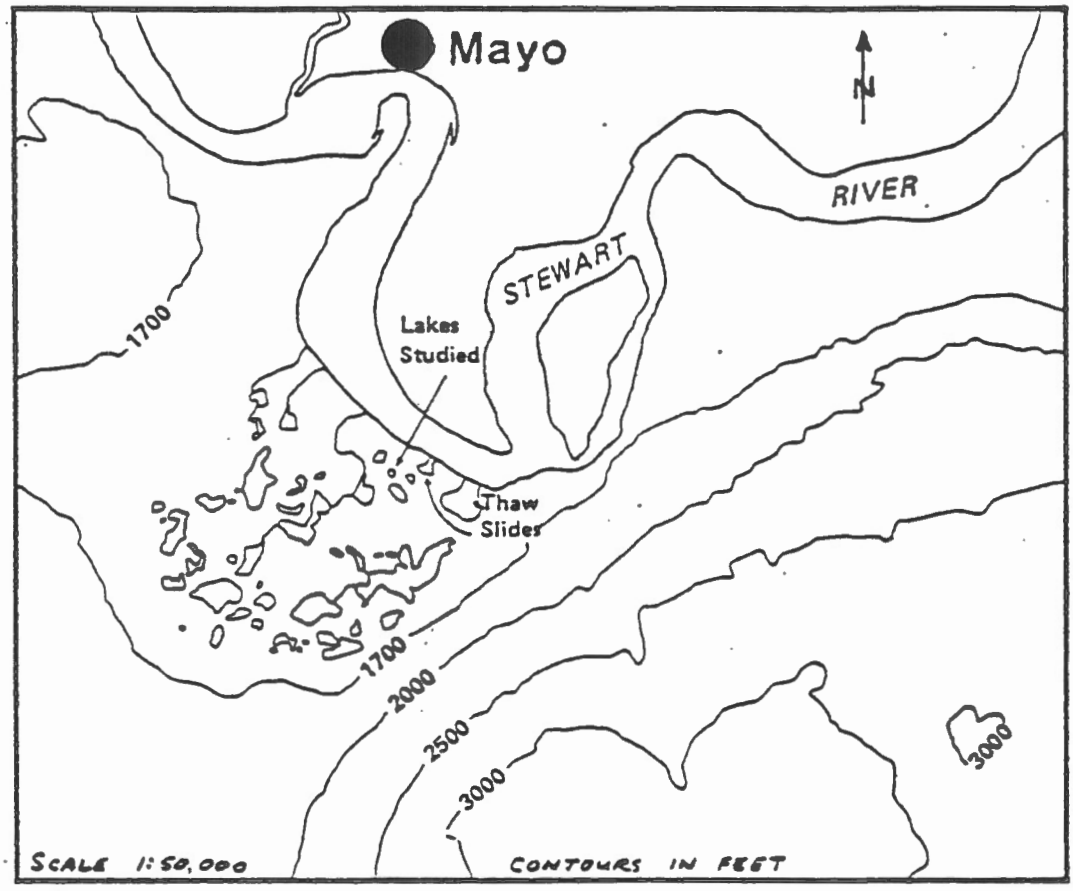

Figure 3.9 Location of thaw slides at Mayo site. (from Burn 1982)

3.6.2 Work Completed

The drilling activity, conducted in 1983, was concentrated along the headwall of the larger thaw slide. The face was actively retreating throughout the summer and by September an average of 10 metres of erosion had occurred. Figure 3.10 depicts the continual enlargement of the slide area and shows the approximate location of drill sites.

In all, three holes were drilled during July and August of 1983 with continuous core recovery from each. Borehole 1 (MBS-1) was completed in early July to a depth of 12.5 metres. It was located approximately 2 metres from the top edge of the slide, but when the overhang of surficial organics is taken into account the borehole was actually less than 1 metre behind the face at the time of drilling. While drilling at a depth of 12.5 metres, a rod sheared without warning, resulting in termination of the hole.

In late July 1983, the drill rods were exposed on the face and it was possible to recover several metres of rod. The height of the face was determined to be 10 metres, leaving the core barrel and lower 2 metres of rod below ground level. Borehole 2 (MBS-2) was drilled at the base of the thaw face adjacent to the original hole. Approximately 2 metres of core material was recovered for comparison with the similar interval in borehole 1.

The third borehole (MBS-3), located approximately 15 metres west of the first two holes, was drilled during the second week of August to a depth of 4.7 metres. The hole was

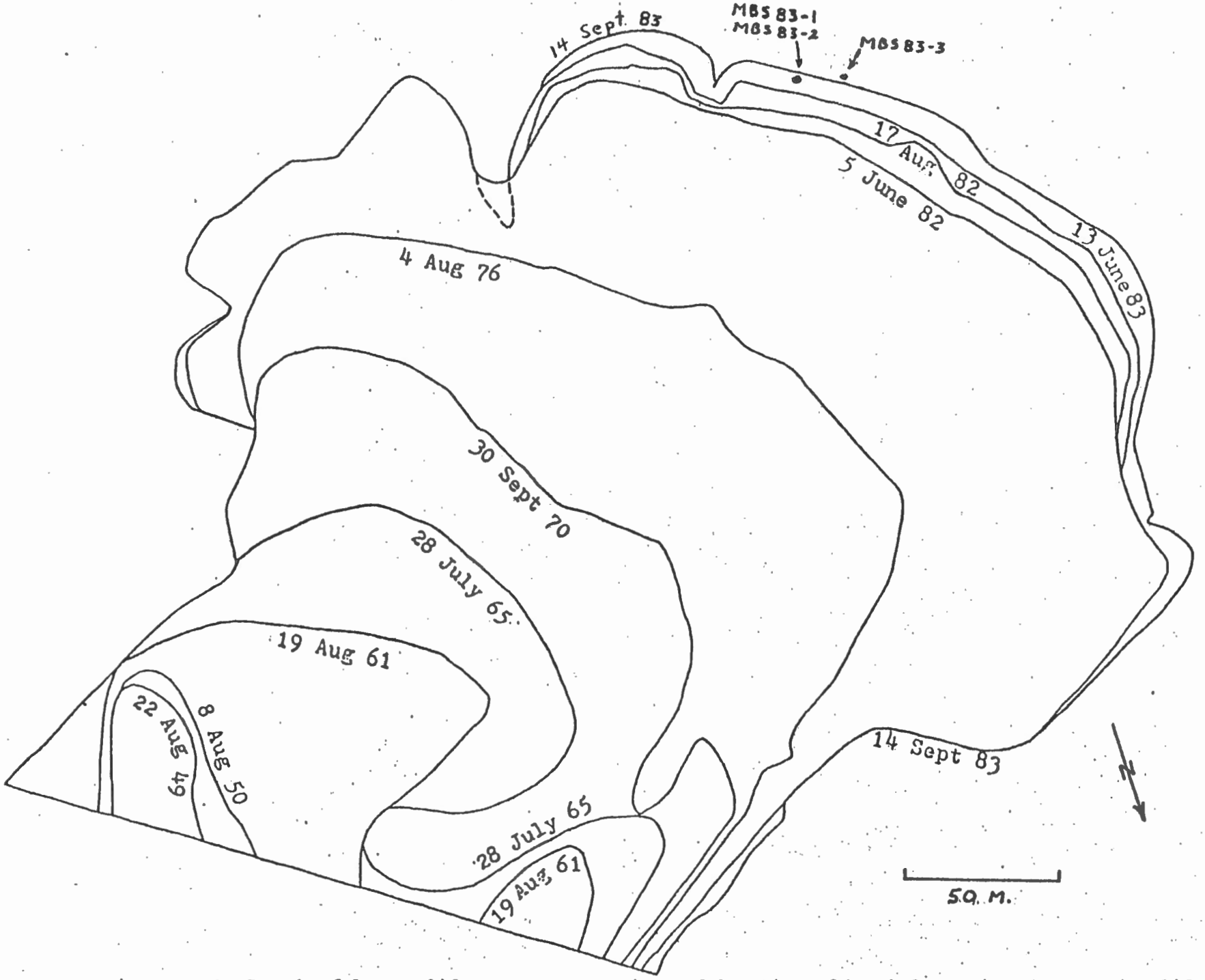

Figure 3.10 Growth of large slide area at Mayo site and location of boreholes. (MBS = Mayo Big Slide)

positioned within two metres of the actual face. The main objective of this hole was for comparison with borehole 1 and to intersect a distinct organic horizon visible in the face of the headwall.

In early January 1984 a brief visit to the study area for other work permitted the collection of four ice samples from various sections of the headwall which are normally inaccessible during the summer. These samples were selected on the basis of stratigraphy.

3.6.3 Stratigraphy

Overall, the face of the slide headwall contains massive ice enclosing blocks of grey clay. The ice could be described as reticulated, comprising 50 to 80% of the total volume. Upon closer examination, the ice can be seen to contain small fragments of clay that have been physically torn apart by the ice. Within the clay blocks, the ice content can be as low as 5 to 10%.

Overlying the massive ice, in the section examined, was an ice-rich silty clay unit. The two units were separated by an organic-rich horizon containing large wood fragments. The upper unit generally contains 25 to 50% ice which occurs primarily as thin lenses. The silty clay is dark grey in colour and contains minor organics and occasional gastropod fragments indicative of a lacustrine environment. The

organic-rich horizon separating the two ice-rich units varied in depth from zero to approximately 4.5 metres within the section.

Covering the upper unit was the modern organic mat which was on average 75 cm thick. At the time of drilling in mid-July, the active layer was 73 cm thick. The ice content of the sediments was low to a depth of 86 cm; at which point it increased sharply to 60 to 80% for the interval 86 to 142 cm. Below 142 cm the ice content decreased to the 25% range. In the ice-rich interval between 86 and 142 cm the ice occurred primarily as lenses up to 1 cm thick.

A detailed report on the stratigraphy and various cryotextures for this site has been prepared by French et al. (1984).

3.6.4 Isotopic Results

Work at the Mayo site is continuing, primarily through the efforts of C. Burn of Carleton University. Isotope data for samples collected during the summer of 1983 and January 1984 are tabulated in Table 3.4.

The single sample from a well at Mayo airport is isotopically similar to unaltered modern precipitation in the central Yukon. The lack of tritium in the sample indicates that this groundwater was recharged prior to 1953. For the following discussion, it will be assumed that this

Table 3.4 Isotope data for Mayo thaw slide site

	DEPTH (CM)	$\delta^{18}O$ (°/oo SMOW)	$\delta^{2}H$ (°/oo SMOW)
MBS-1	93-101	-22.4	-178
	101-110	-19.2	-170
	117-125	-22.5	-184
	133-140		-174
	157-165	-24.2	-188
	180-188		-189
	205-212	-22.0	-189
	225-237	-22.3	-185
	247-255		-183
	270-280	-22.3	-177
	280-290	-20.6	-177
	311-317		-183
	332-341		-181
	341-350		-191
	370-377	-22.5	-191
	377-385	-20.1	
	385-394	-18.8	-191
	400-411		-192
	420-435	-22.5	-190
	445-455		-193
	470-480	-23.6	-191
	480-490		-191
	500-510	-22.4	-190
	518-530		-189
	540-550	-21.8	-181
	550-560		-184
	580-590	-22.8	-184
	610-620		-185
	625-635	-22.8	-185
	651-660		-183
	670-680		-186
	690-700	-21.6	-185
	717-725		-185
	735-745	-21.9	-187
	763-773		-186
	790-800	-21.5	-183
	810-820		-183
	830-840		-179
	848-855	-21.8	-179
	855-872	-21.5	
	872-880	-21.3	-174
	880-892	-20.2	-175
	910-917	-22.2	-181
	923-934		-184
	944-950	-21.7	-185

Table 3.4 Isotope data for Mayo thaw slide site (cont'd)

	DEPTH (CM)	$\delta^{18}O$ (°/oo SMOW)	$\delta^{2}H$ (°/oo SMOW)
MBS-1	970-980		-187
	990-1000	-21.8	-187
	1020-1033	-20.1	-186
	1045-1060		-185
	1070-1080		-187
	1087-1100		-185
	1118-1122	-21.7	-183
	1122-1138		-185
	1145-1151		-183
	1170-1180	-22.7	-195
	1190-1200		-195
	1213-1220	-23.7	-195
	1230-1240	-21.3	-198
MBS-2	0-10		-187
	20-30		-182
	50-60		-181
	70-80		-183
	90-100		-183
	145-160		-183
MBS-3	80-90	-18.7	-174
	140-150	-19.0	-176
	210-220	-20.7	-182
	250-260	-23.0	-189
	292-300	-21.4	-190
	390-400	-21.6	-191
	425-435	-22.6	-193
	445-452	-23.8	-193
	460-463	-21.7	
	463-466	-20.0	-193
Mayo Ice			
84-1		-25.4	-201
84-2		-22.5	-177
84-3		-17.5	-168
84-4		-19.0	-167
	^{3}H (T.U.)		
Mayo Airport Well	not detected	-22.0	-170

groundwater is isotopically representative of the average annual precipitation for the study area, which is usually not an unreasonable assumption.

The four samples of ice collected from the thaw slide headwall in January 1984 demonstrate that isotopic variations exist within these ice-rich sediments. Recent samples collected by Burn and reported separately (Burn et al., in prep.) suggest that the original pore water may have had an ^{18}O composition around -26 ± 0.5 °/oo.

Borehole MBS-1, the deepest at the site, was located within the section containing lacustrine sediments from a former thermokarst lake. It was originally thought that a deep borehole at this location would encounter the transition between ice formed from thermokarst lacustrine water and ice formed from the original glaciolacustrine water. However, as is evident from Figure 3.11, no transition exists isotopically. This means that either both bodies of water were isotopically similar or the original glaciolacustrine pore water has been completely replaced by thermokarst water in the 12.5 metre section which was sampled. Because of other isotope evidence noted earlier, the latter explanation is favoured.

Ice, throughout the headwall of the thaw slide, is segregational in origin. The isotopic profiles shown in Figures 3.11 and 3.12, therefore, have been influenced by the rate of freezing and advancement of the freezing front. The isotope data for both boreholes MBS-1 and MBS-3 display

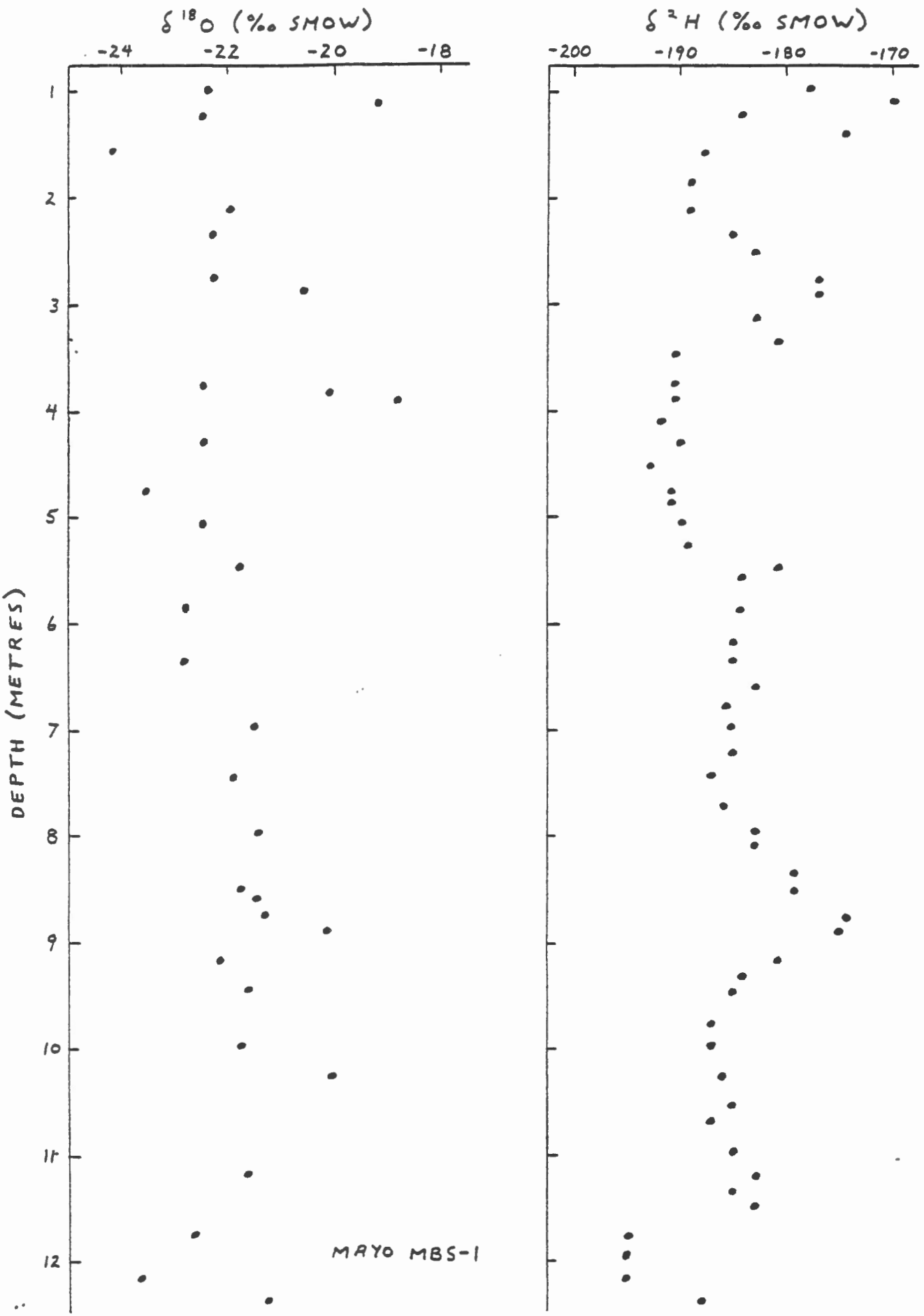

Figure 3.11 Variation ^{18}O and ^{2}H contents with depth for core MBS-1 at Mayo site.

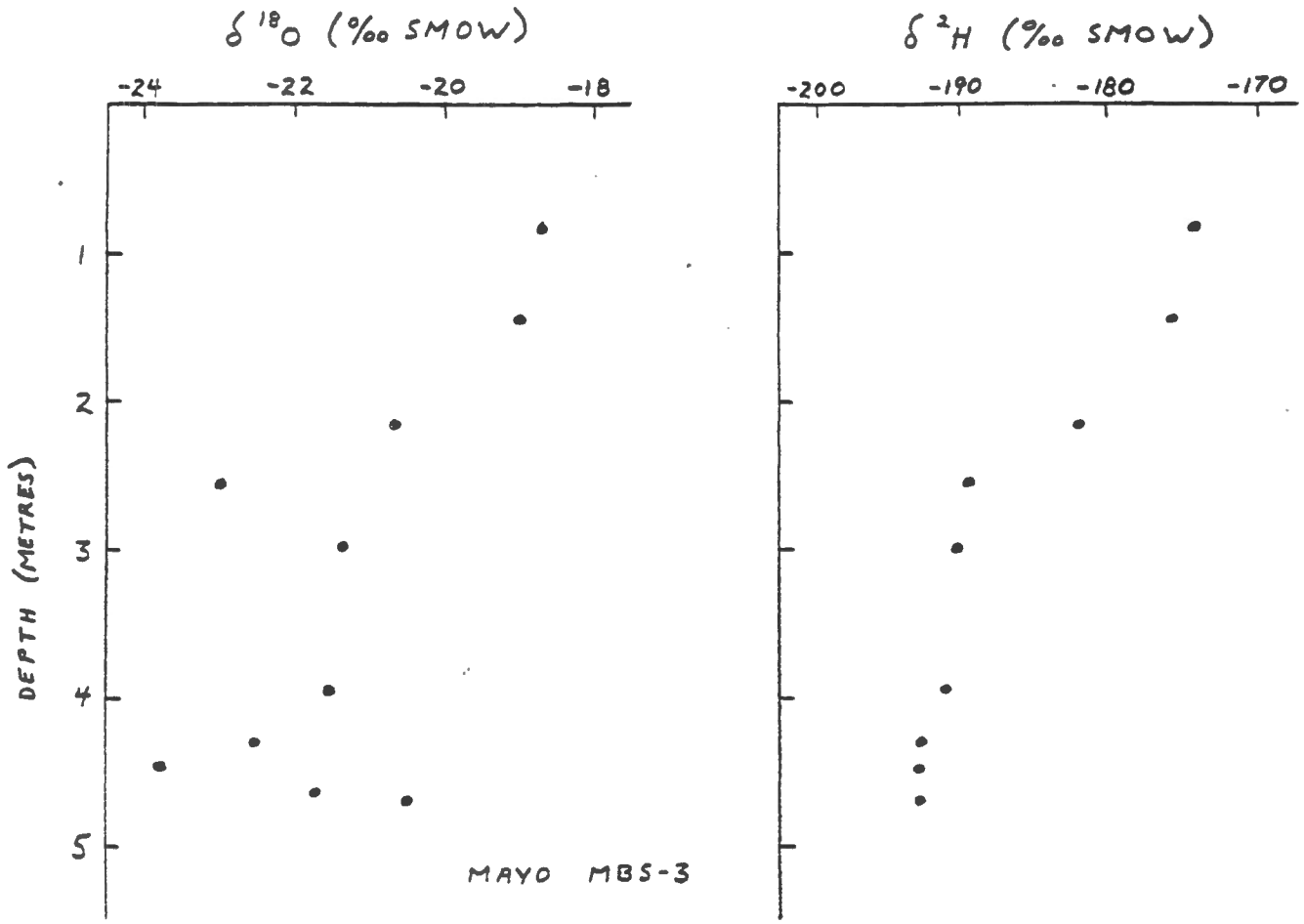

Figure 3.12 Variation in ^{18}O and ^{2}H contents with depth for core MBS-3 at Mayo site.

differences between the oxygen and hydrogen isotope profiles. This is most clearly shown for MBS-3 (Figure 3.12). After a gradual shift to more negative $\delta^{18}O$ and $\delta^{2}H$ values in the upper 2 metres of the section, the two profiles begin to differ. The deuterium profile is uniform (within the 2 °/oo error limits) below 2 metres while the oxygen-18 profile fluctuates sharply.

This divergence in profiles indicates that the freezing rate was sufficiently slow to permit oxygen isotope fractionation while it was too rapid to permit significant hydrogen isotope fractionation. This is in agreement with the isotope data for the North Fork Pass frost blister (section 3.3) where it was noted that equilibrium conditions were reached faster for the oxygen isotopes than for the hydrogen isotopes. The actual freezing rate cannot be determined at present; this must await a series of laboratory experiments.

The ^{2}H versus ^{18}O relationship for each of these two cores is plotted in Figures 3.13 and 3.14. Examination of these figures reveals that the degree of fractionation during freezing was different for each borehole section. The regression line for MBS-1 has a slope of 5.0, while the slope of the line for MBS-3 is 3.6. The global meteoric water line (GMWL) is shown in both figures for comparison. These differences in slope are interpreted as being indicative of substantially different freezing rates, although other possible influences not related to freezing rate cannot be

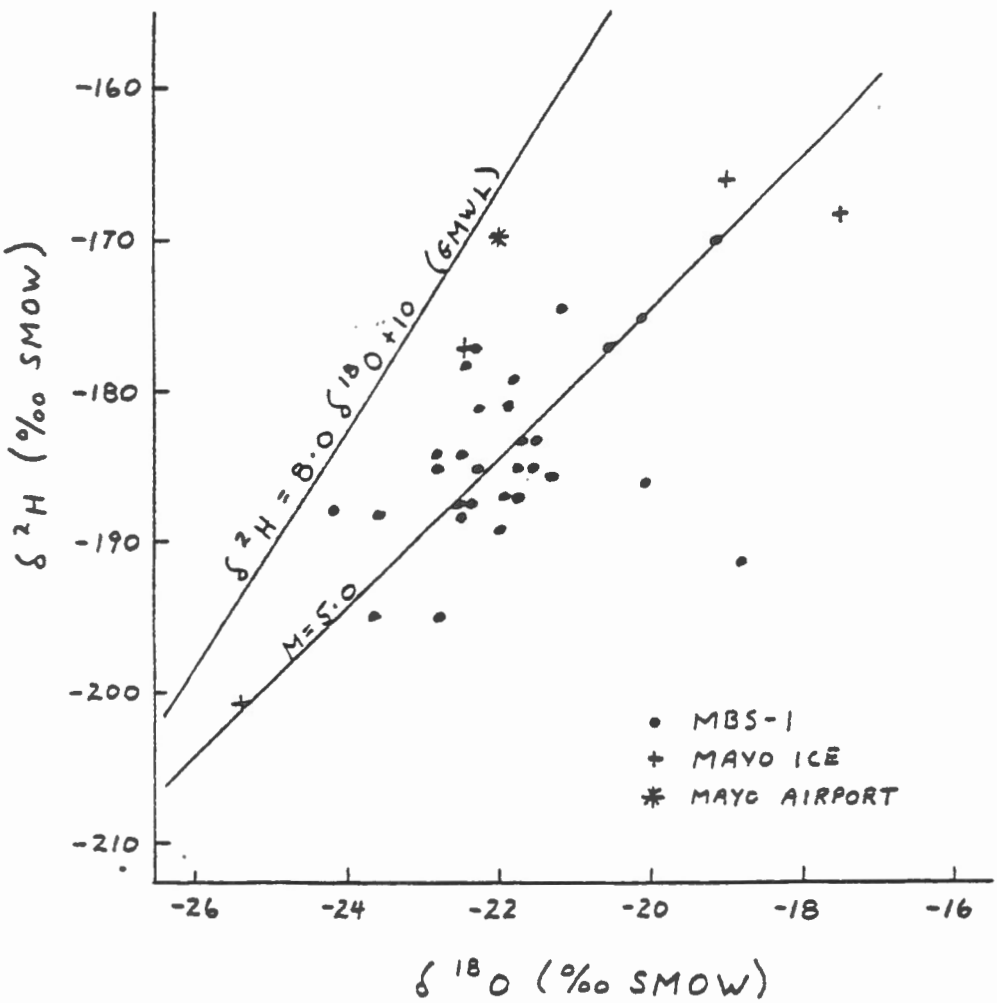

Figure 3.13 Relationship between ^{2}H and ^{18}O contents for core MBS-1. Mayo ice and airport samples shown for comparison. GMWL = global meteoric water line.

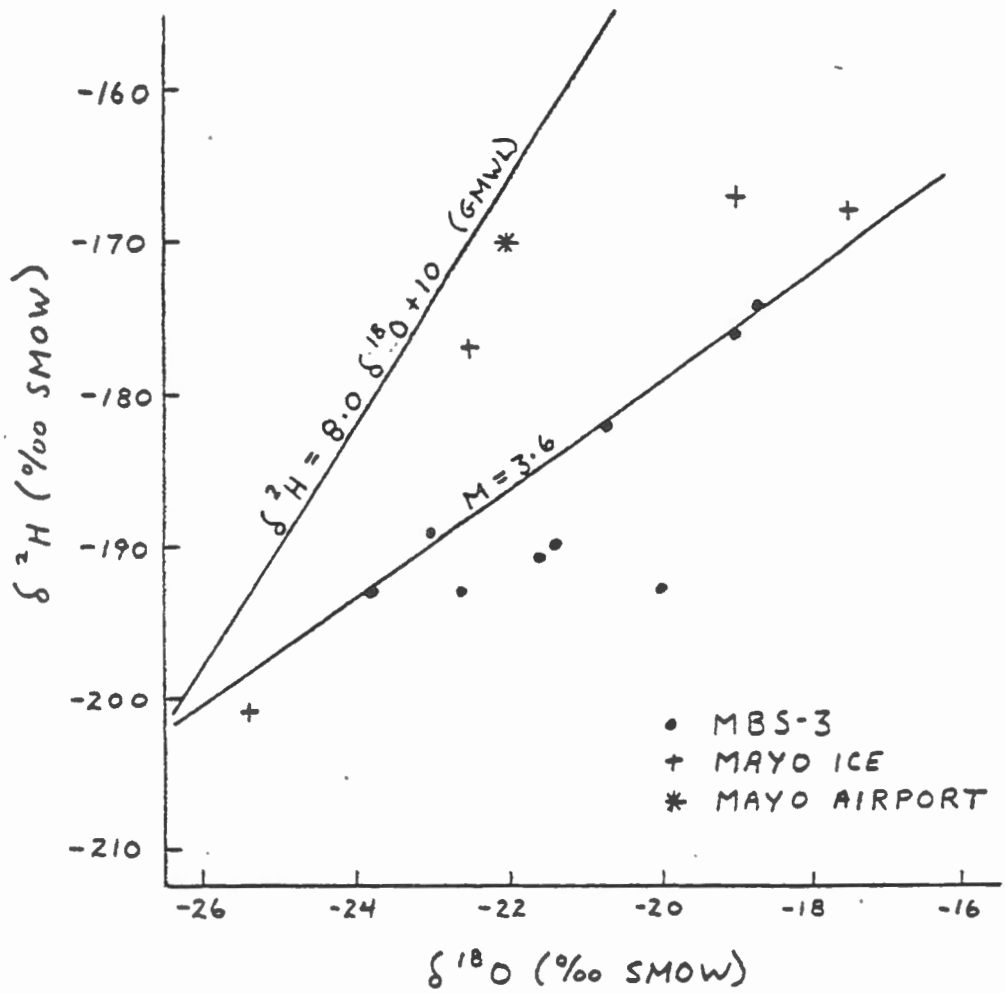

Figure 3.14 Relationship between ^{2}H and ^{18}O contents for core MBS-3. Mayo ice and airport samples shown for comparison. GMWL = global meteoric water line.

ruled out. Again, research on the relationship between fractionation and freezing rate is required for both oxygen and hydrogen isotopes before any further interpretation can be attempted.

4. SUMMARY AND CONCLUSIONS

Massive ice and ice-rich sediments have been examined stratigraphically and isotopically at a number of sites in central and northern Yukon. The principal aim of this study was to attempt to determine the origin and formational process for these ice units using stable isotopes. The initial premise was that each formational process should produce a characteristic isotope signature.

Within the central Yukon, ice-wedge ice, segregated ice and frost-blister ice have been identified and examined. On the basis of stratigraphic and isotopic evidence, massive ice encountered at the Eagle River and Ogilvie River sites along the Dempster Highway is considered to be of an ice-wedge origin, although some segregated ice may also be present. Ice in ice-rich sediments exposed in the headwall of a large retrogressive thaw slide near Mayo is interpreted as forming by segregational processes. The massive ice examined from a frost blister in North Fork Pass proved to be an ideal example of isotope fractionation during complete freezing of a confined water reservoir.

Along the northern Yukon coastal plain, massive ice and ice-rich sediments, exposed in the headwalls of retrogressive thaw slides, have been classifed as ice-wedge ice, segregated ice and buried basal glacier ice. Many of the examined ice wedges for which isotope data are available have $\delta^{18}O$ values similar to modern precipitation occurring in the early spring. One ice wedge, exposed on Herschel Island,

penetrated to much greater depths than modern ice wedges and had an ^{18}O composition which was much more negative than its modern equivalents. It is interpreted as forming during a period of colder glacial conditions.

A massive ice lens up to 3 metres thick, exposed at Sabine Point, is interpreted as segregation ice. Water migrating upward through the underlying marine clay was probably provided by a coarse sand unit beneath the clay. Unfortunately no samples of this sand unit are available for analysis at present.

Banded massive ice and ice-rich sediments were exposed in the headwalls of thaw slides near King Point, Kay Point and on Herschel Island during the summer of 1984. Isotopic profiling of these ice units indicates that they are buried glacier ice, probably from near the base. Since the last glaciation of this region is considered to be early Wisconsisan, this buried ice must be at least as old. Preliminary structural data indicate that the direction of glacier movement was from the southeast toward the northwest.

Each of the ice types examined has produced a characteristic isotope signature. In future, detailed continuous sampling should be undertaken to fully characterize variations in the isotope profile. Further research is also required on the hydrogen isotope distribution and the ^{18}O-^{2}H relationships from these various types of ice.

REFERENCES

Bouchard, M. 1974. Géologie de depots de L'Ile Herschel, Territoire du Yukon; thèse M.Sc. non publiée Université de Montréal, Montréal.

Burn, C.R. 1982. Investigations of thermokarst development and climatic change in the Yukon Territory. Unpublished M.A. Thesis, Carleton University, Ottawa, 142 p.

Burn, C.R., Michel, F.A. and Smith, M.W. in preparation. Stratigraphic, isotopic and mineralogical evidence for an early Holocene thaw unconformity at Mayo, Yukon Territory.

Foothills Pipe Lines (Yukon) Ltd. 1978. Dempster lateral drilling program. Prepared by Klohn Leonoff Consultants Ltd., 2 volumes.

French, H.M., Pollard, W.H. and Burn, C. 1984. Permafrost and ground ice investigations, Mayo, Interior Yukon. Report for Canada Department of Energy, Mines and Resources, Earth Physics Branch, Serial No. OSU83-00158, University of Ottawa, 78 p.

Fritz, P. and Michel, F.A. 1977. Environmental isotopes in permafrost related waters along two proposed pipeline routes. Report on Project No. 606-12 for Canada Department of Energy, Mines, and Resources, Earth Physics Branch, File No. 05SU.23235-6-0681, Waterloo Research Institute, University of Waterloo, 51 p.

Hambrey, M.J. 1984. Sedimentary processes and buried ice phenomena in the pro-glacial areas of Spitsbergen glaciers. Journal of Glaciology, vol. 30, no. 104, pp. 116-119.

Harris, S.A., Heginbottom, J.A., Tarnocai, C and van Everdingen, R.O. 1983. The Dempster Highway-Eagle Plains to Inuvik, in H.M. French and J.A. Heginbottom 9 eds.), Northern Yukon Territory and Mackenzie Delta, Canada, Guidebook 3 for Fourth International Conference on Permafrost. pp. 87-111.

Harry, D.G., French, H.M., and Pollard, W.H. 1985. Ice wedges and permafrost conditions near King Point, Beaufort Sea coast, Yukon Territory, in Current Research, Part A, Geological Survey of Canada, Paper 85-1A, pp. 111-116.

Johnston, G.H. 1980. Permafrost and the Eagle River bridge, Yukon Territory, Canada: Permafrost Engineering Workshop, September 27-28, 1979, Proceedings, National Research Council of Canada (Associate Committee in Geotechnical Research) Technical Memorandum 130, pp. 12-28.

Langway, C.C., Jr. 1970. Stratigraphy analysis of a deep ice core from Greenland. Geological Society of America, Special Paper 125, 186 p.

Mackay, J.R. 1983. Oxygen isotope variations in permafrost, Tuktoyaktuk Peninsula area, Northwest Territories, in Current Research, Part B, Geological Survey of Canada, Paper 83-1B, pp. 67-74.

Michel, F.A. 1982. Isotope investigations of permafrost waters in northern Canada. Unpublished Ph.D. thesis, University of Waterloo, 424 p.

Michel, F.A. 1983. Isotope variations in permafrost waters along the Dempster Highway corridor. Proceedings, 4th International Conference on Permafrost, Fairbanks, Alaska, National Academy of Science, Washington, D.C., vol. 1, pp. 843-848.

Michel, F.A. and Fritz, P. 1980. Laboratory and field studies to investigate isotope effects occurring during the formation of permafrost, Part 2. Report on Project No. 606-12-04 for Canada Department of Energy, Mines and Resources, Earth Physics Branch, Serial No. 0SU79-00064, Waterloo Research Institute, University of Waterloo, 139 p.

Michel, F.A. and Fritz, P. 1982a. Significance of isotope variations in permafrost waters at Illisarvik, N.W.T. Proc. Fourth Canadian Permafrost Conference, Calgary, Alberta, pp. 173-181.

Michel, F.A. and Fritz, P. 1982b. Laboratory and field studies to investigate isotope effects occurring during the formation of permafrost, Part. 4. Report on Project No. 606-12-06 for Canada Department of Energy, Mines and Resources, Earth Physics Branch, Serial No. OSU81-00076, Waterloo Research Institute, University of Waterloo, 76 p.

Michel, F.A. and Fritz, P. 1982c. Study of the environmental isotopes of permafrost related waters along the Alaska Highway pipeline route. Report on Project No. 104-15 for Canada Department of Energy, Mines and Resources, Earth Physics Branch, Serial No. OSU81-0016, Waterloo Research Institute, University of Waterloo, 16 p.

Michel, F.A. and Fritz, P. 1983. Isotope investigations in permafrost regions. Report on Project No. 205-17 for Canada Department of Energy, Mines and Resouces, Earth Physics Branch, Serial No. 0SU82-00161, Waterloo Research Institute, University of Waterloo, 63 p.

Pollard, W.H. 1983. A study of seasonal frost mounds, North Fork Pass, Northern Interior Yukon Territory. Unpublished Ph.D. Thesis, University of Ottawa, Ottawa, 236 p.

Rampton, V.N. 1982. Quaternary geology of the Yukon coastal plain. Geological Survey of Canada, Bulletin 317. 49 p.